See Page 137

OCT 1965

B0649641

NMI-4999

TECHNICAL PAPERS OF THE SEVENTEENTH METALLOGRAPHIC GROUP MEETING, HELD MAY 21 TO 23, 1963 AT LOS ALAMOS SCIENTIFIC LABORATORY, LOS ALAMOS, NEW MEXICO

Compiled by
H. Roth Roman

April 1, 1965

Division of Textron
Nuclear Metals, Inc.
West Concord, Massachusetts

UNITED STATES ATOMIC ENERGY COMMISSION · DIVISION OF TECHNICAL INFORMATION

Other issues of this report bear the number CONF - 105.

LEGAL NOTICE

Printed in USA. Price $5.00. Available from the Clearinghouse for Federal Scientific and Technical Information, National Bureau of Standards, U. S. Department of Commerce, Springfield, Va.

NMI - 4999
METALS, CERAMICS, AND MATERIALS
(TID - 4500, 43rd. Ed.)

Technical Papers of the Seventeenth Metallographic Group Meeting, Held May 21 to 23, 1963 at Los Alamos Scientific Laboratory Los Alamos, New Mexico

Compiled by
H. Roth Roman
Nuclear Metals
Division of Textron, Inc.
West Concord, Massachusetts

Steering Committee

A. E. Guay	Past Chairman
C. L. Angerman	Chairman
R. J. Van Thyne	Sr. Member
H. C. Kloepper	Jr. Member
H. Roth Roman	Secretary

Date of Issuance

April 1, 1965

Nuclear Metals
Division of Textron, Inc.
West Concord, Massachusetts

ATTENDANCE LIST

E. N. Hopkins	Ames Laboratory
F. W. Cotter	Army Materials Research Agency
R. A. Harlow	Atomics International
M. S. Farkas	Battelle Memorial Institute
M. F. Garufi	Bridgeport Brass Company
G. L. Kehl	Columbia University
A. E. Calabra	Dow Chemical Company, Rocky Flats
R. L. Greeson	Dow Chemical Company, Rocky Flats
G. P. Rauscher	Dow Chemical Company, Rocky Flats
T. Van Vorous	Dow Chemical Company, Rocky Flats
J. V. Furth	General Atomics
W. J. Gruber	General Electric, HAPO
A. E. Guay	General Electric, HAPO
L. A. Hartcorn	General Electric, HAPO
D. D. Hays	General Electric, HAPO
R. Teats	General Electric, HAPO
A. F. Steeves	General Electric, KAPL
E. W. Filer	General Electric, NMPO
J. R. Dvorak	IIT Research Institute
R. J. Van Thyne	IIT Research Institute
H. L. Barker	Los Alamos Scientific Laboratory, CMB-1
J. S. Barthell	LASL, CMB-6
J. E. Boyer	LASL, CMB-6
J. R. Bradberry	LASL, CMF-5
S. E. Bronisz	LASL, CMF-5
C. C. Burwell	LASL, CMB-14
S. A. Daily	LASL, N-1
D. L. Douglass	LASL, CMF-5
W. E. Ferguson	LASL, K-2
J. C. Groen	LASL, CMB-6
E. A. Hakkila	LASL, CMB-1
C. G. Hoffman	LASL, N-1
P. Hull	LASL, CMB-14
C. A. Javorsky	LASL, CMB-6
K. A. Johnson	LASL, CMF-5
T. I. Jones	LASL, CMB-6
L. S. Levinson	LASL, CMF-13
G. H. Mottaz	LASL, CMB-14
R. D. Reiswig	LASL, CMF-13
J. W. Schulte	LASL, CMB-14
V. Shadden	LASL, CMF-5
D. S. Shaffer	LASL, CMB-14
M. C. Smith	LASL, CMF-13
D. R. Stoller	LASL, K-2
K. E. Thomas	LASL, CMB-14
L. A. Waldschmidt	LASL, K-2
M. Wilson	LASL, CMB-14
H. C. Kleopper, Jr.	Mallinckrodt Chemical Works
C. F. Hall	National Lead Company of Ohio
B. W. Schoolfield	National Lead Company of Ohio
H. Roth Roman	Nuclear Metals
R. S. Crouse	Oak Ridge National Laboratory
R. J. Gray	Oak Ridge National Laboratory
E. J. Manthos	Oak Ridge National Laboratory
C. L. Angerman	Savannah River Laboratory
H. E. Watts	Sylvania Electric Products

TABLE OF CONTENTS

TABLE OF CONTENTS (continued)

INVESTIGATION OF VIBRATORY POLISHING VARIABLES

E. N. Hopkins and D. T. Peterson
Iowa State University

Several variables in vibratory polishing have been investigated. The characteristics of the sample polishing varied with the lapping material, abrasives, sample weight, and voltage.

INTRODUCTION

Vibratory polishing since its introduction to the field of metallography in 1956 (1) has shown considerable merit. The principal advantages with respect to rotating wheel methods of polishing have been the ease of operation, the saving of skilled operators' time and the reduction in relief polishing. This report is concerned with the influence of some of the many variables in vibratory polishing and an attempt to measure the effect of these variables on the rate of metal removal. The variables under consideration in this report are the effect on the rate of metal removal of the lap material, vibrational amplitude, specimen and holder weight, number of samples in the bowl, type of abrasive and the hardness of the material to be polished.

PROCEDURE

The test specimens were mounted in bakelite and ground through 600 grit silicon carbide paper. Most of the investigation was done with annealed specimens of 1020 steel. Diamond pyramid hardness impressions were made using a 1000 gram load and the diagonal lengths measured. The specimens were then polished for a measured length of time and the diagonals were remeasured. The rate of metal removal was calculated from the difference in the diagonal measurements and the known geometry of the diamond indenter. Photographs were taken of representative areas to show the quality of the polish.

A standard vibratory polisher (2) was used for all tests. The lap or cloth used for polishing was secured with a standard retaining ring. When necessary, cloths and laps were glued to surface of bowl with Pliobond cement. The amount of abrasive used was 20 grams and the abrasive was suspended in 500 ml water and 10 ml liquid Vel detergent. The rheostat used with the vibratory polisher was the Model LPC-01 Separate Controller purchased with the vibratory unit.

RESULTS AND DISCUSSION

Very early in the investigation, an unexpected result became apparent. The amount of metal removal was not directly proportional to the vibrational amplitude. Figure 1 shows typical examples of the variation in the rate of

metal removal as the rheostat setting is varied. It is apparent that small differences in the rheostat setting can produce considerable differences in the rate of metal removal. The rate of metal removal could be reproduced at a given rheostat setting if the setting were not changed but the rheostat setting could not be reproduced. The setting at which maximum polishing occurred also varied with the type of material being polished. For example, a zinc specimen did not reach the maximum rate of metal removal at the same rheostat setting as a steel specimen even when both were polished simultaneously. This sensitivity of the polishing rate to the rheostat setting required that a number of tests be made at various rheostat settings as other variables were changed.

The maximum, minimum, and average rates of metal removal by different cloths and laps are shown in Table I. From this table it is seen that a wax lap has the highest rate of metal removal followed quite closely by Pellon discs and nylon cloth. It should be noted that the maximum rate of metal removal did not occur at the same rheostat setting for the different lap media. The Pellon cloth, epoxy resin, and wax gave the maximum metal removal at rheostat settings between 70 and 80 whereas the other cloths and laps gave maximum removal at rheostat settings below 30. Figure 2 shows the quality of polish obtained with various lap materials. With the exception of the epoxy resin lap and Microcloth, the quality of the polished surfaces are comparable. Plastic laps when used with Linde A abrasive leave the surface with scratches comparable in depth to the original 600 grit scratches. The surface obtained with Microcloth showed considerable irregularity and relief polishing.

TABLE I

RATE OF METAL REMOVAL AS A FUNCTION OF LAP MATERIAL

Lap Material	Rate of Metal Removal -- Microns Per Hour		
	Minimum	Average	Maximum
Microcloth	2	7	13
Rubber	1	5	19
Leather	2	9	22
Wood	2	14	34
Neoprene	5	14	35
Epoxy resin	24	36	45
Nylon cloth	12	28	52
Pellon disc	21	43	59
Wax	37	57	80

The effect of the abrasive as a factor in the rate of metal removal is shown in Table II. The specimens were polished on wax laps and with identical conditions except for the use of different abrasives. The abrasives used were 600 grit silicon carbide, 600 grit aluminum oxide, 15 microns aluminum oxide, 1 micron magnesium oxide, 0.3 micron aluminum oxide, and .05 micron aluminum oxide. The 600 grit abrasives were not as effective in removing metal as the smaller 15 micron abrasive and produced fewer but deeper scratches. This condition is probably the result of poor sizing in the larger abrasive materials. It is possible that the sample was not in contact with the entire abrasive bed but was supported by the small number of large particles, thus not removing as much material as would be expected from a coarse abrasive. The magnesium oxide abrasive did not remove as much metal as the much finer 0.3 micron aluminum oxide. Aluminum oxide appears superior to magnesium oxide in the rate of metal removal. Figure 3 shows the quality of polish obtained with the various abrasives.

TABLE II

RATE OF METAL REMOVAL AS A FUNCTION OF ABRASIVE

	Rate of Metal Removal--Microns per Hour		
Abrasive	Minimum	Average	Maximum
0.3 micron Aluminum Oxide	37	57	80
1.0 micron Magnesium Oxide	4	16	29
15.0 micron Aluminum Oxide	70	115	239
600 grit Aluminum Oxide	36	106	177
600 grit Silicon Carbide	7	66	141

The fourth variable studied was the specimen weight. A comparison of the rate of metal removal as a function of specimen weight is shown in Table III. The standard holder and specimen weighed 375 grams. Increasing the weight increased the rate of polishing up to 600 grams but decreased the polishing rate after this point. The standard specimen holder did not give the maximum rate of metal removal but the difference is not great enough to warrant a change in the weight of the standard specimen holder.

TABLE III

THE RATE OF METAL REMOVAL AS A FUNCTION OF THE SAMPLE AND HOLDER WEIGHT

Weight of Sample in Grams	Rate of Metal Removal--Microns per Hour
100	16
200	4
375	53
600	60
800	45

It was observed that the maximum, minimum, and average rates of metal removal decrease with an increasing number of specimens in the bowl. The maximum rate does not decrease rapidly or to any great extent but the minimum rate decreases rapidly and is much less with 14 specimens than at one specimen. The polishing rates for various numbers of specimens in the bowl are given in Table IV.

TABLE IV

THE RATE OF METAL REMOVAL AS A FUNCTION OF THE NUMBER OF SAMPLES POLISHED

Number of Samples Simultaneously Polished	Rate of Metal Removal--Microns per Hour		
	Minimum	Average	Maximum
1	37	57	80
5	11	45	65
9	4	39	65
14	4	25	51

Table V illustrates the effect of differences in hardness on the rate of metal removal. The hardness of material is certainly not the only contributing factor in the polishing characteristics. As is seen from this table, a harder material can polish faster than softer material. Some of the reasons for this may be the amount of surface worked metal and the ductility or the brittleness of sample as well as the hardness.

TABLE V

THE RATE OF METAL REMOVAL AS A FUNCTION OF SAMPLE HARDNESS

Sample Material	Diamond Pyramid Hardness 1000 Gram Load	Rate of Metal Removal--Microns per Hour
Zinc	90	41
Steel	170	33
Steel	200	46
Steel	350	24
Steel	510	33
Steel	600	32
Steel	790	32
Vanadium Carbide	875	41

CONCLUSIONS

The vibratory polisher is easy to operate and gives an excellent quality of polish. However, the large variations in the rates of metal removal with changes in vibrational amplitude and other factors are undesirable. These differences are believed to be due in part to the vertical component of vibratory movement. An increase in the horizontal motion and a decrease in the vertical motion might cause much of the erratic behavior of the vibratory polisher to disappear. A polisher which would still be easy to operate but would be considerably more effective and reproducible might be developed by modification of present types or the evolution of new types of vibratory polishers.

The desirability of an intermediate polishing step using a 15 micron aluminum oxide abrasive between the 600 grit abrasive papers and the 0.3 micron Al_2O_3 is clearly indicated. With the use of the 15 micron Al_2O_3 abrasive, the time of polishing would be considerably decreased. The use of the 600 grit powder abrasives is of no advantage.

The weight of the standard specimen holder is in the correct range for most efficient polishing.

Increasing the number of specimens in the bowl decreases the rate of polishing, particularly the minimum rate of metal removal. With a more effective polisher this would not be a problem since polishing would be done in the maximum rate of metal removal region.

The hardness of the metal to be polished is not the only factor to be considered in the rate of polishing, and no quantitative prediction can be made to fit all metals at the present time.

The vibratory polisher is a step forward in the field of metallography. With the further improvement of this type of metallographic polishing, sample polishing will some day be relegated a minor role in metallography.

ACKNOWLEDGMENT

The authors would like to acknowledge Mr. H. Baker, who helped with a considerable portion of the experimental work covered in this paper.

REFERENCES

1. F. M. Krill, "Vibratory Polishing of Metallographic Specimens," Metals Progress 70 (1), 81-82 (1956).

2. Syntron Model LP-01, Type C, Synthron Company, Homer City Pa.

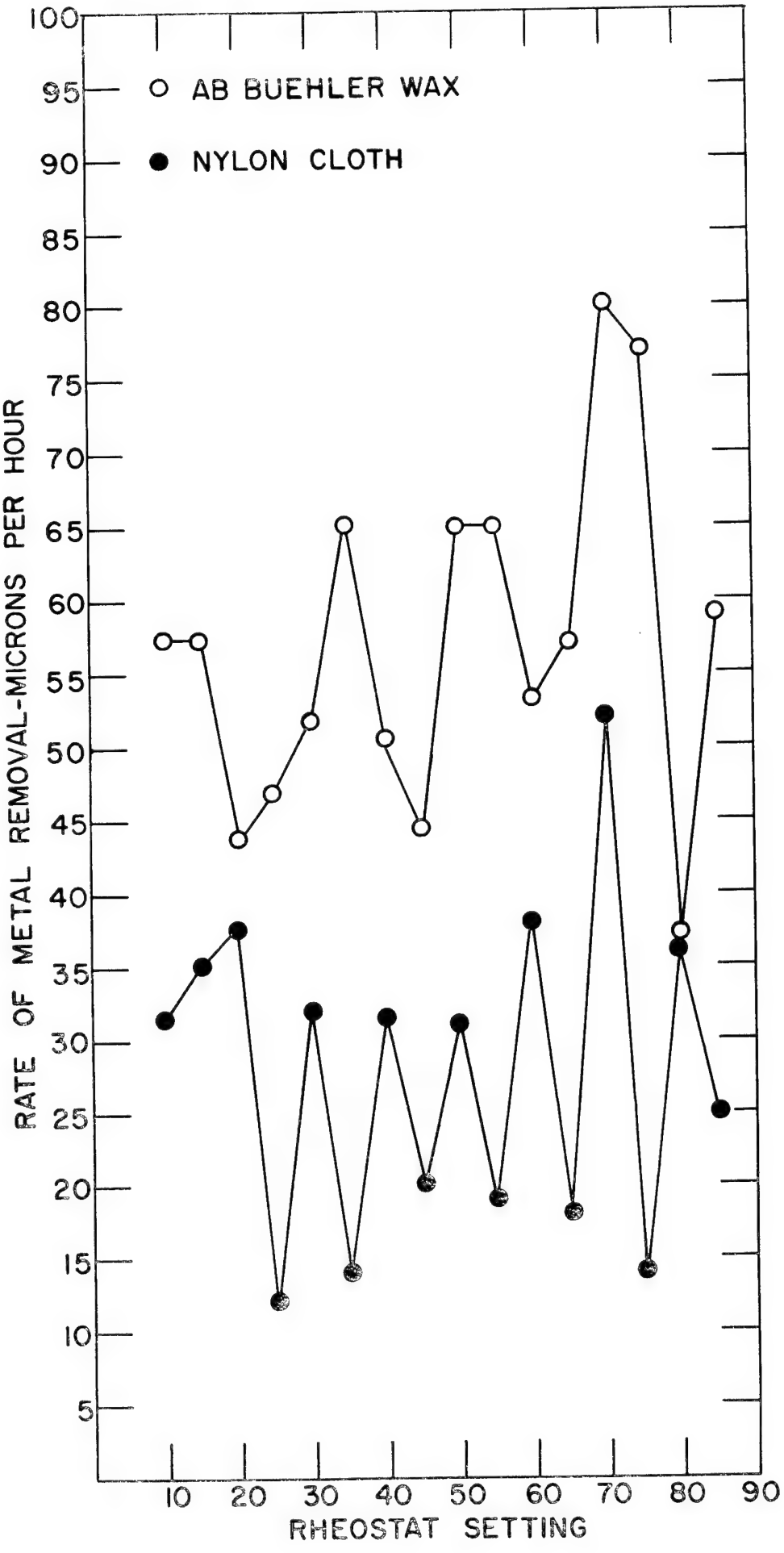

Figure 1. Variation in the Rate of Metal Removal Produced by Various Rheostat Settings.

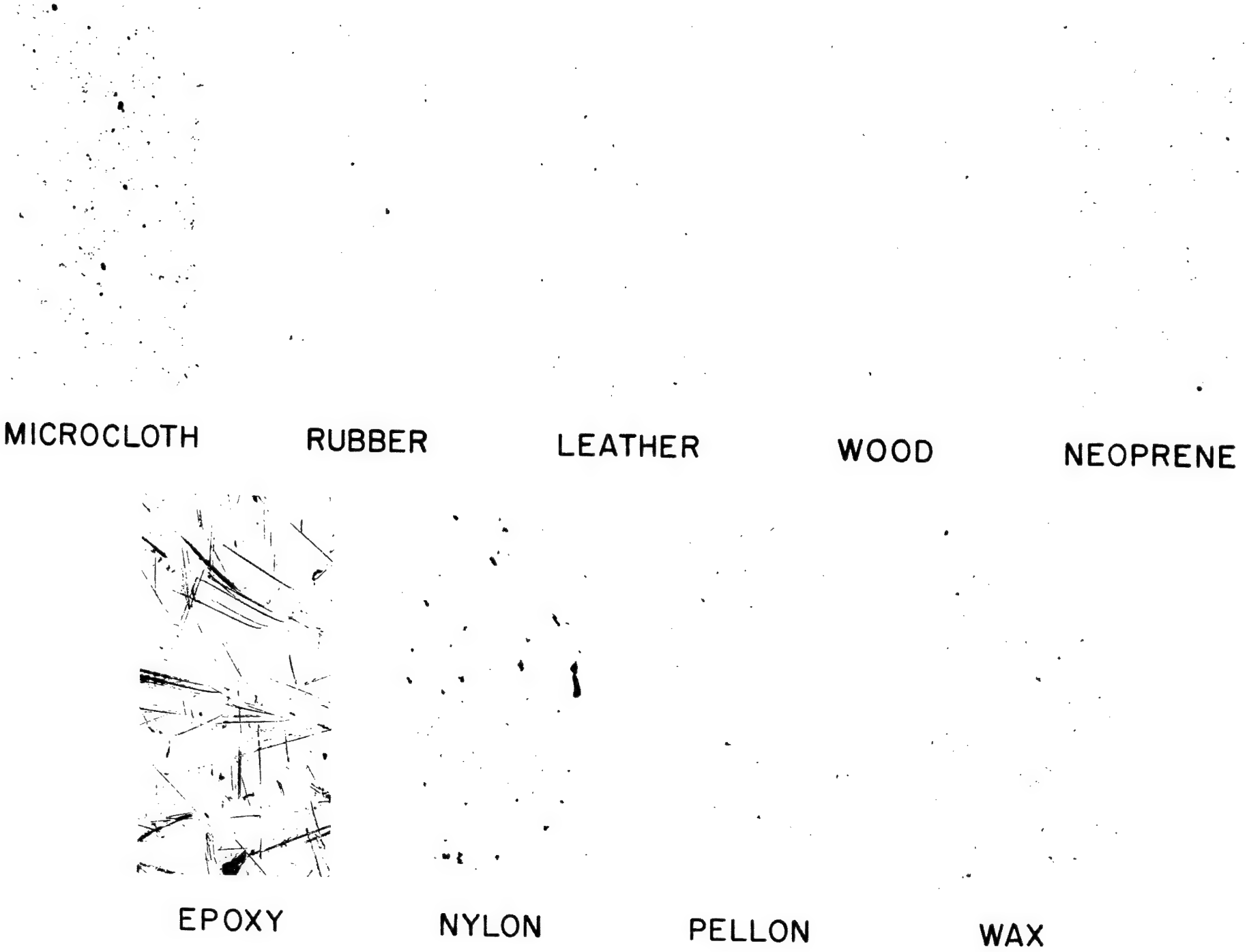

Figure 2. Quality of Polish Obtained with Various Lap Materials.

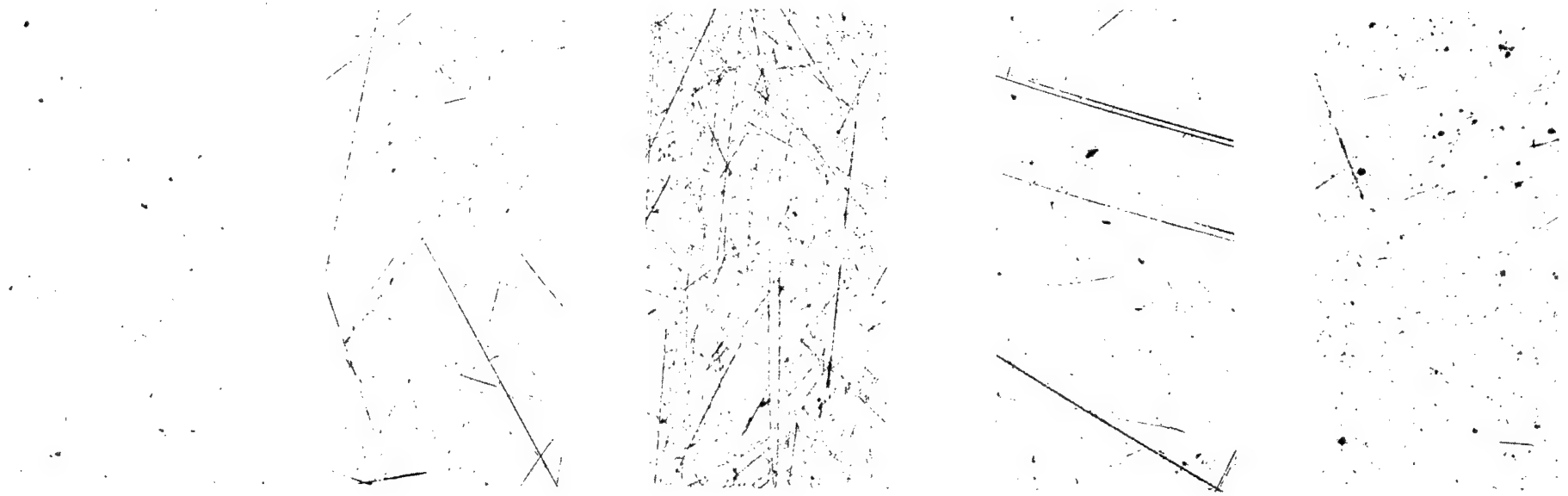

Figure 3. Quality of Polish Obtained with Various Abrasives.

METALLOGRAPHY OF THERMIONIC CONVERSION COMPONENTS*

T. I. Jones
Los Alamos Scientific Laboratory

Modification of standard preparation procedures was required to evaluate the very hard components and dissimilar materials used in a design for thermionic conversion.

INTRODUCTION

A great deal of interest is currently being expressed in a method of direct conversion of heat to electricity which is generally termed "thermionic conversion." At Los Alamos, the effort is being made to convert heat from fissioning material directly into electricity. Attention has centered on thermionic cells in which an ionized cesium gas fills the space between the anode and the cathode. The path through the cesium plasma together with the external leads to the cell electrodes forms a closed electrical circuit. A circuit of this kind can be thought of as a "plasma thermocouple" since the interface between the emitter electrode and the cesium gas corresponds to the hot junction while the interface between the collector and the cesium gas represents the cold junction. Figure 1 shows a drawing of an early plasma thermocouple design. The UC-ZrC fuel pin became the incandescent emitter which ionized part of the cesium. The positive ions thus produced neutralized the electron space charge so that the electron current received by the Nb-Zr collector was no longer space charge limited.

This drawing illustrated the desired goal; however, a number of fabrication problems had to be solved first on an individual component basis. For example, suitable techniques had to be found to join the fuel pin to the body and for joining the body and the collector to the Al_2O_3 insulator.

METALLOGRAPHIC PREPARATION

It was apparent that the size of many of the shapes to be examined would exceed the 1-1/4 inch diameter standard mounts used for metallographic examination. Figure 2 shows the standard molds and mounts and the new ones which were developed for the larger size specimens. The two molds and mounts on the left are the standard 1-1/4 inch diameter units. The molds were made from silicone rubber (Silastic RTV 501). The mold dimensions were such that the final epoxy resin mounts cast in them were about 0.003 to 0.005 inch less than 1.250 inch diameter.

- - - - - - - - - - -

*This research was done under the auspices of the Atomic Energy Commission.

Two varieties of epoxy resin were used for mounting the metallographic specimens. Epon 815 was used when vacuum mounting was desired to force the resin into the cavities of porous samples. This resin had considerable shrinkage on hardening and the molds were larger than those used for routine mounting using Epon 828. The larger molds used for vacuum mounting were colored a reddish-brown to distinguish them from the regular tan-colored molds. The figure shows that a sample designation may be written on the mold with a ball point pen before pouring the resin. After the epoxy has hardened, the designation can be scribed on the mount and the mold cleaned for future use.

The two larger molds and mounts are also shown on Figure 2. These molds will produce mounts having flat surfaces of 1-1/4 inch by 2 inch and 1-1/4 inch by 4 inch.

Figure 3 shows the apparatus used for vacuum casting the epoxy resin. The resin and hardener were mixed in a glass beaker and the beaker was placed in the clamp on the shaft. The mold containing the specimen was placed in the chamber and the door closed. The chamber was usually evacuated until the vacuum gauge indicated between 20 and 23 at which time and resin was poured into the mold. The resin effervesced indicating some loss of more volatile material. When the mold had been filled, the vacuum pump was turned off and air was admitted to the chamber which forced the resin into the open pores of the specimen. It has been found desirable to allow the molds to remain at room temperature for 2-1/2 hours before placing them in an oven controlled at 75°C for overnight curing.

Figure 4 shows the two larger mounts after the machining operation which adapted them for use in 1-1/4 inch diameter specimen holders.

All specimen mounts were ground and polished using the Buehler Automet apparatus. Usually the final polish was made using a diamond abrasive. When examination of the soft Nb-Zr metal was desired, an additional operation using the vibratory polishing unit was required.

The larger mounts necessitated a modification in the Automet specimen holder. Figure 5 shows the conventional specimen holder and the two new units. The top unit is the conventional five-position holder for standard 1-1/4 inch diameter mounts. The bottom two units, from left to right, are used for the medium and large mounts. Figure 6 shows the three specimen holders with the mounts each would normally use. It was found necessary to use two spacer mounts with the largest mount to prevent specimen rounding during the grinding operation.

The integrity of each plasma thermocouple component as well as the joining of the various components was examined metallographically. Figure 7 shows the fuel pin which was the first component to be examined. The metallographic procedures used on these hard carbide pins deviated from standard practice. The machined mount was sent to the shops department for sectioning. The shops ground these pins to a diameter using a diamond grinding wheel on a surface grinder. The surface being ground was flooded with a water-oil mixture. Approximately 0.001 inch of material was removed per traverse of the specimen. When the diameter of the pin was reached, the mounts were inserted in the specimen holders and ground on abrasive papers using the Automet fixture. It was discovered that by using a stream of water on the grinding paper and heavy loads on the holder (about 45 to 60 lbs), a polished surface was obtained after using several 600 grit papers. The polished surface could not be obtained using kerosene or lighter loads. It was presumed that the water imparted an attack-polish technique to the UC-ZrC pin.

RESULTS

Using the water-heavy load technique, the various inclusions were retained and had sharp interfaces. The periphery of the pin was not polished but showed a finely fractured structure. Figure 8 shows UC_2 inclusions in a UC-ZrC pin ground through the 600 grit paper. The dark areas were voids and probably represented some pull-out or drop-out of fractured material. Figure 9 shows the same field after prolonged etching in a nitric-acetic-water etchant. Figure 10 shows UC_2 inclusions in a similar sample after a suitable etching time. Note the UC striations in the UC_2 particles. Subsequent polishing using 0-2μ diamond on Metcloth succeeded in polishing the periphery of the pin but had little effect on the internal structure. Only the nitric-acetic-water etchant was used since in the early development stages it was thought that the presence of non-solid solution inclusions were of more importance than the possible effects of grain size. Figure 11 shows UC_2 inclusions in an apparent grain boundary network as well as massive, random inclusions. Figure 12 shows the structure of the UC-ZrC after etching with an HF etchant. It was much more difficult to discover the UC_2 inclusions in this background that it was in the as-polished condition. Figure 13 shows a UC_2 inclusion and a grain boundary phase in an HF-etched pin.

A number of brazing materials were investigated to attempt to join the carbide pin to the Nb-Zr body. Figure 14 shows the results of one such attempt; note the porosity in the braze zone. Figure 15 shows a higher magnification view of the brazed section made using V foil. This figure shows that the V wet both surfaces but porosity developed as the liquid solidified. The Nb-Zr was not polished well enough to eliminate the scratches because only the interface was being examined. If the structure of the Nb-Zr had been desired, a subsequent vibratory polishing operation would have been necessary. The inclusions in the Nb-Zr were thought to be carbides.

Figure 16 shows the penetration of the V into the carbide pin. The cracks were believed to have been caused by the surface grinding operation but may have indicated a very brittle zone in the brazed joint. Figure 17 shows a brazed joint in which Zr foil was used to join the carbide pin to a Mo base. Figure 18 shows the braze metal-carbide interface. Figure 19 shows the penetration of the braze metal into the carbide pin.

In the plasma thermocouple design, it was necessary to insulate the body from the collector and form a vacuum seal. This insulator also had to withstand the corrosive effects of the cesium vapor. Pure Al_2O_3 fulfilled these requirements. In order to join a metal to the Al_2O_3, some metallized layer had to be bonded to the ceramic surface. Figure 20 shows a ceramic insulator with a metallized coating around the top and bottom of the cylinder. The cylinder was coated by spraying WO_3 on the zones shown. The WO_3 was reduced by firing the insulator in a wet H_2 atmosphere. Figure 21 shows the polished metallographic section of this insulator. Figure 22 shows the W-metallized layer on one of the surfaces of the ceramic. The W particles appeared to be intimately bonded to a non-metallic matrix.

Figure 23 shows a W-metallized Al_2O_3 insulator brazed to the Nb-Zr body with Pd. Figure 24 shows the brazed joint. The scalloped surface was the machine marks on the Nb-Zr which was etched to distinguish the braze metal from the body metal. It was apparent that the Pd was extensively alloyed with the Nb-Zr. The ceramic-braze metal interface was in intimate contact. This sample was polished only enough to reveal the condition of the bond. It was felt that the true porosity of the ceramic would be much lower than that shown and could be revealed by prolonged diamond polishing at the expense of putting the metal layer in relief. Figure 25 shows the intimate ceramic-braze metal bond at higher magnification. Apparently some of the non-metallic matrix of the original metallized layer had been transported into the braze metal.

Figure 26 shows a double brazed joint. This early section indicated a need for better alignment during brazing. Figure 27 shows a typical brazed joint on one of the four brazed sections.

With the development of fabrication and metallographic techniques fairly well established for individual components, the problem of complete assembly remained. In order to test the mounting and polishing techniques for long assemblies, a rough mock-up was made of the early plasma thermocouple design. Figure 28 shows the mock-up which was made by inserting into a Cu tube a steel rod suspended between two brass plugs. The brass plugs had an interference fit with the Cu tube. Holes 1/16 inch diameter were made in each end to simulate the openings in the designed assembly. This unit was mounted in the vacuum chamber using a large mold. The polished section shown in this figure indicated that the

vacuum casting technique would force the epoxy through the end openings and completely fill the internal cavity. Also, the polished section was reasonably flat from end to end and side to side.

Figure 29 shows the polished longitudinal section of a plasma thermocouple assembly of an early design. Although the fuel pin was slightly less than full length because of the broken tip, the assembly was otherwise standard. The structures of the fuel element and the brazing which joined the fuel element to the body and the body to the collector through the ceramic insulator were similar to those microstructures of the individual components previously shown. Thus, what initially appeared to be an extremely difficult metallographic problem has become one of routine examination.

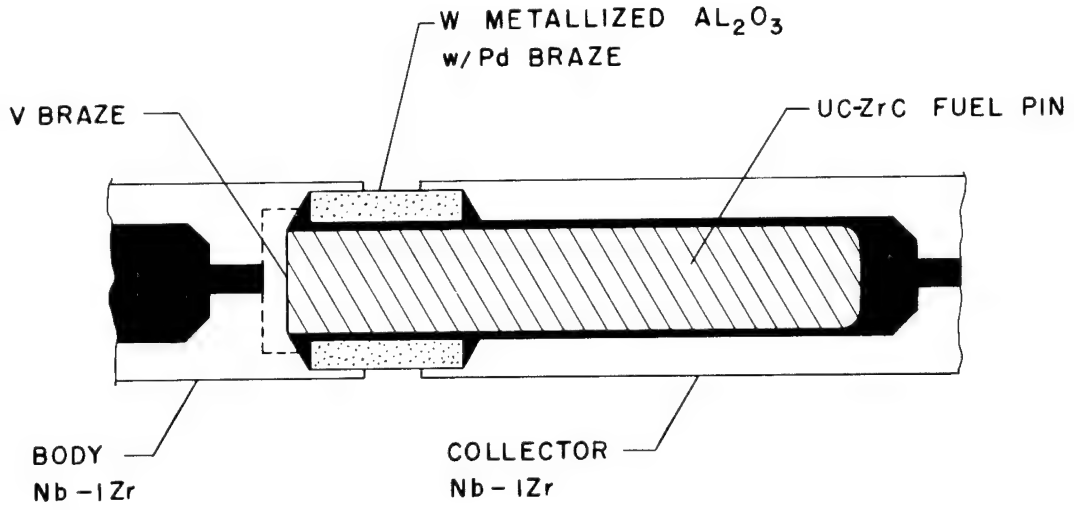

Figure 1. Early Plasma Thermocouple Design

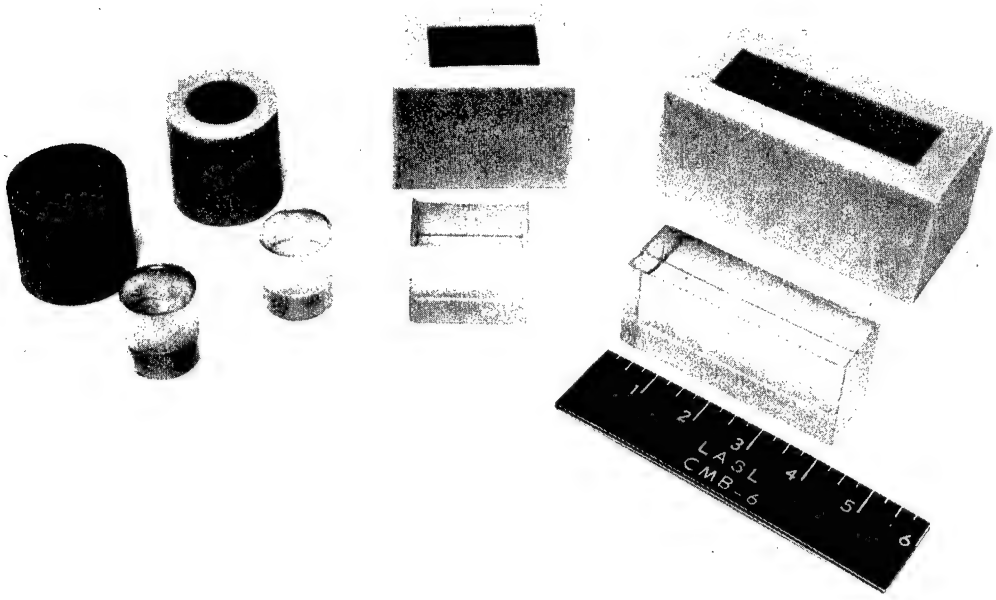

Figure 2. Standard Molds and Mounts (left), and New Molds and Mounts (right) Developed for Larger Size Specimens.

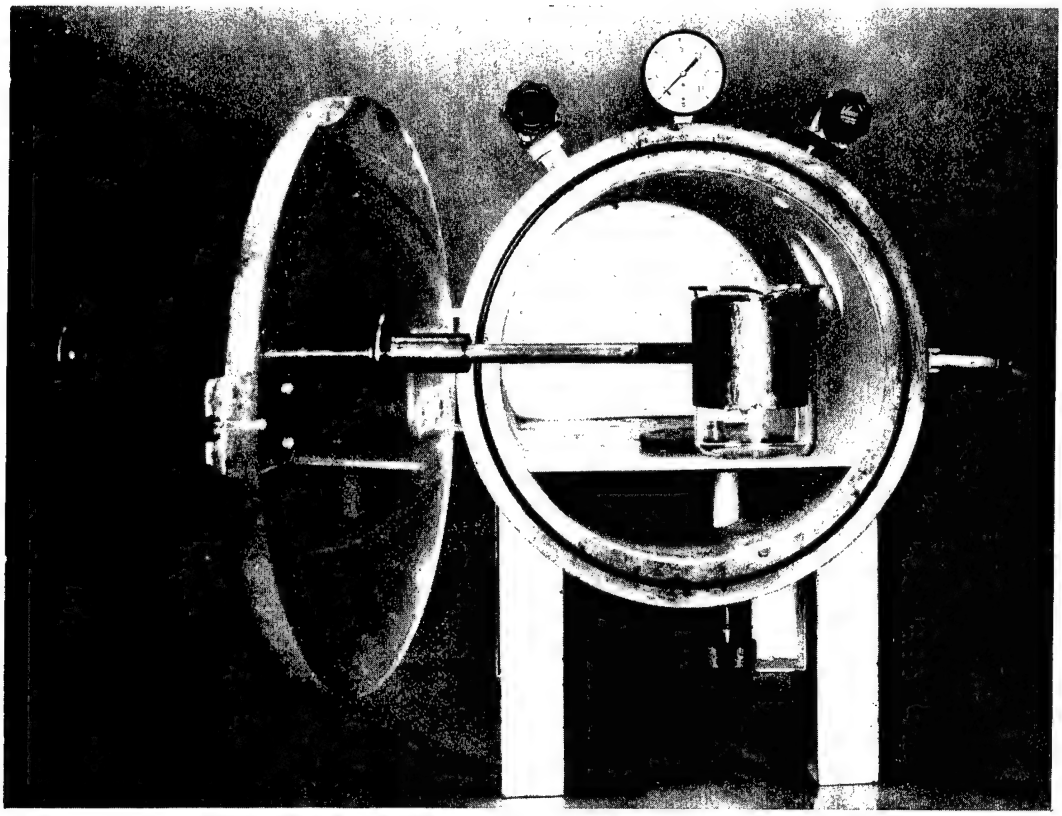

Figure 3. Apparatus Used for Vacuum Casting the Epoxy Resin.

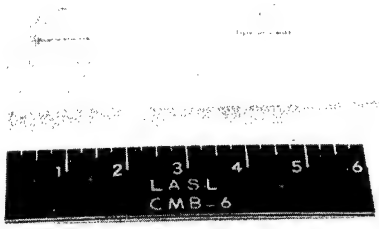

Figure 4. The Two Larger Mounts after Machining.

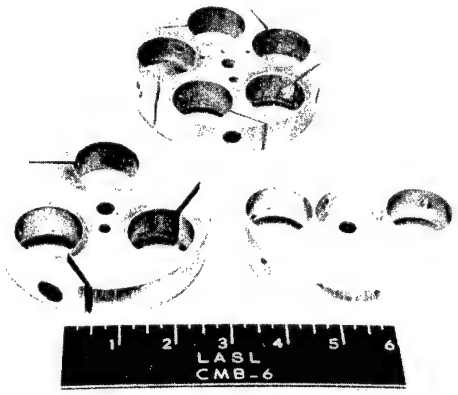

Figure 5. Conventional Specimen Holder (lower right) and the Two New Units.

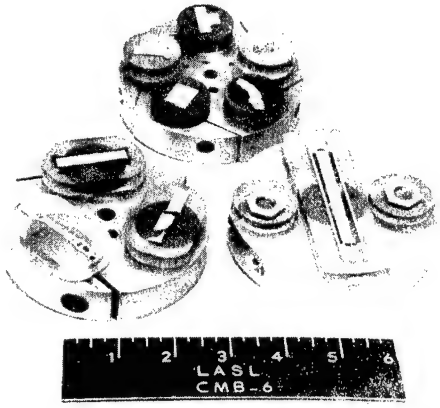

Figure 6. The Three Specimen Holders with Normally Used Mounts.

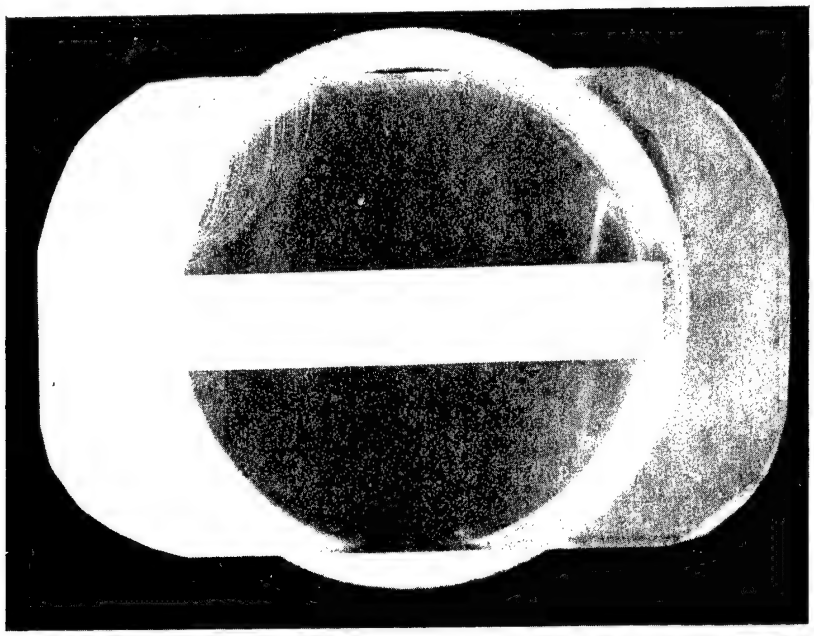

Figure 7. Fuel Pin from Plasma Thermocouple. 2X.

Figure 8. UC_2 Inclusions in a UC-ZrC pin Ground Through the 600 Grit Paper. 500X.

Figure 9. Same Field as Figure 8 after Prolonged Nitric-Acetic-Water Etch. 500X.

Figure 10. Same as Figure 9, showing UC Striations in the UC_2 Particles. 500X.

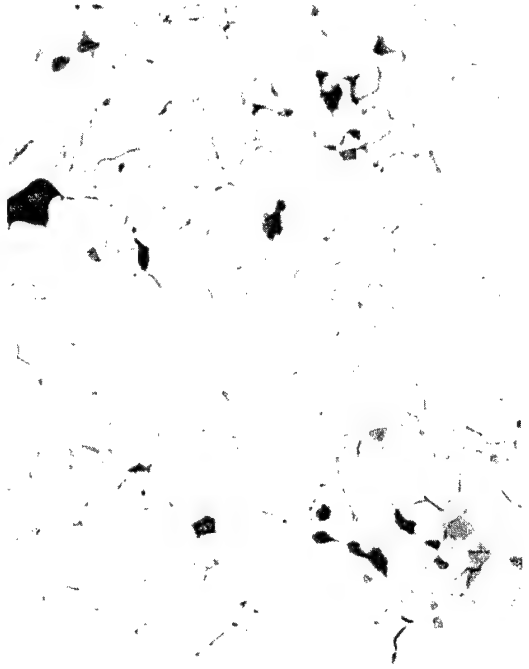

Figure 11. UC_2 Inclusions in an Apparent Grain Boundary Network as well as Massive, Random Inclusions. 500X.

Figure 12. Structure of UC-ZrC after HF Etch. 250X.

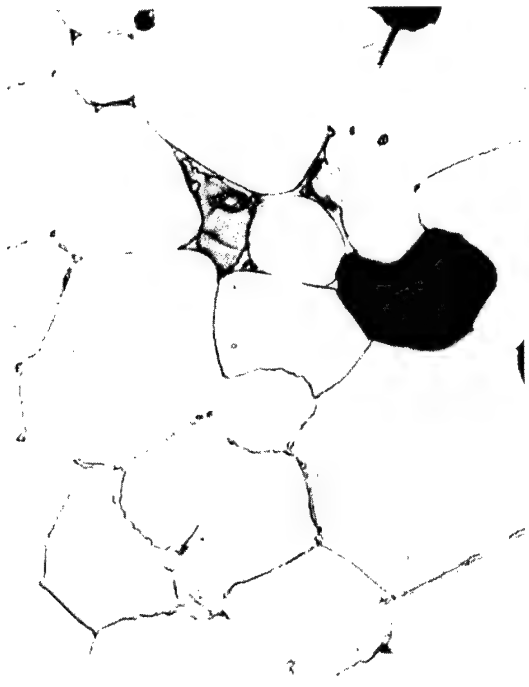

Figure 13. UC Inclusion and Grain Boundary Phase in an HF-Etched Pin. 1000X.

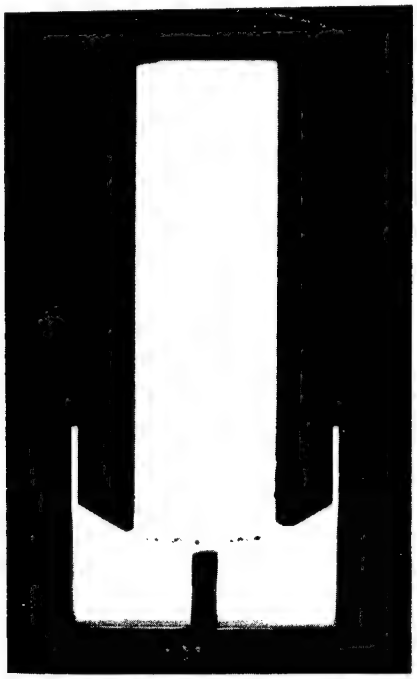

Figure 14. Carbide Pin after an Attempted Braze to Nb-Zr Body. 3X.

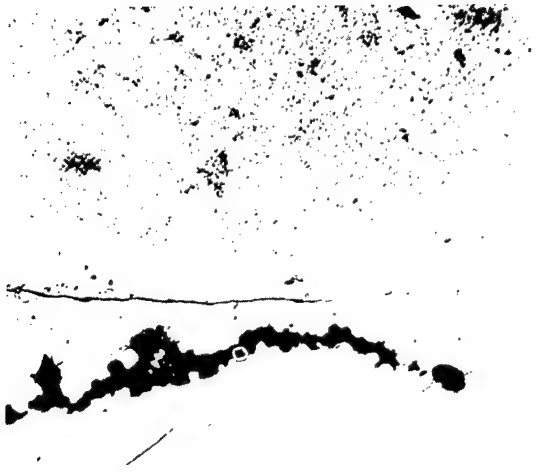

Figure 15. Higher Magnification (100X) of Brazed Section. Made with V Foil.

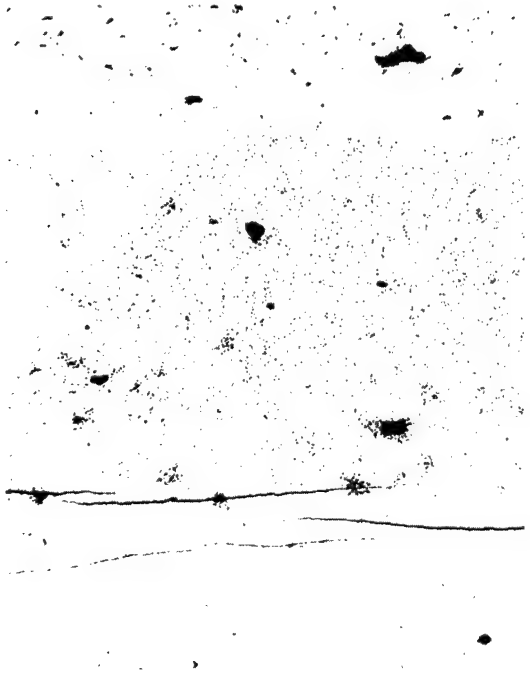

Figure 16. Penetration of the V into the Carbide Pin. 100X.

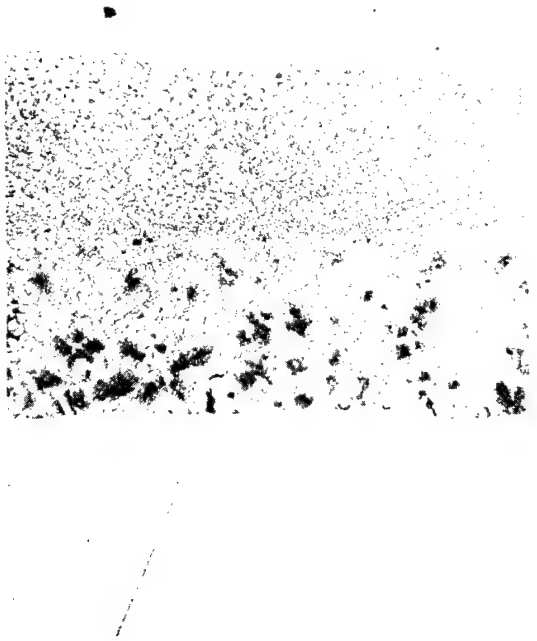

Figure 17. Brazed Joint in which Zr Foil was Used to Join the Carbide Pin to a Mo Base. 100X.

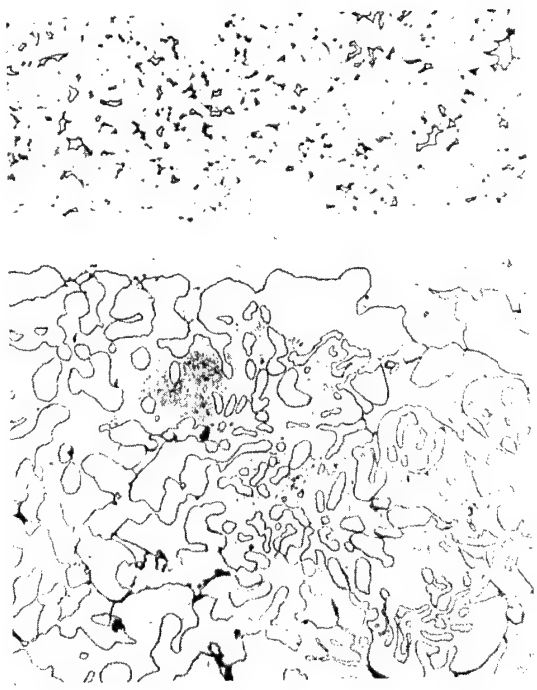

Figure 18. Braze Metal-Carbide Interface. 500X.

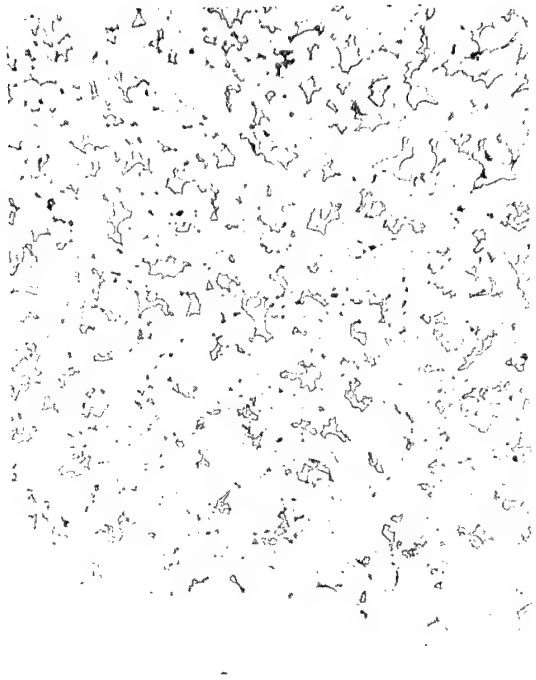

Figure 19. Penetration of the Braze Metal into the Carbide Pin. 500X.

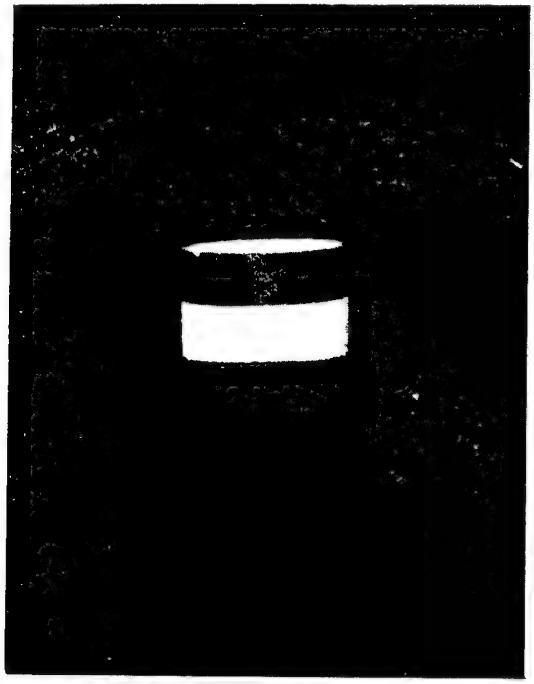

Figure 20. Ceramic Insulator with Metallized Coating around Top and Bottom of Cylinder. 2X.

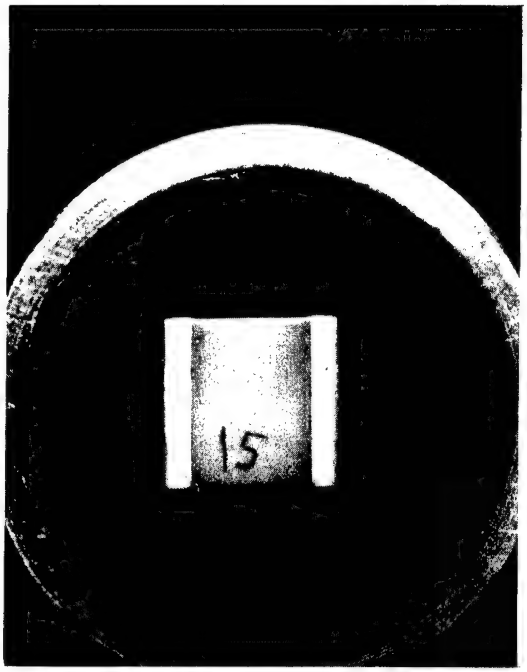

Figure 21. Polsihed Metallographic Section of Ceramic Insulator. 2X.

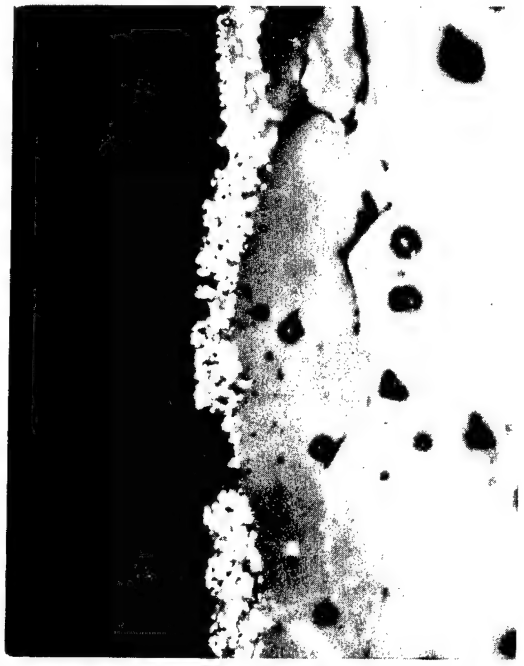

Figure 22. W-Metallized Layer on One of the Surfaces of the Insulator. 500X.

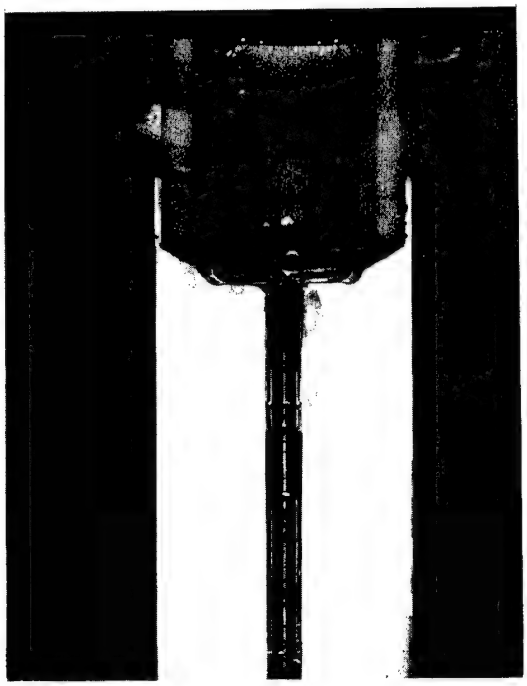

Figure 23. W-Metallized Al_2O_3 Insulator Brazed to the Nb-Zr Body with Pd. 3X.

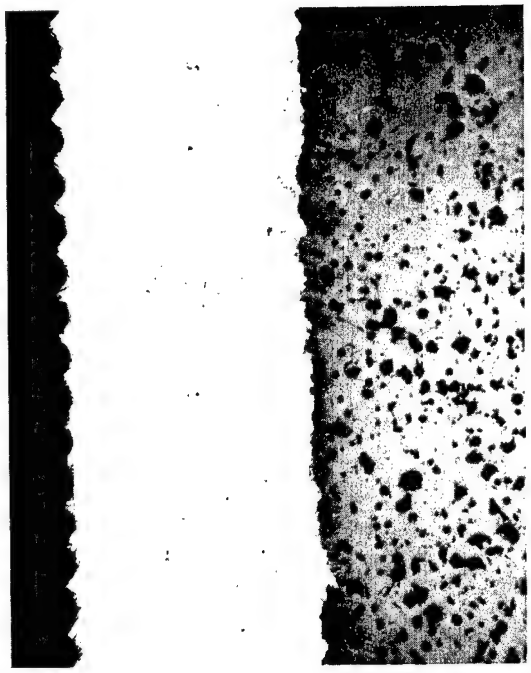

Figure 25. Ceramic-Braze Metal Bond at Higher Magnification (500X).

Figure 24. Brazed Joint of Insulator at Higher Magnification (100X).

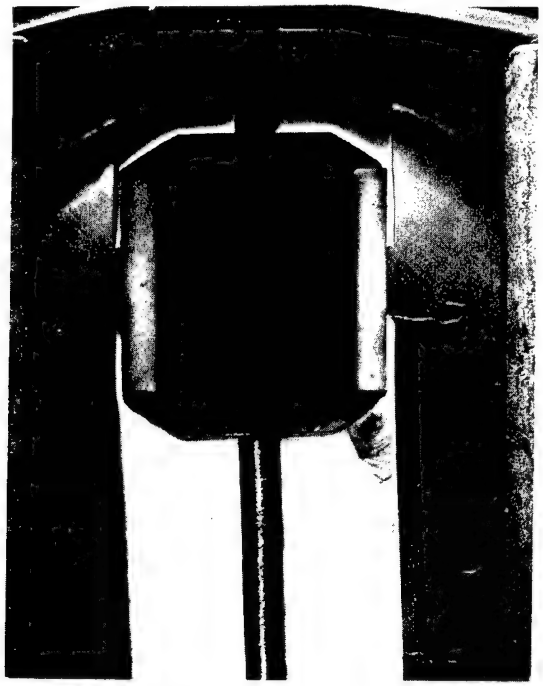

Figure 26. Double Brazed Joint. 3X.

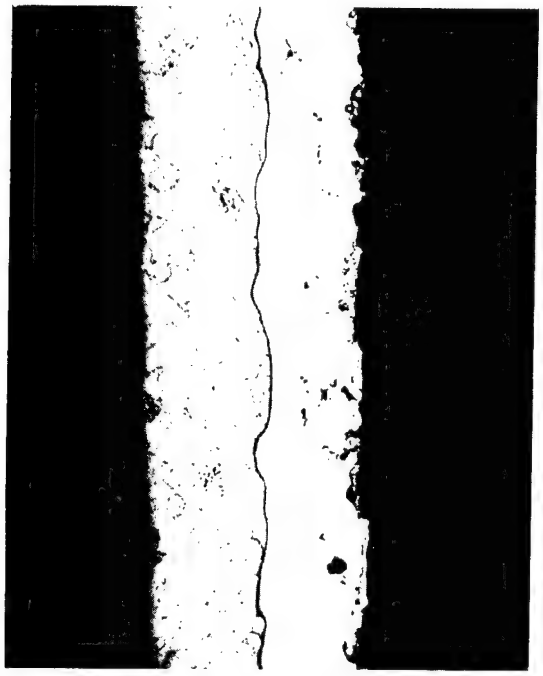

Figure 27. Typical Brazed Joint on One of the Four Brazed Sections. 100X.

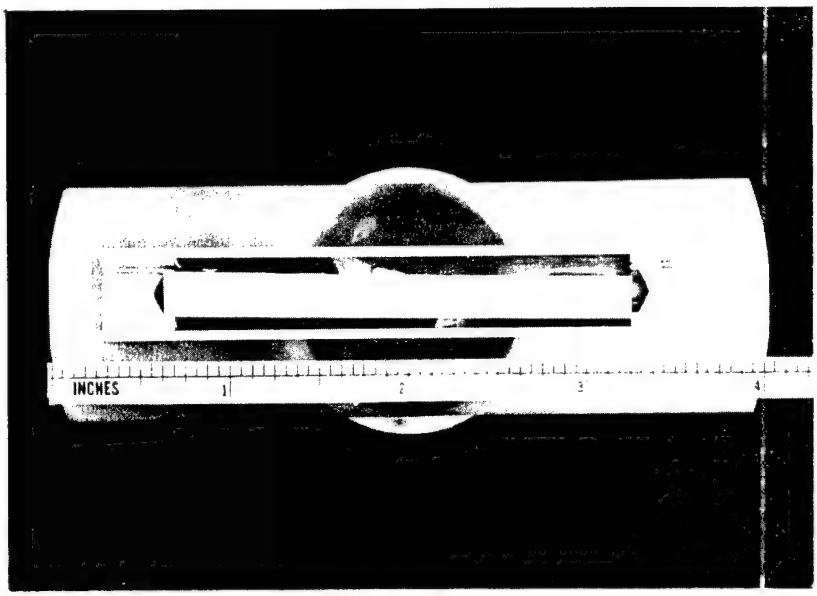

Figure 28. Mock-Up Made by Inserting a Steel Rod Suspended between Two Brass Plugs into a Copper Tube.

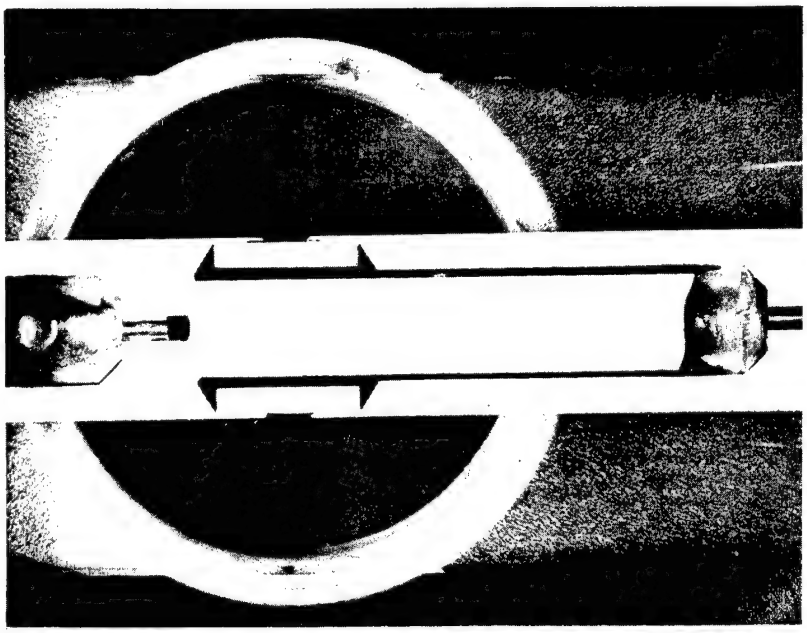

Figure 29. Polished Longitudinal Section of a Plasma Thermocouple Assembly of an Early Design.

A PROCEDURE FOR COLOR MICROPHOTOGRAPHY *

W. J. Gruber
Hanford Atomic Products Operation

This paper describes the criteria and a procedure for successful color photography with a metallograph. Some of the fundamentals of color photography, which are considerations affecting the method selected, are discussed.

INTRODUCTION

In recent years the demand for color photomicrographs has increased. There are several reasons for this trend. The metallographer wants to show the characteristic colors of constituents of phases. Increased use of color slides makes it desirable to use color photomicrographs in order to maintain continuity in presentations. The cost of color film and processing has been drastically reduced in the past decade, making it economically feasible to employ color metallography.

A successful procedure has been developed at the Hanford Radiometallurgy Laboratory to ensure that the color produced on transparancies and finished prints will closely match that of the subject. This paper describes the procedure established and some of the fundamentals of color photography (1) which affected the final methods selected.

ILLUMINATION

Selection of light source is probably the most important item as the spectral quality of the source must be compatible with the response of the color film to ensure true color rendition. In metallographic applications, three sources which are suitable are; zirconium arc, carbon arc, and tungsten lamps. Two which are not suitable are mercury vapor lamps and tungsten arc with a mercury vapor starter.

The zirconium arc is the most simple to use as the spectral quality of the light requires no correction for color photography. The color temperature of the illumination is 3200°K and Type B film can be used with no color temperature correction.

Carbon arc illumination has greater intensity than the zirconium arc, but some correction must be made before it can be used. The carbon arc light spectrum has an excess of ultraviolet light which affects the blue component of color film and must be filtered out. The color temperature of the illumination is a function of the current and can be reproduced when current is controlled. Color temperature of illumination from a standard 8 mm carbon anode with excess ultraviolet

- - - - - - - - - - -

* The etchants used for this procedure are described in Appendix A to this publication, page 158.

removed varies from 3650°K at 4.5 amp. to 3800°K at 10 amp. d.c. Since the color temperature range does not fall at any of the points where commercial films are balanced, a light corrector (photometric) filter is required.

Tungsten lamps can be used as light sources for remote color photography but, in some instances, are not desirable because of the difficulty in reproducing exact color temperatures. The light intensity is less than that of either carbon or zirconium arc. During the life of a lamp, the color temperature varies with age. The color temperature also varies from lamp to lamp of the same type. Tungsten lamps are usually employed where exact color rendition and reproducibility are not required.

OPTICS

In general, combinations of objectives and eyepieces are recommended for photomicrography on the assumption that a narrow spectral band of yellow-green light will be used to illuminate the subject and photography will be with black and white film.

Illumination used in color metallography is polychromatic, differing from the essentially monochromatic source used for black and white. With the introduction of polychromatic light, a second factor, lateral color, which requires correction is encountered (2). Lateral color, or chromatic difference of magnification, results in separation of the spectrum in objects some distance from the axis of the optical path in the image projected by the objective lens. The amount of separation increases as the distance from the axis becomes greater. Like curvature of the field, lateral color increases with magnification and is corrected with the metallograph eyepiece.

Because lateral color has not been properly considered, it will be found that combinations of objectives and eyepieces best suited for color metallography may differ from those recommended for black and white, especially at magnifications greater than 500X.

Also, certain optical components may act as a filter and affect either the color balance or color temperature of the light. If either or both occurs, then the induced change in the light must be corrected.

PROCEDURE USED IN THE RADIOMETALLURGY LABORATORY AT HANFORD

Metallography in the laboratory is performed on two Bausch and Lomb Research Metallographs. One has been remotized for examination of radioactive materials and the other is a conventional unit. Our procedure for color photography is affected by the fact that developing and printing will be done outside our organization and the person doing the processing will not be familiar with the object photographed.

ILLUMINATION

A direct current carbon arc with an 8 mm diameter anode was selected as the light source for color work as high intensity light is required for the remote unit because of its extended optical path. Carbon arc illumination was selected as a light source for the conventional metallograph so a second procedure would not be required. In order to control the color temperature of the light sources, d.c. ammeters were installed in the power leads. To insure reproducibility, all color photography is done with the current adjusted to 10 amp. Excess ultraviolet light is filtered out by a solution of 1 weight % sodium nitrite added to the water in a 3 cm thick water cell. When the sodium nitrite solution is used, the efficiency of the water cell is reduced so that an infra-red cutoff filter is required to protect the metallographoptics and the photometric and/or color-correcting filters from the excess heat. The color temperature of the filtered light passing through the cutoff filter is 3800°K. A Wratten 81C filter adjusts the color temperature to 3200°K where Type B film is balanced and a Wratten 82C filter adjusts the color temperature to 5800°K where daylight film is balanced.

OPTICS

Objective and projecting lens combinations which were found to be compatible for color microphotography are as follows:

(1) For magnifications of 25 to 150X, achromat objectives with huygenian projecting lenses.

(2) For magnifications from 150 to 500X, achromat objectives with hyperplane projecting lenses.

(3) For magnifications from 500 to 1000X, apochromat objectives with compensating lenses.

PHOTOGRAPHY

Since processing is done by personnel not familar with the objects photographed, a neutral color guide must be supplied. This is provided by including an exposure of the 111 plane of an electropolished, single aluminum crystal photographed under the same conditions as the subject. The negative is used to determine the color correction required during printing to provide an accurate color reproduction of the subject.

The use of the single aluminum crystal proved invaluable during the testing of lens combinations for quality of transmitted light when the procedure for color photography was being established.

For proper exposure, the ideal method is to run a series of test strips of the film that is being used. However, this is impractical where processing is done by another group. Black and white panchromatic film with an A.S.A. rating near that of the color film is used for test exposure purposes and the difference in rating between the films is extrapolated using an exposure meter as a guide.

POST IRRADIATION METALLOGRAPHIC LABORATORY AT GE-NMPO *

S. A. Leighton and E. W. Filer
Nuclear Materials and Propulsion Operation

The construction of the cell and equipment used in preparing irradiated materials for metallographic evaluation are discussed. The mounting, grinding, polishing, etching and photomicrographic procedures used in preparing the various metallic and ceramic materials are given along with representative results. The various pitfalls to be avoided are stressed. The methods used and the results obtained in replicating materials remotely for electron microscopic studies are discussed.

INTRODUCTION

The facility used in preparing irradiated materials for Metallographic evaluation at General Electric's Nuclear Materials and Propulsion Operation was constructed and the first specimens prepared in 1956. Since that time the facility or cell has been modified in order to more nearly meet the present program requirements, with the latest change being made in 1961. The following report covers the construction of the cell, a general description of the equipment and techniques used in preparing both metallic and ceramic material for metallographic evaluation, the methods used in replicating specimens for electron microscopy, and the various pitfalls that have been encountered along with some of the results.

DESCRIPTION OF CELL

The cell used for the metallographic evaluation of irradiated metallic and ceramic materials is located in the center of the room so that all sides are easily accessible, Figure 1. This cell was designed so that an operator limited to working in a radiation field of 2.5 millirems per hour could handle a Co^{60} radioactive specimen which had an activity sufficiently high to give a dose rate of about 330,000 millirems per hour at an unshielded distance of 6 inches. This cell was constructed of curved lead bricks 6 inches thick in order to minimize the danger of the operating personnel being exposed to stray radiation. The inside wall of the cell is lined with 3/4 inch steel boiler plate covered with a 1/16 inch sheet of stainless steel to facilitate cleaning and decontamination. This leaves an area 4 by 6 feet for all the equipment required for the metallographic preparation, including the metallograph. The floor is constructed

- - - - - - - - - - - -

* Published as General Electric Advanced Technology Series TM-63-5-9. Nuclear Materials and Propulsion Operation. Cincinnati: 1963. Etchants and polishing procedures are in a report which is available on request.

in the same manner as the walls, while the roof of the cell is covered with 4 inch thick interlocking lead slabs which are supported by 3/4 inch stainless steel plates. The four viewing windows in the cell are of high density leaded glass, 12 inches thick and the operation of the equipment in the cell is controlled from the large window shown in Figure 2. The cell is always kept at a negative pressure to prevent airborne contamination from spreading into the operating area. A lead lined drawer beneath the cell collects the liquid waste and is easily removed for waste disposal. Two loading ports provide for the insertion of specimens and the necessary materials for the metallographic preparation. The interior of the cell is illuminated by four 15 watt flourescent tubes and two individually controlled flood lamps. The working deck of the cell is one foot above the cell floor and is made in sections of 3/4 inch plywood covered with Textolite laminated plastic. Since the deck is divided into small sections that are easily removable, it is possible to make changes in the layout or add additional equipment to the cell as required. In the case of equipment failure, the defective unit is easily disconnected and the wood section containing the equipment quickly removed from the cell for repair or replacement. This type of installation minimizes radiation exposure to personnel effecting repairs.

The cell is serviced by a pair of Model No. 7 Master Slave Manipulators. Most of the equipment used throughout the cell is controlled from the panel located under the large viewing window, Figures 2 and 3. There are two quick disconnect boxes in the electrical circuits between the control panel and the equipment in the cell, one located outside the cell and the other under the deck inside the cell. This permits checking the operation of any equipment prior to placing it in operation in the cell, as well as checking equipment that has failed in operation. Water for washing and air for drying the metallographic specimens are controlled by foot operated solenoids. An air blower is also available for drying the specimens. There is a two inch thick lead shielded storage cave in the cell which has room for 90 specimens.

The radiation level in the room is monitored by 3 units. Fastened on the wall in back of the operator is an Eberline radiation monitor (model RM-1A). The top of the cell and waste storage drawer are monitored by Nuclear Measurements Corporation remote area monitors (models 715B and 715A).

DESCRIPTION OF EQUIPMENT

The location of the equipment in the cell used for the metallographic preparation and evaluation of irradiated material is shown in the schematic drawing, Figure 4. The materials for evaluation are sectioned in the Radioactive Materials Laboratory, then transferred to the cell using a small lead cask, Figure 5, and placed in the cell, Figure 6.

The drying oven, which has an automatic timer in the electrical circuit, is for curing the epoxy resin used in mounting the specimens. Buehler Automets and Syntron Polishers are used in grinding and polishing mounted specimens for metallographic evaluation. A sponge filter. Figure 7, is placed in the drain of the Automet polishing bowls to retain the solid radioactive waste in the cell rather than have it go into the waste drain drawer. Measured levels of radiation have shown 10 - 15 R/hr in the Automet bowl but less than 100 mr/hr in the waste drain drawer. The specimens are cleaned in the ultrasonic tanks between each step of the polishing procedure.

A Castle Manipulator (model M3500) is used to transfer the specimens to the stage of the Bausch and Lomb Research Metallograph. A photograph, Figure 8, shows the metallograph as it was remotized before installation in the cell. Variable speed d.c. motors have been installed in place of the manual controls on the X-Y translations of the stage. Illumination is supplied by a tungsten filament lamp, which is cooled by a separate air line, thus resulting in longer bulb life. Four objectives are on the turret of the metallograph, 8X, 20X, 41X, and 50X, giving a range for photomicrography of 50 to 1500 magnification. Specimens are examined and photographed using bright field, polarized and sensitive tilt illumination. Panatomic-X film is normally used without filters.

SAMPLE PREPARATION

If any specimens are to be mounted in Bakelite plastic, this is done prior to transferring, otherwise they are mounted in the metallographic cell, where an epoxy resin* is used. The specimen is placed in a prepared aluminum mold, 1-1/4 inches in diameter by one inch deep and covered with the epoxy resin, which is then cured overnight at 200°F. Shorter times can be used, but leaving them overnight is more convenient. The timer included in the electric circuit of the oven makes possible late afternoon casting with the unit automatically being shut down at a predetermined time. A numbered iron washer is placed on the back of the mount for identification and ease of handling.

In preparing the metallic samples, three grades of abrasive paper are used for rough grinding, α alumina (0.3 micron) and γ alumina (0.05 micron) are used for final polishings. The various abrasives, cloths, times and pressures for preparing metallic specimens are given in Table I.

- - - - - - - - - - - -

* Maraglas No. 655, Hardener No. 555 manufactured by Marblette Co., 37-31 Thirtieth Street, Long Island City 1, New York

TABLE I

PROCEDURE USED IN PREPARING IRRADIATED METALS FOR METALLOGRAPHIC EXAMINATION

Step	Equipment	Polishing Media Backing Material	Abrasive Size	Time Min.	Weight Per 1-1/4" Mount
1	Automet	SiC Paper	240	5	6 pounds
2	Automet	SiC Paper	240	5	6 pounds
3	Automet	SiC Paper	400	3	4 pounds
4	Automet	SiC Paper	600	3	4 pounds
5	Automet	αAl_2O_3 Billard	0.3μ	2	4 pounds
6	Automet	γAl_2O_3 Gamal	0.05μ	2	4 pounds
7	Syntron	$\gamma\ Al_2O_3$ Microcloth	0.05μ	30	350 grams

Water is the lubricant in all steps.

The procedure for preparing ceramics is modified slightly from that used for metals and is given in Table II. A better finish is obtained after grinding on a 400 grit silicon carbide abrasive paper than from a 600 grit paper. If a large amount of stock is to be removed from a specimen, a 240 grit abrasive paper charged with 45 micron diamond paste is used on the Automet. Using this procedure it is possible to remove approximately 1/8 inch of a 1/4 inch diameter BeO rod in 30 minutes.

TABLE II

PROCEDURE USED IN PREPARING IRRADIATED CERAMICS FOR CERAMOGRAPHIC EXAMINATION

Step	Equipment	Polishing Media Backing Material	Abrasive Size	Time Min.	Weight Per 1-1/4" Mount
1	Automet	Diamond Paste on 240 SiC Paper	45μ	10	6 pounds
2	Automet	Diamond Paste on 240 SiC Paper	45μ	10	6 pounds
3	Automet	SiC Paper	240	10	6 pounds
4	Automet	SiC Paper	400	15	6 pounds
5	Automet	Diamond Paste on Nylon Cloth	3μ	15	6 pounds
6	Automet	αAl_2O_3 - Nylon	0.3μ	15	6 pounds
7	Syntron	αAl_2O_3 - Microcloth	0.3μ	30-60	350 grams

Water is the lubricant except step 5 where Dymo-Thinner is used.

The Syntron Vibratory polishers are used mainly for touching up both the metallic and ceramic specimens after they are removed from the Automet holders and for repolishing after etching. A microcloth charged with a slurry of γ alumina (0.05 micron) for metals and α alumina (0.3 microns) for ceramics is normally used. The specimen holders for the Syntron polishers weigh approximately 350 grams.

All types of etching are carried out in the cell. Electropolishing is accomplished using the same set up as for electroetching. The specimens are cleaned between each operation using the ultrasonic cleaners. A number of the steps in the preparation of specimens are shown in Figures 9 and 10.

After completing the metallographic evaluation, the specimen is repolished and etched before trying to prepare a replica for electron microscopy. The specimen is held in the manipulator at an angle and the replicating solution flowed over the surface with an eye dropper and allowed to dry. Normally a 1% nitrocellulose solution is used in replicating metals. Ceramics are replicated with one mil cellulose acetate sheet softened in methyl acetate. Steam is directed on the specimen surface containing the replicating material until it is thoroughly fogged. The replica is stripped from the sample using scotch tape and passed out of the cell where it is checked for radioactive contamination. If there is contamination, the replica is discarded and a new one made. From here, the replica is handled in the normal manner for electron microscopy. Some of the steps in the preparation of a replica are shown in Figure 11.

DISCUSSION AND EXAMPLES OF WORK ACCOMPLISHED IN CELL

In the cell, as discussed previously, a large number of different types of irradiated metals, ceramics and cermets, have been prepared and evaluated using both optical and electron microscopic techniques. A few typical examples of the type of work performed are presented in the following discussion.

One of the difficulties encountered in ceramographic evaluation of materials was deciding whether damage occurred in sectioning and mounting or was actually caused under test conditions. A good example of the type of damage that can occur when mounting in Bakelite plastic is shown in Figure 12. Here, three sections of a hex tube are normally mounted with the outside faces touching in order to help in edge retention. In this case one of the tubes turned and in applying pressure the corners of the hex were forced against the faces of the adjacent tubes. As a result the two tubes were cracked starting at the point of contact. In this case it was right at the surface of the mount and the cause of the cracking could be readily determined. If this should happen back in the mount or in an area that was ground away, it would be almost impossible to determine the cause. For this reason all ceramics are mounted in an epoxy resin which requires no pressure in mounting. As you will note, there is good edge retention of all specimens without the necessity of using backup material.

Two segments of the same BeO rod, one unirradiated the other irradiated to 3.6×10^{20} nvt, at pile ambient temperature, were mounted in the same metallographic mount in order to receive identical handling. In the as-polished condition, grain boundaries are difficult to see in the unirradiated specimen but are quite noticeable in the irradiated segment, Figure 13. In addition, the irradiated specimen shows many large voids in the microstructure because of pull out in polishing. The large amount of pull out is related to the grain boundary separation which is the only observed radiation induced effect noted on BeO irradiated at realtively low (approximately 100°C) temperatures. In the low temperature irradiations the severity of this grain boundary separation increases with the neutron dose, until finally the damage to the microstructure becomes so great that the grains no longer cohere and the sintered rods crumble to powder. Replicas of these specimens were then prepared for electron microscopic studies and the results are shown in the electron micrographs, Figure 14. Figure 14a shows a typical as-polished, unirradiated BeO microstructure, containing both inter- and intragranular pores packed with polishing debris. A grain boundary traversing this micrograph is just barely visible due to relief polishing. Its presence is best established by the elongated intergranular pores in the upper half of the micrograph. Grain boundaries are quite readily visible in the irradiated microstructures, Figure 14b. This micrograph shows that the boundaries are open to such an extent that the replicating material has flowed into them, forming a dark ridge which casts a shadow on adjacent portions of the replica. In addition, the upper right hand corner of Figure 14b shows an area caused by pullout or loss of a grain which corresponds to the dark areas seen in the irradiated segment in Figure 13.

Considerable work has been done on the preparation of some of the precipitating hardening alloys for both optical and electron microscopy. A specimen of Rene 41 nickel base alloy which had been irradiated at 6×10^{19} nvt at 1200°F was polished and etched, Figure 15. Here we see large carbides and a grain boundary precipitate. A replica, which was prepared remotely in the cell, was then examined in the electron microscope. Here can be seen the grain boundary carbides ($M_{23}C_6$) and a gamma prime phase, $Ni_3(Ti,Al)$, in the matrix.

Another example of the type of work performed in the metallographic cell is preparing and evaluating cermet fuel elements. An example is a fuel element made by dispersing uranium dioxide in nichrome and then cladding with nichrome. Figure 16 shows a general view of the core of the fuel element and a 1000X magnification of a fuel particle. Figure 17 shows a cross section of a blister. As can be seen, our method of preparation gives us good edge retention and uniform polishing. Figure 18 shows the oxidation that has taken place in a refractory metal cladding after testing.

SUMMARY

A description has been given of the cell and equipment used in the metallographic preparation and analysis of irradiated materials. A few representative optical and electron micrographs have been shown to illustrate the type of results that have been obtained in using the facility and equipment.

ACKNOWLEDGEMENT

The authors wish to thank the personnel of the Metallographic Laboratory who assisted by preparing the unirradiated material and developing required techniques for metallography; R.C. Rau and J.P. Smith for performing the electron microscopy; H. Bodner who assisted in the design and construction of the cell; H. W. McLaughlin for technical assistance in the operation of the cell.

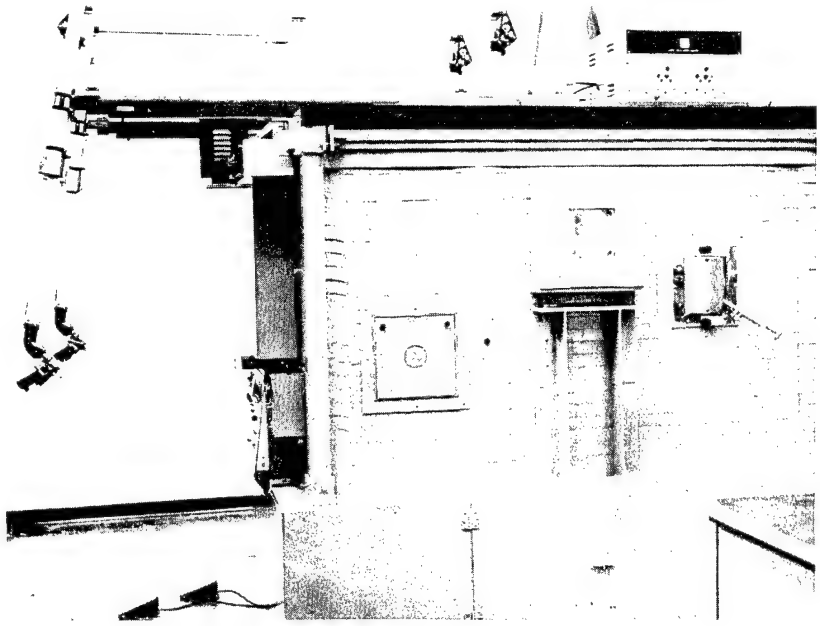

Figure 1. General View of the Cell Used in the Metallographic Preparation and Analysis of Irradiated Materials.

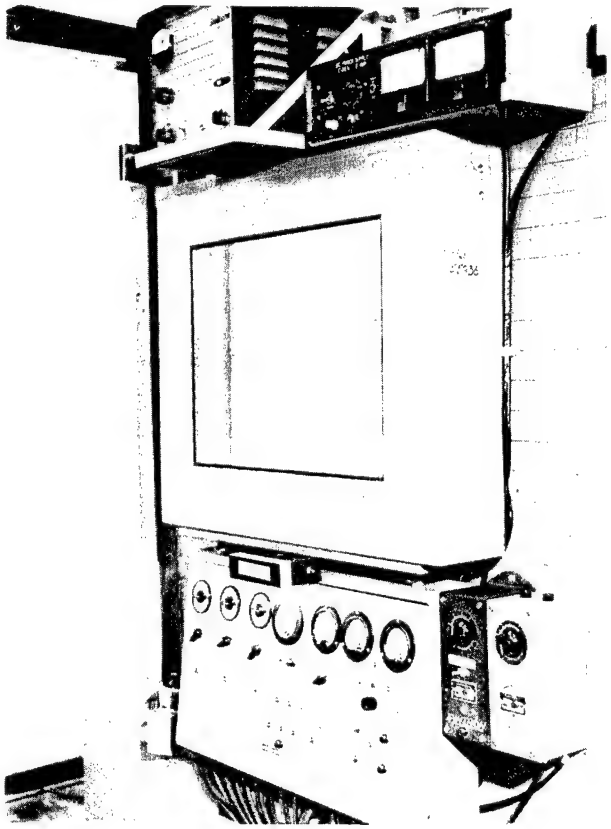

Figure 2. The Operator's Side of the Cell Showing the Large Viewing Window and the Control Panel.

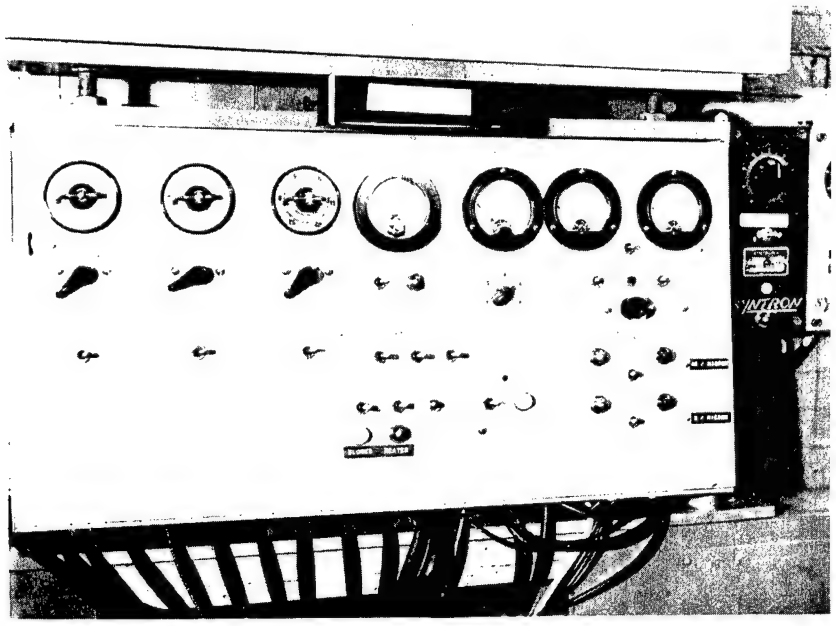

Figure 3. Panel for Controlling Equipment Used in the Metallographic Preparation of Samples of Irradiated Materials.

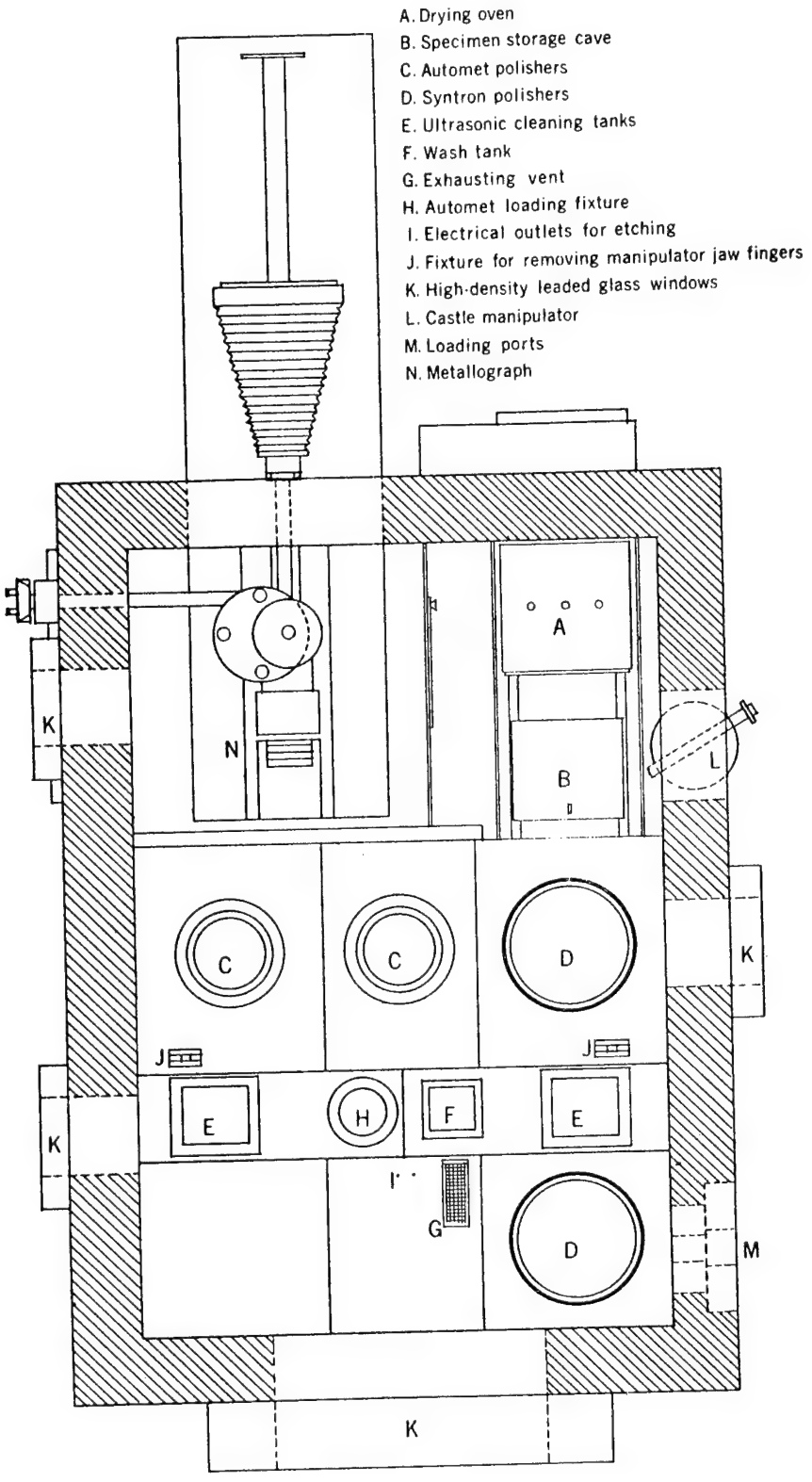

Figure 4. Schematic Showing the Arrangement of the Various Items Used in the Metallographic Preparation and Analysis of Irradiated Materials.

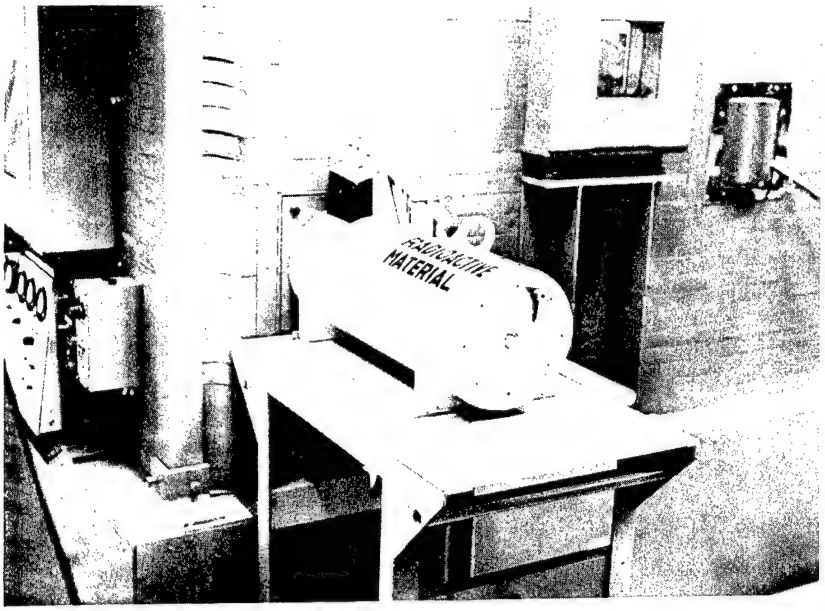

Figure 5. Transfer Cask in Position at Loading Port for Moving Samples into Cell.

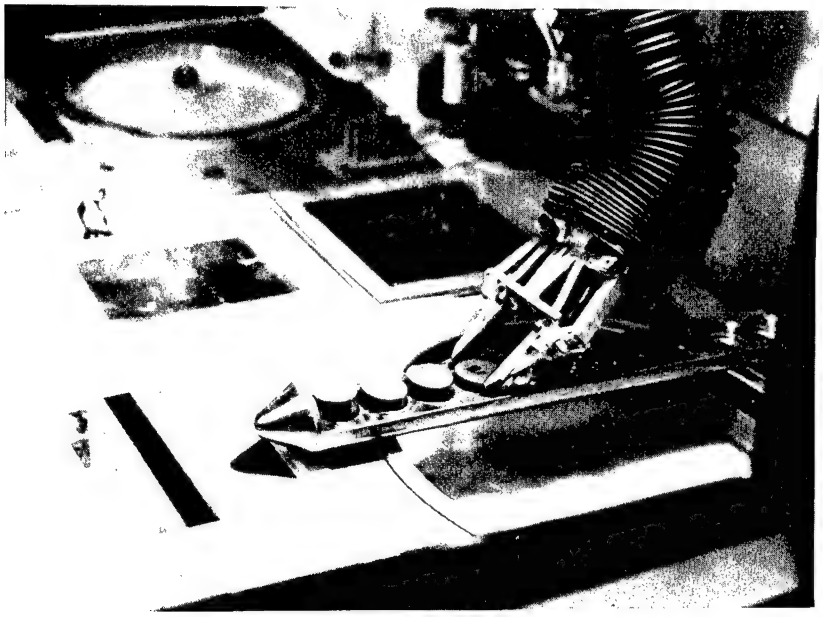

Figure 6. Specimens in Sample Carrier of Transfer Cask After Being Moved Through the Loading Port into Cell.

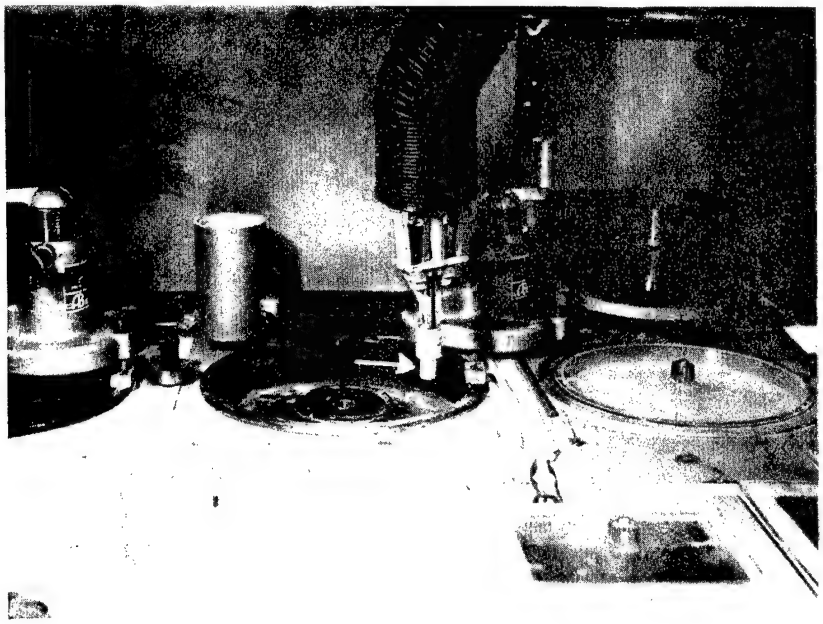

Figure 7. Sponge Filter (arrow) Used in the Drains of the Polishing Bowls to Retain Contaminated Waste.

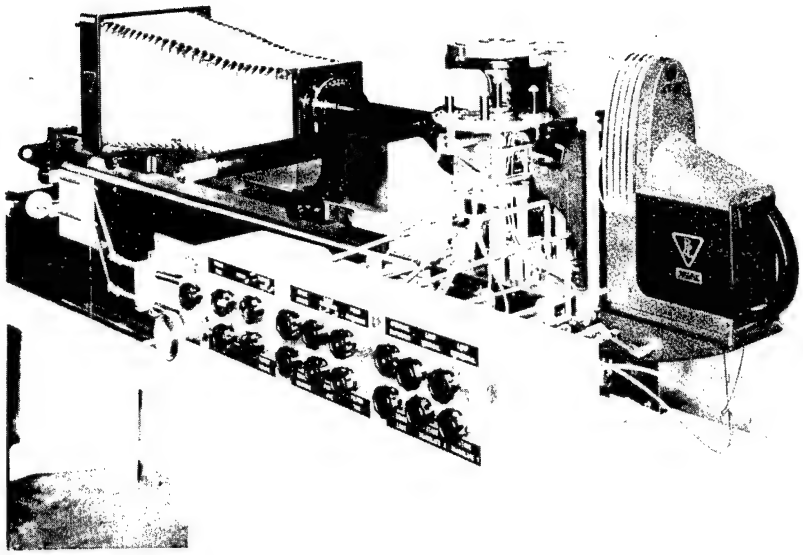

Figure 8. B and L Research Metallograph as Modified for Remote Operation Prior to Being Placed in the Cell.

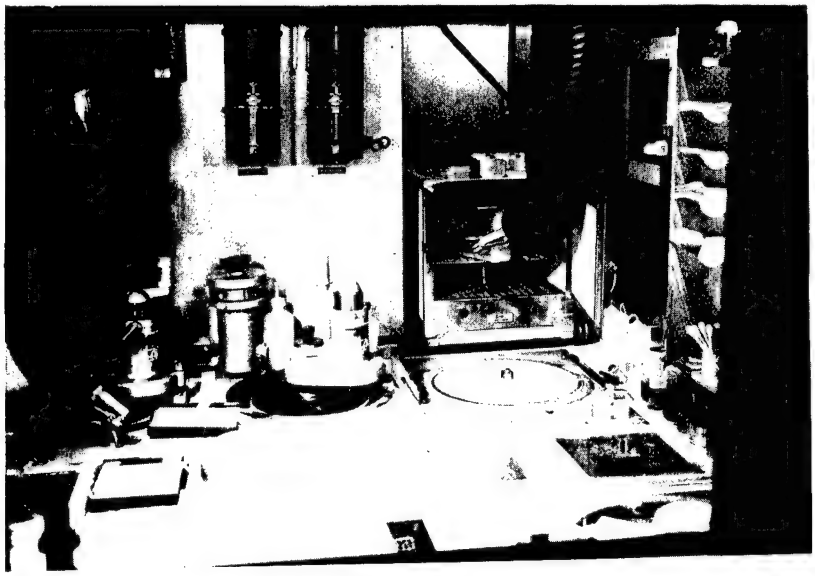

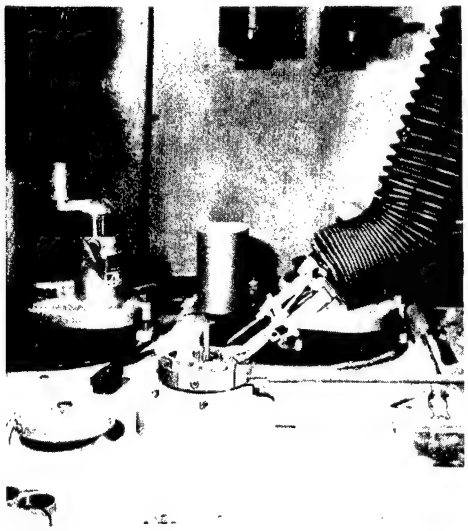

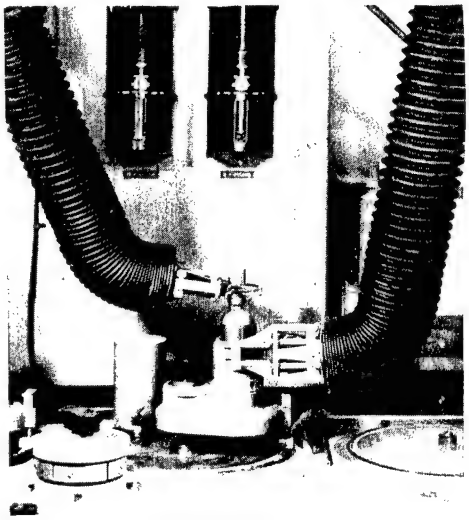

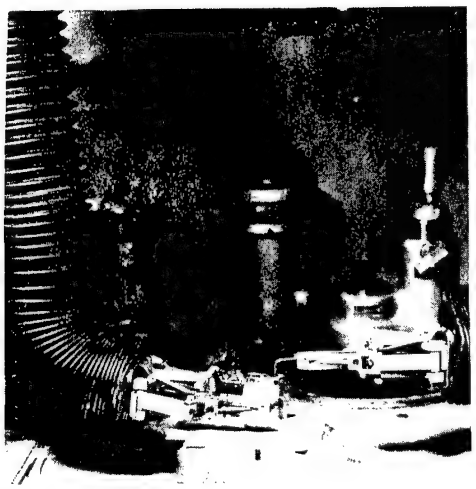

Figure 9. Top - Equipment in Cell as Viewed Through Large Window.
Middle- Specimen Holder and Automet Polisher.
Bottom- Specimen Weight and Syntron Polisher.

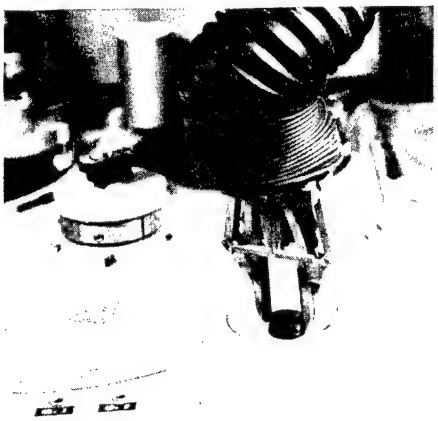

Immersion

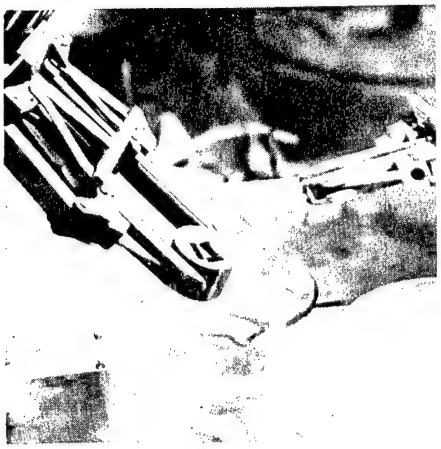

Swab

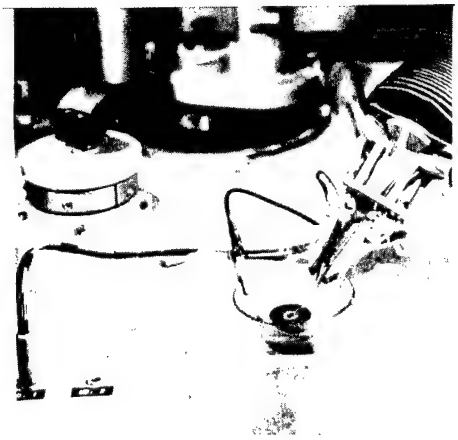

Electrolytic

Figure 10. Shows how the Various Types of Etching are Handled Remotely.

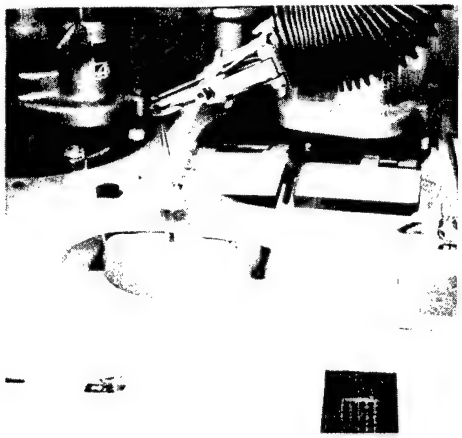

Applying replicating solution

Applying moisture before stripping replica

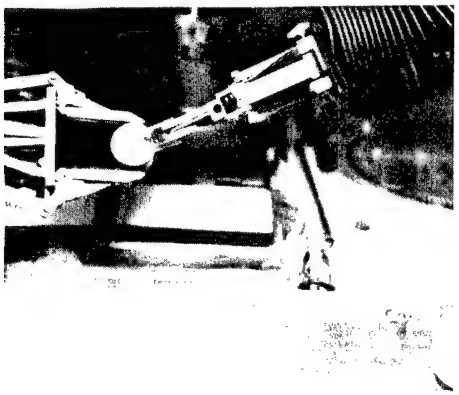

Stripping replica from specimen

Figure 11. Various Steps Used in Replicating a Specimen for Electron Microscopy.

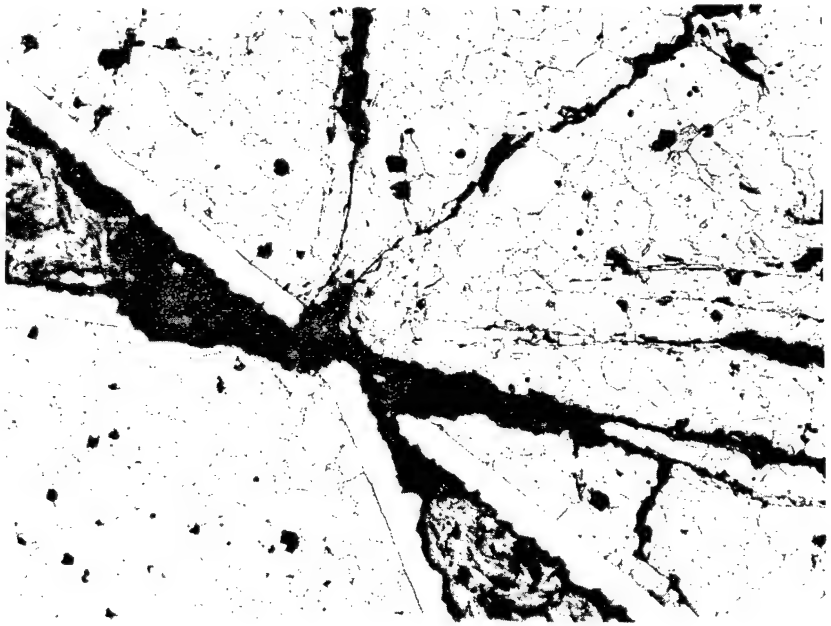

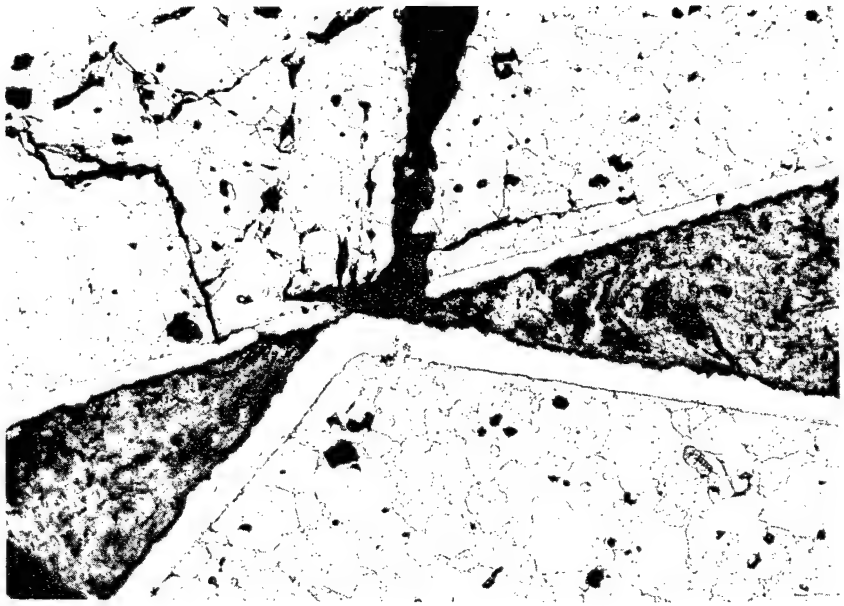

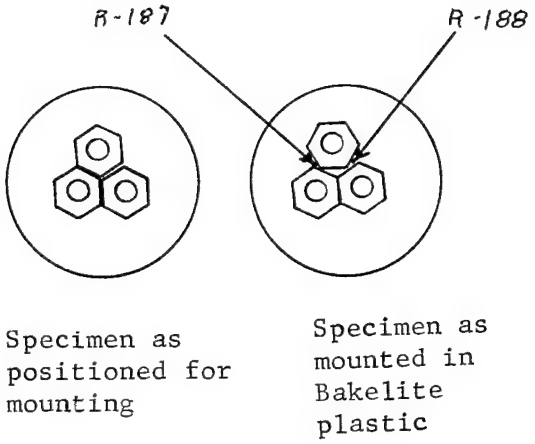

Figure 12. Photomicrographs and Schematic of the Mount Showing the Effects of Pressure on Ceramic Hexes that were Turned in the Process of Mounting in Bakelite Plastic. As polished 100X.

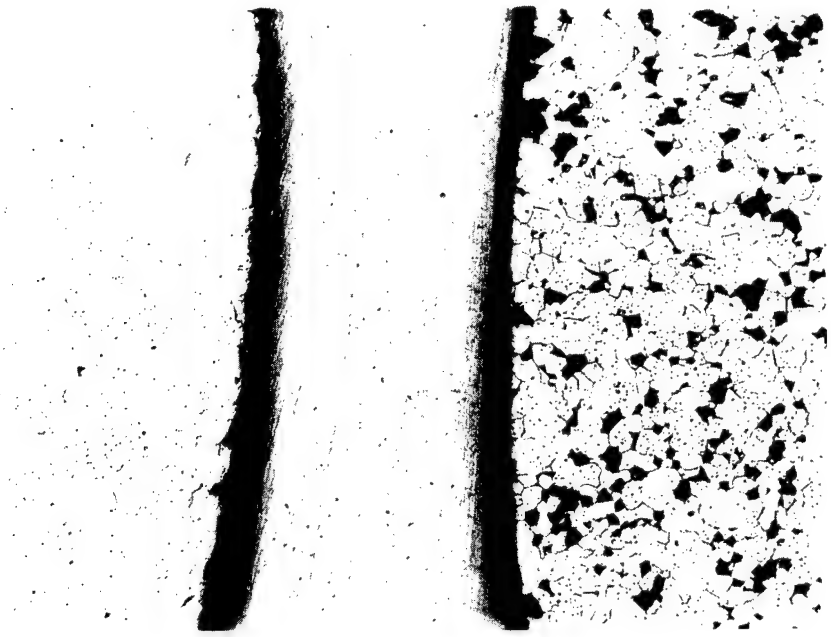

(a) Unirradiated (b) Irradiated 3.6×10^{20} nvt at 100°C

Figure 13. Optical Micrograph of Unirradiated and Irradiated BeO Rod in the Same Mount. As polished 100X.

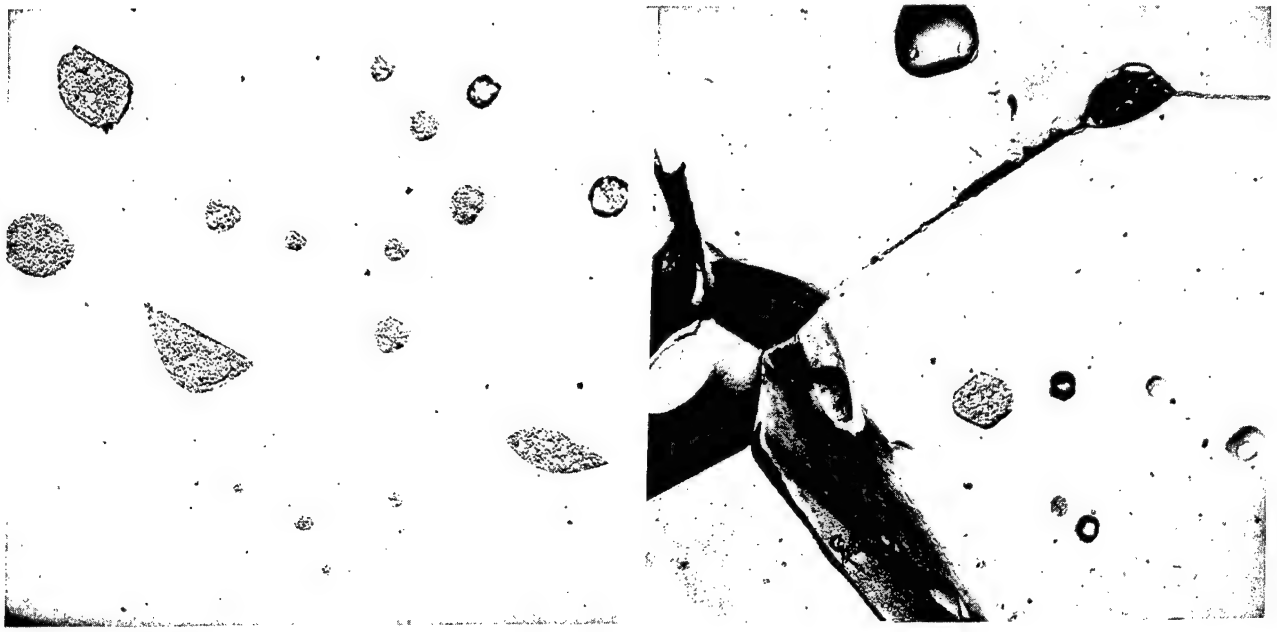

(a) Unirradiated (b) Irradiated

Figure 14. Electron Micrographs of BeO Rod as Seen in Figure 13. As polished. 3200X.

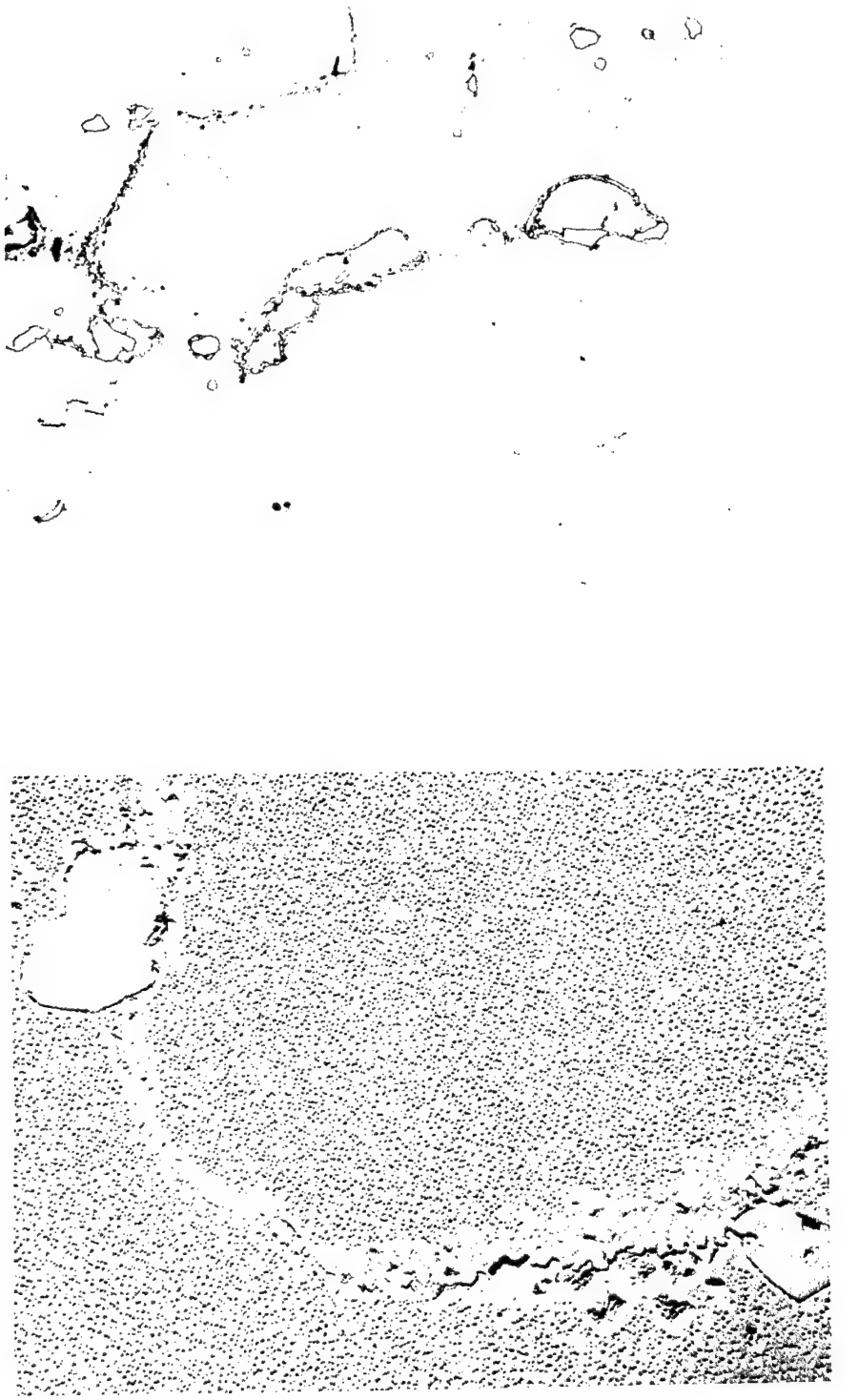

Figure 15. Rene 41 Nickel Base Alloy Irradiated at 6 x 10^{19} nvt, 1200°F.

Top - Optical Micrograph, 500X, Etch-Marbles.
Bottom - Electron Micrograph, 4600X, Etch-Marbles.

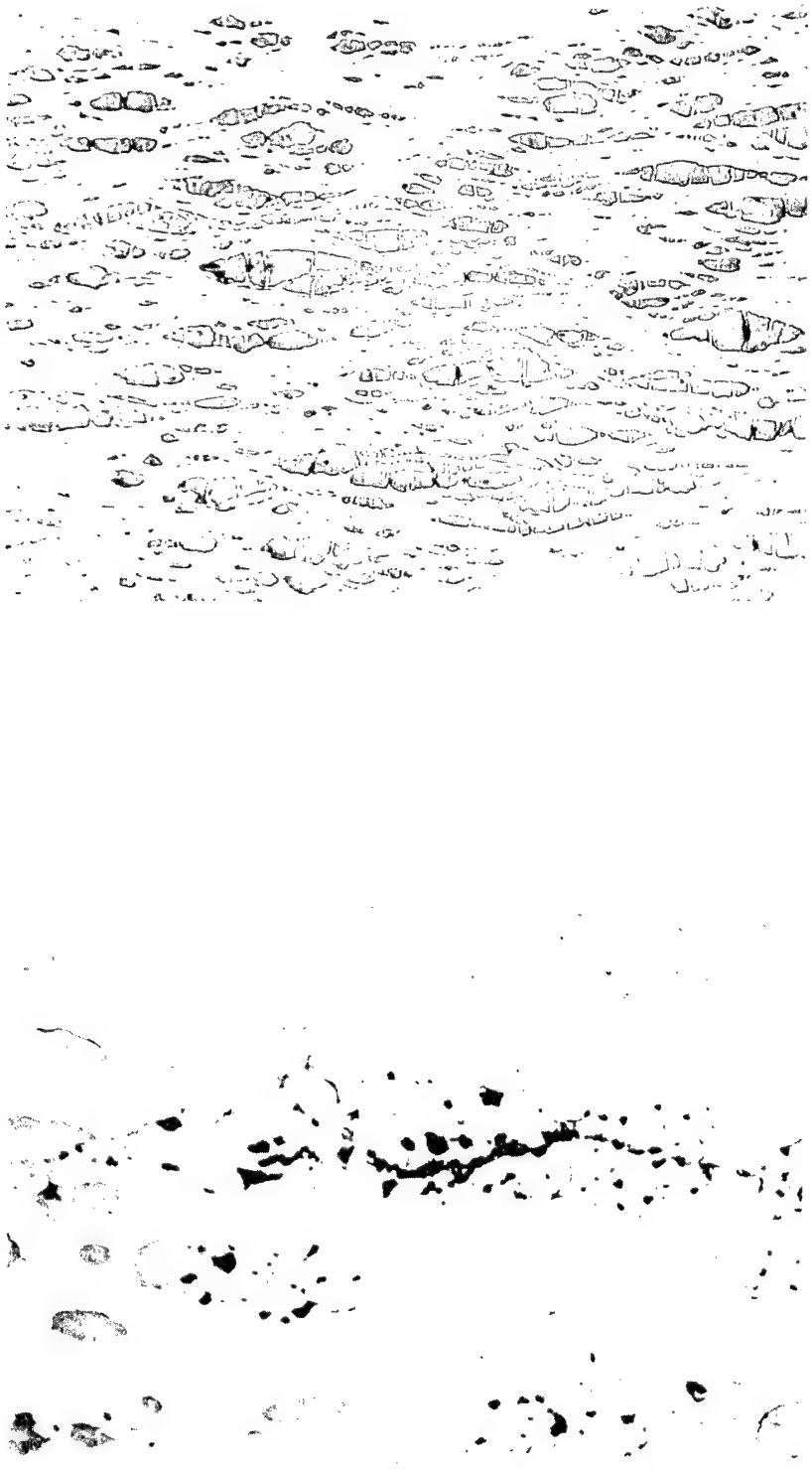

Figure 16. Modified 80 Nickel, 20 Chromium - UO_2 Fuel Element. As polished.

Top - 250X
Bottom - 1000X

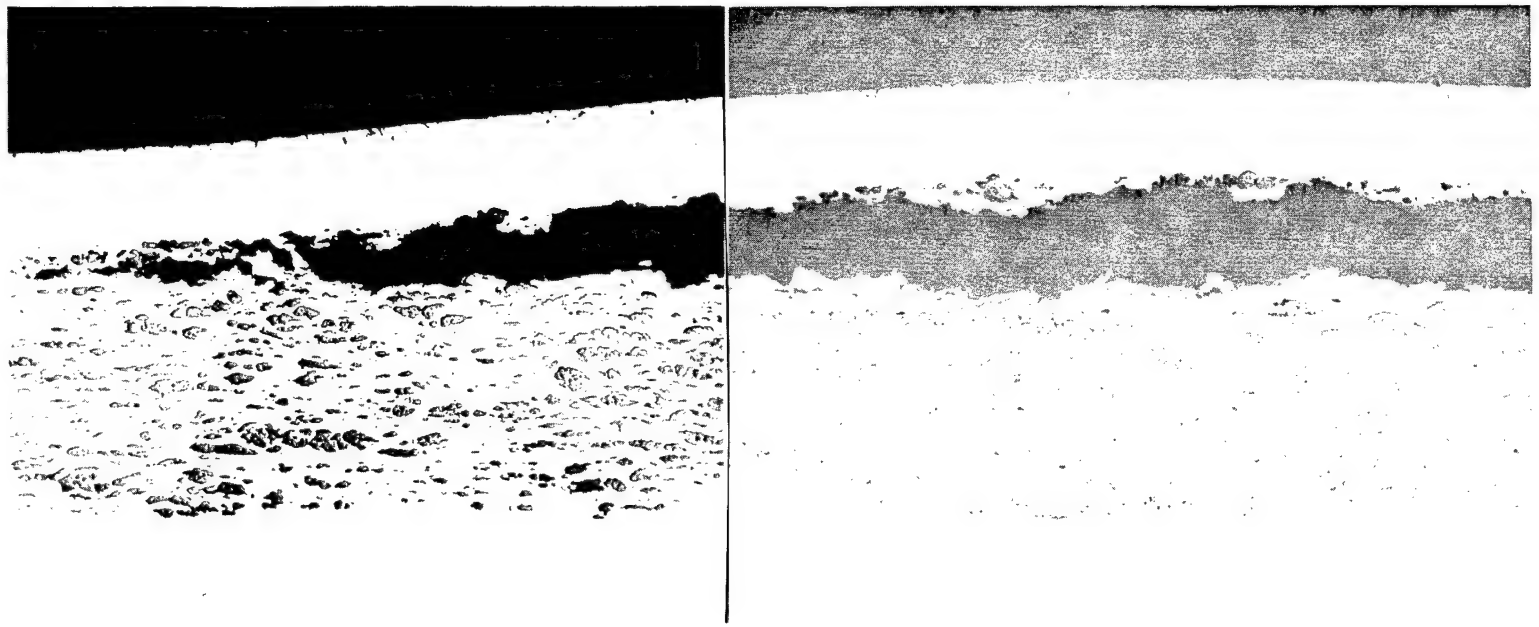

Figure 17. Cross Section of a Blister in a Modified 80 Nickel, 20 Chromium - UO_2 Fuel Element Showing How Well Our Polishing Procedures Retains the Edge and Fuel Particles in the Core. As polished 100X.

Figure 18. Photomicrograph of a Refractory Clad Fuel Element Showing Good Fuel and Edge Retention. As polished. 75X.

USE OF AUTORADIOGRAPHY IN MICROSAMPLING OF IRRADIATED CERAMIC FUEL ELEMENTS

R. Teats
Hanford Atomic Products Operation

The article describes a new technique for making autoradiographs of irradiated ceramic elements using photographic plates. The autoradiograph shows in good detail the distribution of fission products and is used in accurate micro sampling of the element.

INTRODUCTION

Autoradiography is proving to be a useful tool in the examination and sampling of irradiated ceramic fuel elements. During high temperature irradiations ceramic materials undergo physical changes, and the fission products formed migrate throughout the core. It is essential for a good understanding of fuel element performance to know the extent of fission product migration and segregation during irradiation. Autoradiographs used in conjunction with microsampling techniques provide samples by which analysis can be made.

DESCRIPTION OF THE PROCESS

Autoradiography is the process by which an irradiated, or radioactive, material takes its own picture on a nuclear emulsion by virtue of its internal energy. Fission products give off radiant energy in the form of alpha, beta, and gamma rays, all with various energy levels depending on the irradiation received and the length of the decay period. Different kinds of emulsions can be used to make autoradiographs depending upon the type of radiation emitted by the material.

For autoradiographing irradiated ceramic material, beta sensitive, high resolution plates made by Eastman have worked very well. The high resolution emulsion has an extremely fine grain size of only one-tenth micron and is insensitive to gamma activity. The method of using these photographic plates for making autoradiographs of irradiated ceramic fuel elements was originally developed at the General Electric Vallecitos Laboratories. The techniques used to apply this method at Hanford have been changed, largely because of differences in equipment and operating conditions. The autoradiographs have been used primarily in the macro-examinations of ceramic materials to determine how fission products migrate and to aid in the microsampling of finite areas in the samples.

Ideally, the best autoradiographs are made by placing the sample directly on the sensitized emulsion. This presents several problems, especially since the entire operation must be done remotely in a hot cell. First, the equipment needed to introduce the plate into the cell, handle it remotely in the dark along with

the sample, and then remove the exposed plate in a light type container is necessarily complicated and difficult to use. Secondly, the danger of spreading contamination which is picked up on the plate emulsion to the outside of the cell is a serious problem and one that is difficult to control.

To get around these problems, a plan was devised to expose the plate through a thin opaque sheath that would still adequately transmit most of the beta radiation. Both aluminum foil and aluminum coated Mylar have been used successfully; however, Mylar has the advantage of being more flexible and slightly thinner. Mylar coated on both sides with aluminum is only 0.0005 inch thick and permits almost intimate contact of the sample with the emulsion. The closer the sample is to the emulsion, the better definition attained because of the smaller amount of scatter.

The procedure followed is to wrap the high resolution plate in Mylar forming a light type packet. The plates are relatively insensitive to light and may be handled under a safe light. The enclosed plate is introduced into the hot cell and the prepared sample is placed on the plate. The sample has been polished previously by standard metallographic procedures to a flat surface. Ceramic samples are usually mounted in an epoxy resin which also acts as a binder to help hold loose particles in place.

The exposure time varies from one minute to several hours depending on the irradiation received and the age of the sample. The required exposure time can be estimated by monitoring the sample for gamma activity. Most of the samples processed at the Radiometallurgy Laboratory at Hanford have required exposures of less than five minutes.

Improved definition is attained by attaching a weight to the sample that will press out any wrinkles in the Mylar screen.

As soon as the packet containing the exposed plate is removed from the cell, it is covered with a layer of masking tape which confines all the loose contamination on the outside of the packet. The plate can now be safely removed for a standard developing process without any danger of contaminating the dark room and other noncontrolled areas. The plate itself is clean and can be safely handled during subsequent enlargements and reproductions. The problem of contamination control is very important because ceramic materials are often cracked and subject to spalling. The average radiation reading from loose particulate contamination on the packet as it is removed from the cell is 10 mrad and occasionally is as high as 50 mrad.

Microdrilling equipment has been developed for remote microsampling of both metallic and ceramic materials. The method of sampling consists of drilling out a minute portion to be analyzed, collecting the resulting chips by vacuum on a plastic filter disk, transferring the filter together with the chips for analysis by microchemistry or other methods.

The sampling equipment is mounted on a plug so that components can be removed easily from the cell for maintenance. Major components include a specimen positioner, a precision spindle, a vacuum sample collector, an air motor, and a macroscope. Design of the equipment includes provisions for read-out of sampling locations, remote changing of drills, remote replacement of filters, magnified visual control of the drilling operation, and micrometer control of drill in-feed.

Two types of drills have been used for sampling; one is a twist drill and the other is a diamond drill made by bonding diamond dust to the tip of a small wire. Both high speed steel and tungsten carbide twist drills are used to sample materials below Rockwell C-65 hardness. The diamond drills are used to sample ceramic or other materials above Rockwell C-65 hardness. Drilling speeds vary from 2500 to 7000 rpm depending on the material being sampled and the type and size of drill used. The lower speeds are used for twist drills while a speed of 7000 rpm is best when sampling irradiated UO_2 with a diamond drill.

Material removed by the drill is picked up with a vacuum probe and deposited on a 0.8 micron mean pore diameter plastic filter disk. Sample weight may be controlled by varying the drill size or hole depth so that the mass of material necessary for quantitative analysis may be obtained. Drilling of hard ceramic materials with a 0.014 inch diameter diamond drill is possible, but sintered material that is badly cracked or has been impregnated with an epoxy resin is best sampled with a 0.020 inch drill. A UO_2 sample 0.020 inch diameter by 0.010 inch deep is large enough for quantitative analysis by microchemistry.

ONE-STEP REPLICATION IN THE HOT CELL

F. E. McGrath
Battelle Memorial Institute

A technique for obtaining replicas from irradiated material for direct examination is described. The use of this method represents considerable savings of time as compared to the triple replication technique.

INTRODUCTION

Metallography is regarded as one of the more useful tools in the studies of radiation effects. Since the finer details of structure cannot be resolved by light microscopy, the use of electron microscopy is sometimes necessary. Replication of irradiated materials is complicated by two factors not encountered in "cold" replication. These are: (1) the replication must be performed using manipulators and (2) particles of radioactive material may be removed from the specimen when the replica is removed. These complications have been eliminated in the past by use of a triple replication technique, which is effective but time consuming. It has been found that a direct replication method can be used on irradiated materials which do not contain fission products. Direct replication results in time savings, while yielding replicas which are equivalent to those obtained by triple replication.

TRIPLE REPLICATION METHOD

The triple replication procedure utilized in hot cell operations is as follows:

(1) A thick sheet of cellulose acetate is softened in acetone and placed on a metallography prepared specimen.

(2) After a drying period of 30 min. to 1 hr., the sheet is stripped from the specimen and removed from the hot cell. Additional strippings may be made if the first is highly radioactive or if a higher quality replica is desired.

(3) The first replica is then replicated by applying a collodion, amyl acetate solution. When dry, the replica is stripped and shadowed with platinum.

(4) A thin carbon film is deposited, by evaporation, over the platinum.

(5) The collodion is dissolved leaving a thin carbon film with platinum shadowing.

REMOTE DIRECT REPLICATION

For hot cell replication of metallographic samples which do not contain fission products the direct replication method can be used to advantage.

The direct method is as follows:

(1) Several drops of collodion or parlodion thinned with amyl acetate are applied to the specimen using an eye dropper. In several minutes the solution dries, leaving the specimen coated with a thin layer of collodion or parlodion.

(2) A 200-500 mesh, stainless steel grid is placed on a piece of Scotch tape. The tape and grid are firmly applied to the specimen. The tape is then stripped off with the grid and the collidion or parlodion replica.

(3) The replica is removed from the hot cell and shadowed.

Although this method does represent a time saving compared to the triple replication method, there are two problems encountered which require skill on the part of the hot cell operator. First, in order to insure that the stainless steel grid adheres to the replica, it is necessary to apply a slight amount of moisture. Normally this is done by breathing on the collodion layer. In the hot cell the moisture must be applied with a vaporizer, and thus involves a certain amount of trial and error.

Second, the application of the Scotch tape and grid, so that the grid is positioned at the proper location on the specimen, requires a skilled hot cell operator.

PREPARATION AND RESULTS OBTAINED ON INCONEL X AND A286

Irradiated specimens of Inconel X and A286 were prepared for replication and electron microscope examination in the following manner: Bakelite is used for mounting, rather than an epoxy resin which will react and soften when in contact with the solvents used in replication. The mounted specimens are ground on a Buehler Automet using progressively 240, 400, and 600 grit SiC paper.

Polishing is performed on Syntron vibratory polishers covered with Microcloth. They are polished for 1 hr. on 1 μ alumina, 2 hr. on Linde A and 2 hr. on Linde B. Since cold working of the specimen surface is sometimes noticeable upon examination, a final electropolish is performed using a 20 per cent perchloric-ethanol bath. Althouth the electropolishing step gives a more distinct structure, rounding of the carbides and some pitting occurs.

The specimens are etched by dipping in a solution of 92 per cent HCl, 5 per cent H_2SO_4, and 3 per cent HNO_3. This etch deteriorates quickly and is effective for about 15 minutes after mixing. Replicas are then made and examined in the electron microscope.

Examples of the electron-micrographs obtained are shown in Figures 1-6. Figure 1 shows the unirradiated microstructure of A286, and Figures 2 and 3 show the irradiated structure as produced by triple and direct replication, respectively. No significant microstructural difference is noted between the irradiated and unirradiated material. Figure 4 shows the microstructure of Inconel X in the unirradiated condition, and Figures 5 and 6 are electron-micrographs of the same material after irradiation as shown by triple and direct replication techniques, respectively. Comparison of the irradiated and unirradiated structures shows that irradiation is responsible for the depletion of the gamma prime phase near the grain boundaries (Figure 6). The depletion of the gamma prime phase near carbide particles also occurs on irradiation of Inconel X (Figure 5).

ACKNOWLEDGEMENTS

The author wishes to acknowledge the direction and assistance of Dr. John Radavich of Purdue University.

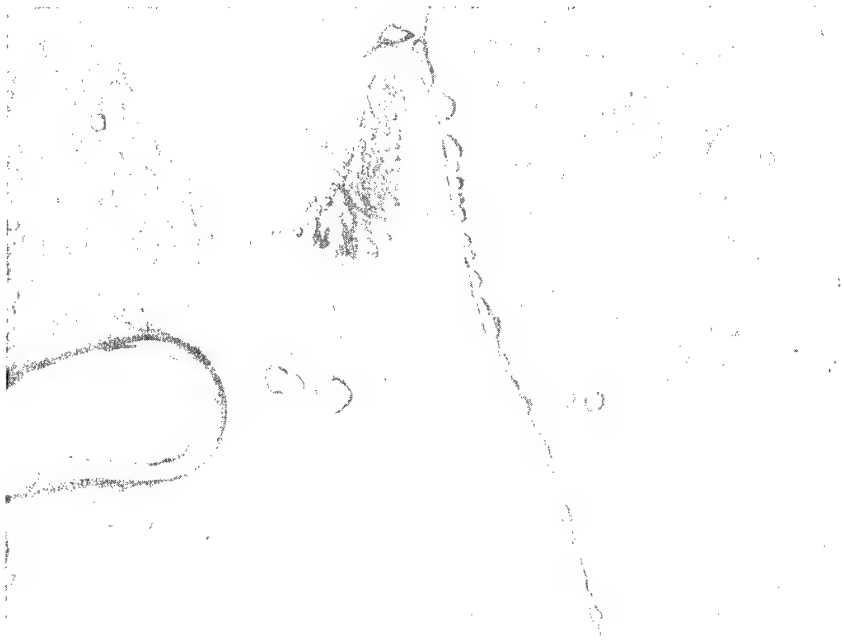

Figure 1. A286 - Unirradiated. 10,000X.

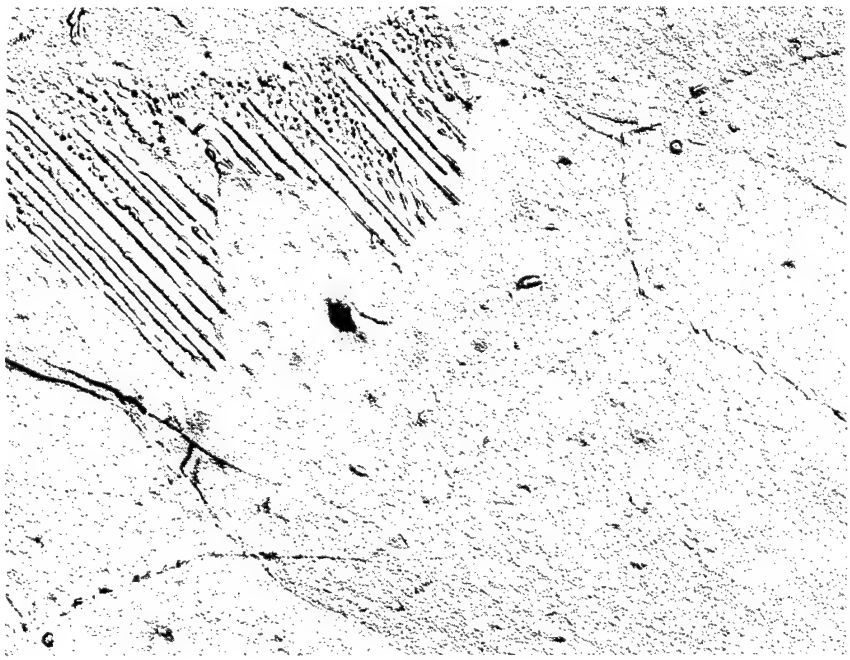

Figure 2. A286 - Irradiated to $\sim 2 \times 10^{20}$ nvt at Ambient Temperatures. Triple replica technique used to obtain a carbon-platinum positive. 8,750X. J1451.

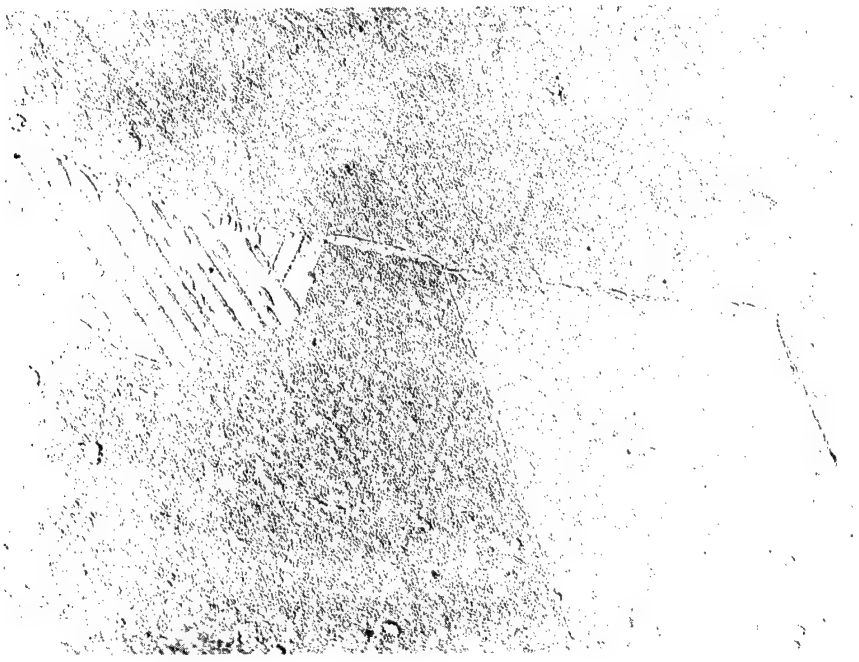

Figure 3. A286 - Irradiated to $\sim 20 \times 10^{20}$ nvt at Ambient Temperatures. Direct replica. 10,000X.

Figure 4. Inconel X - Unirradiated. 10,000X.

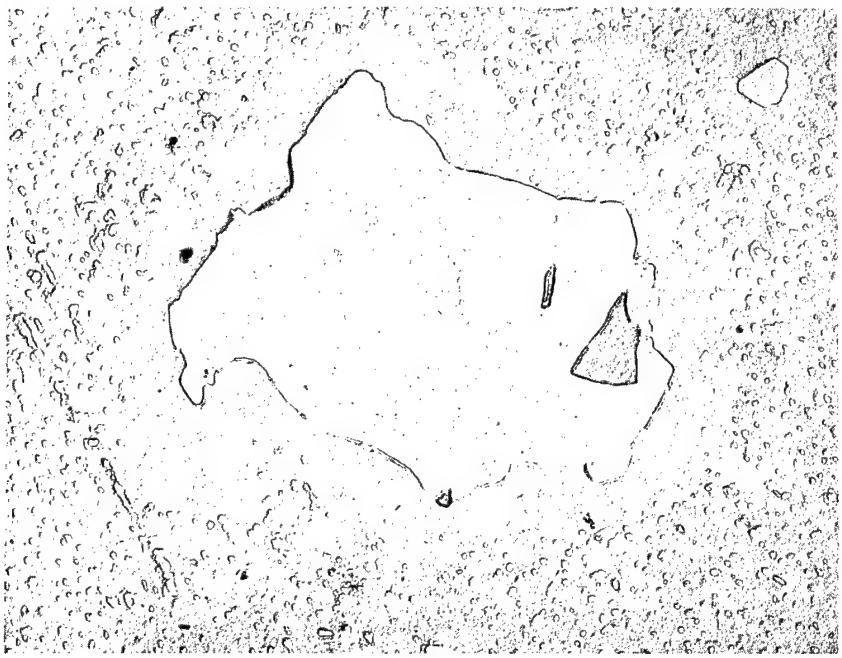

Figure 5. Inconel X - Irradiated $\sim 2 \times 10^{20}$ nvt at Ambient Temperatures. Triple replica. 8,750X. J1614.

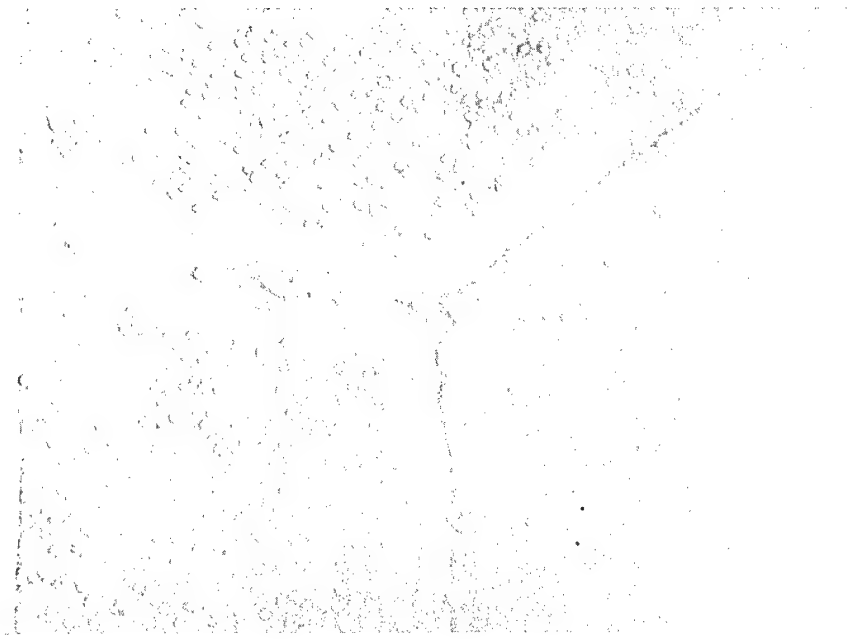

Figure 6. Inconel X - Irradiated $\sim 2 \times 10^{20}$ nvt at Ambient Temperatures. Direct replica. 10,000X.

REPLICATION OF MICROSTRUCTURES USING SILICONE * RUBBER AND EPOXY RESIN

R. S. Crouse
Oak Ridge National Laboratory

INTRODUCTION

The introduction of room-temperature and low-temperature vulcanizing silicone rubber a few years ago has resulted in many interesting and novel ideas on the part of materials people. These substances are liquid or paste-like semi-solids that can bemade to solidify into flexible solids by the addition of a chemical catalyst. While in the uncured state the silicone rubbers can be poured like syrup or spread like thick jam or peanut butter and will conform to the surface to which they are applied. After curing, which may take several hours or only minutes, depending on the rubber and its catalyst, the rubber releases readily, leaving a near perfect impression of the surface.

Silicone rubbers are available from many different suppliers, Dow-Corning, General Electric, Union Carbide and Hysol, to name a few; and exhibit widely varying properties. They are available with properties to suit practically any use one might find for them.

Replication of surfaces using silicone rubber was first used at Oak Ridge National Laboratory by R.E. McDonald(1) of the Metals and Ceramics Division. McDonald's application involved surfaces on a macro scale but his success pointed to more sophisticated endeavors on a micro scale. M.L. Picklesimer, also of the Metals and Ceramics Division, has demonstrated the feasibility of microstructural replication in the case of Zircaloy-2, as shown in Figure 1.

Following the lead of McDonald and Picklesimer, the Metallography Group has developed a technique of replication which gives quite good results. This report describes the technique and gives some examples of the application.

PROCEDURE

For replication of microstructures, three properties are important. They are (1) low viscosity for penetration into all surface irregularities, (2) rapid cure and (3) low shrinkage to minimize replica distortion. The silicone rubber chosen by the Metallography Group was LTV-602 manufactured by General Electric. This rubber is water white with a room-temperature viscosity of 800-1500 centipoises, about the same as glycerin. It cures in 1 to 2 hr at 65°C or overnight at room temperature.

- - - - - - - - - - - -

* The etchant used for this procedure is described in Appendix A to this publication, page 158.

A polished and etched metallographic specimen is wrapped in clear acetate sheet so the polished surface forms the bottom of a hollow cylinder about an inch deep. The catalyst is mixed with the LTV-602 in the amount of 0.5% by weight in a small paper cup. After mixing thoroughly, the catalyzed rubber is degassed in a vacuum to remove air entrapped in mixing. After the initial frothing has subsided the mixture is removed from vacuum and poured over the polished specimen to some convenient depth such as 3/8 in., see Figure 2. Curing of the rubber takes place under a heat lamp in about 1 hr.

When the rubber is sufficiently cured to withstand handling, the specimen is removed and the rubber negative replica becomes the bottom of the cylinder. This cavity is filled with epoxy resin, (2) as in Figure 3. After the resin sets up in place, the two replicas are separated as in Figure 4, and the epoxy positive is metal coated by vacuum deposition. Figure 5 shows the original specimen, the rubber negative and the metallized positive replica. In this case, the deposited metal is platinum, but may be aluminum, copper or any convenient metal or alloy.

Figure 6 (a and b) shows the effect of too heavy a metal coating. The original specimen here was a piece of type 304 L stainless steel which has been exposed to brine for a number of hours at high temperature. Notice the "orange peel" effect on the replica and loss of detail. Aluminum also has a tendency to introduce other artifacts as shown in Figure 8 (a and b).

This figure is a comparison of the INOR-8 in Figure 6 with an aluminized replica. Notice what appears to be extra precipitation in the replica. This may be bits of aluminum oxide from the wire used in metallizing.

Figure 1 shows the use of copper as a metallizing material, which produces a better surface than aluminum, relatively free from artifacts. Neither copper nor aluminum gives as good a surface as platinum, which is illustrated in Figure 6.

This technique is useful in cases where progressive changes in the microstructure of a single specimen need to be preserved. A case in point is the study of the development of slip systems and grain nucleation and growth in deformed Cb single crystals as a result of deformation and subsequent heat treatment (Figure 9). Other cases might be in the metallography of toxic and radiological materials in glove boxes where direct microscopic reviewing is difficult. Technetium and plutonium are examples of materials in this category. Thorium carbide is a material that is extremely reactive, which, if compatible with the rubber, might be replicated for later leisurely examination. So far, replication of hot or reactive metallographic samples by this technique has not been attempted, but the success of McDonald in his work leads one to the opinion that it should be successful. Some questions may remain to be answered but the technique definitely has promise.

REFERENCES

1. R. E. McDonald, B. W. McCollum, G. A. Moore, "Replication of Surface for Hot Cell Application", Proceedings Conference, Hot Lab Equipment Conference, ANS, Chicago Illinois, 1961.

2. Araldite 502, Ciba Products Company, Fairlawn, New Jersey.

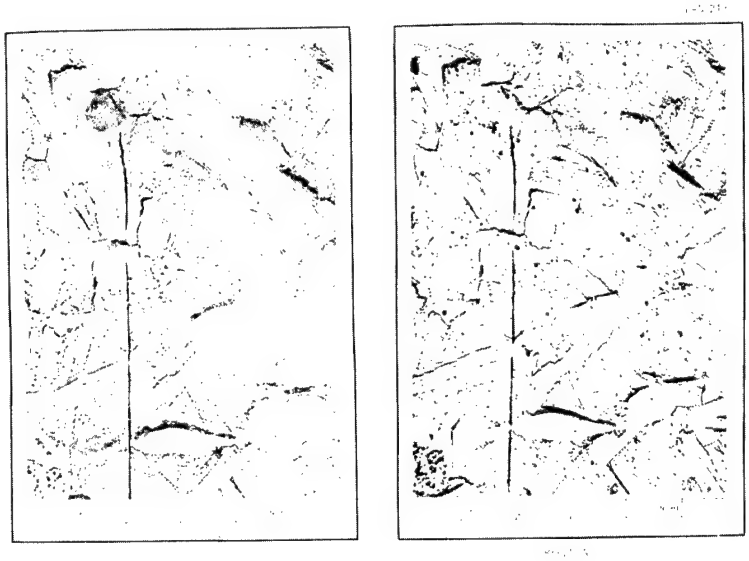

Figure 1. Original and Replica of Zircaloy-2 Microstructure. Y-50213.

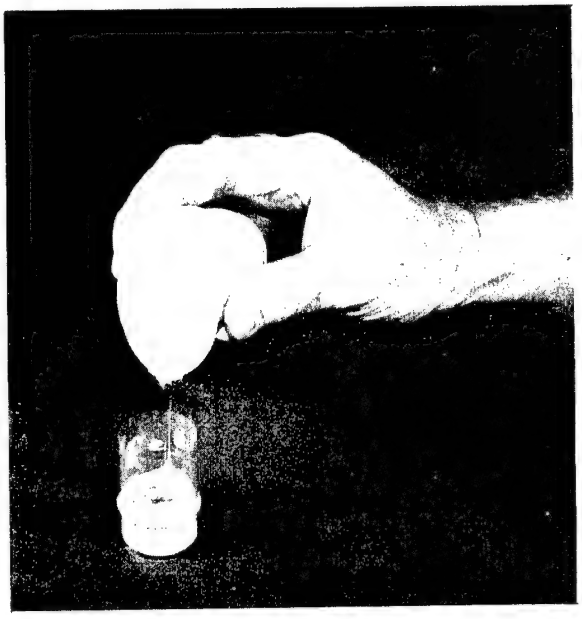

Figure 2. Pouring Rubber Over Polished Specimen. Y-50522.

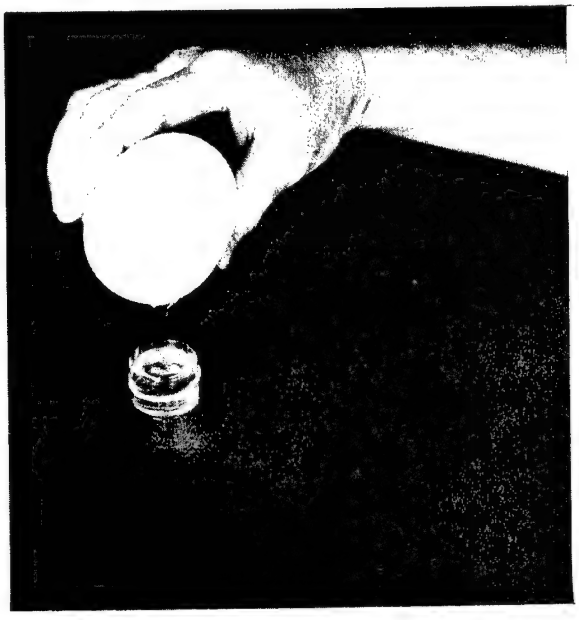

Figure 3. Epoxy Resin Being Poured Over Rubber Negative Replica. Y-50520.

Figure 4. Separating Replicas. Y-50519.

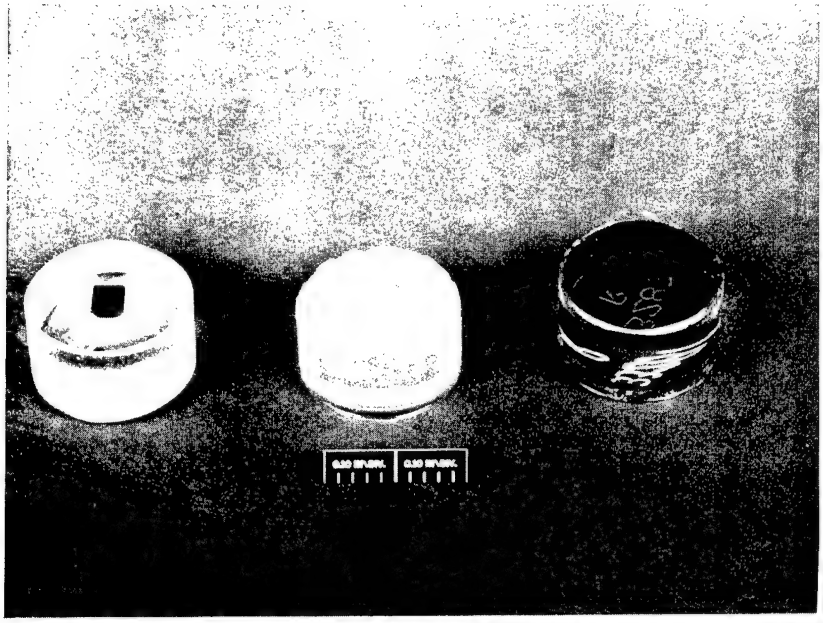

Figure 5. Original Specimen, Rubber Replica Metallized Epoxy Resin Positive Replica. Y-50521.

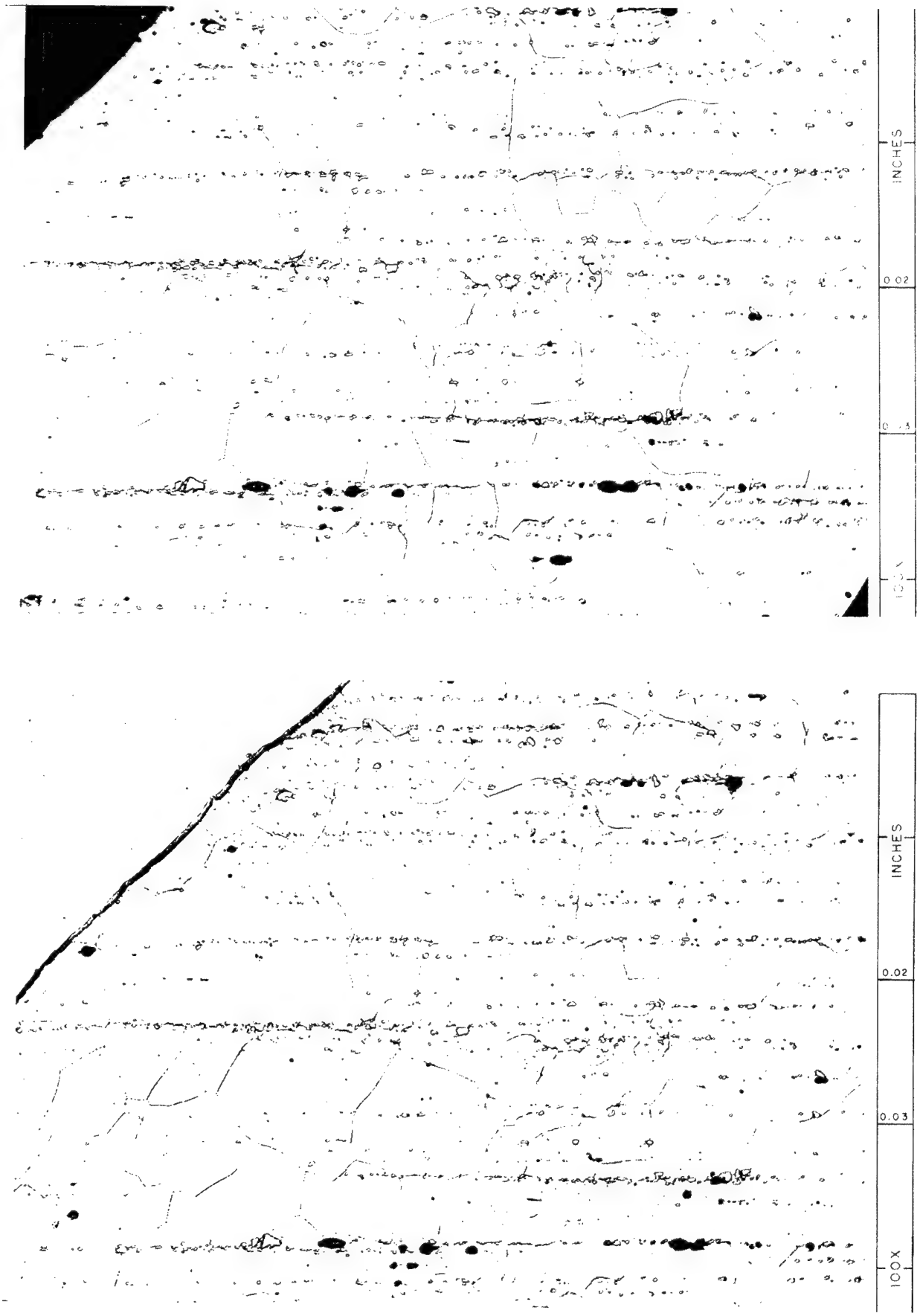

Figure 6. Comparison of Original Microstructure and Epoxy Replica. (a) Original Microstructure. 100X. Y-50540. (b) Epoxy Replica Coated with Platinum. 100X. Y-50701.

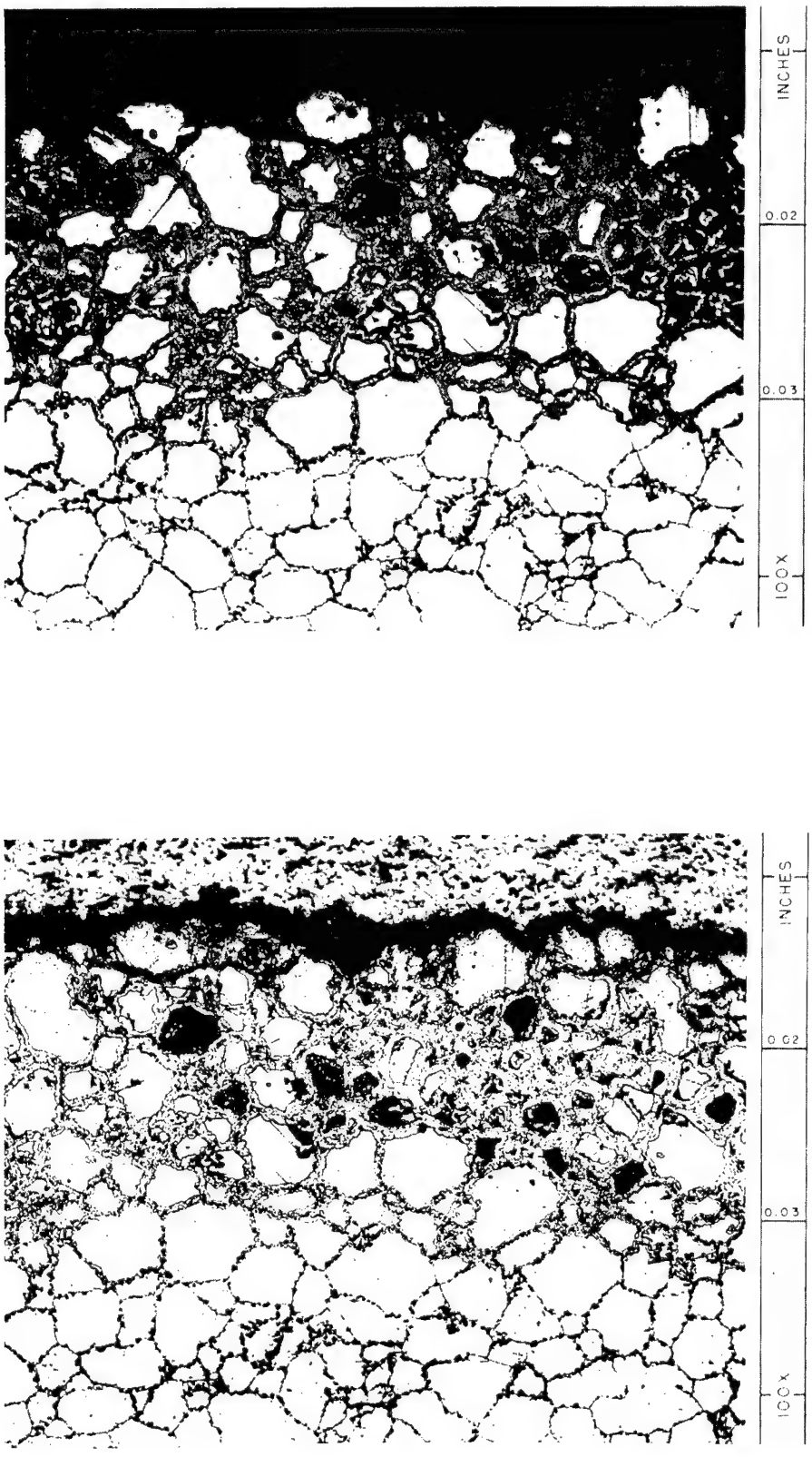

Figure 7. Comparison of Original of Type 304 L Stainless Steel Corrosion Specimen and Heavily Aluminized Epoxy Replica. (a) Original. 100X. Y-50212. (b) Aluminized Epoxy Replica. 100X. Y-50701.

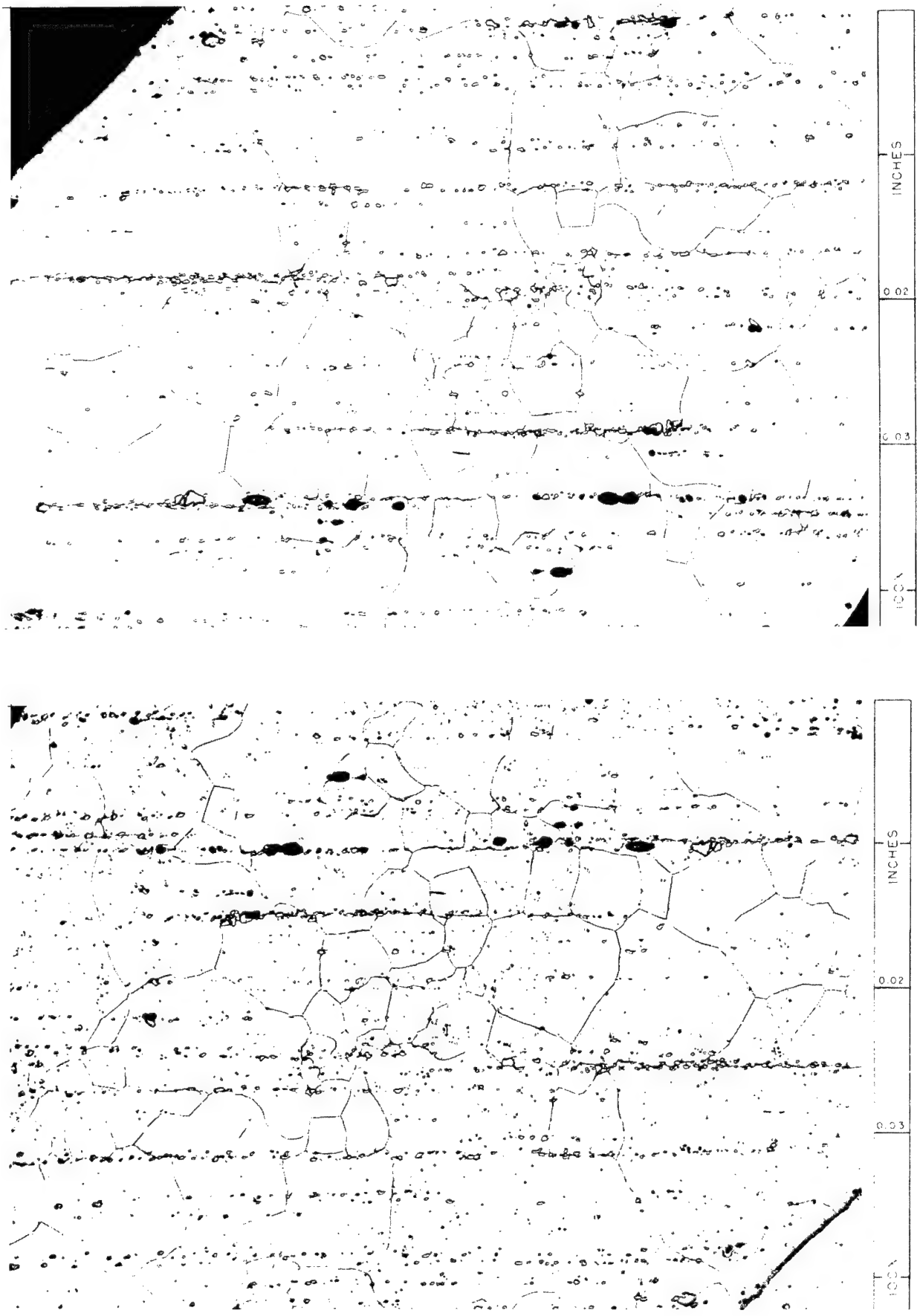

Figure 8. Original and Replica Showing "Precipitate" Artifact Introduced by Aluminizing. (a) Original. 100X. Y-50540. (b) Aluminized Replica. Y-50541.

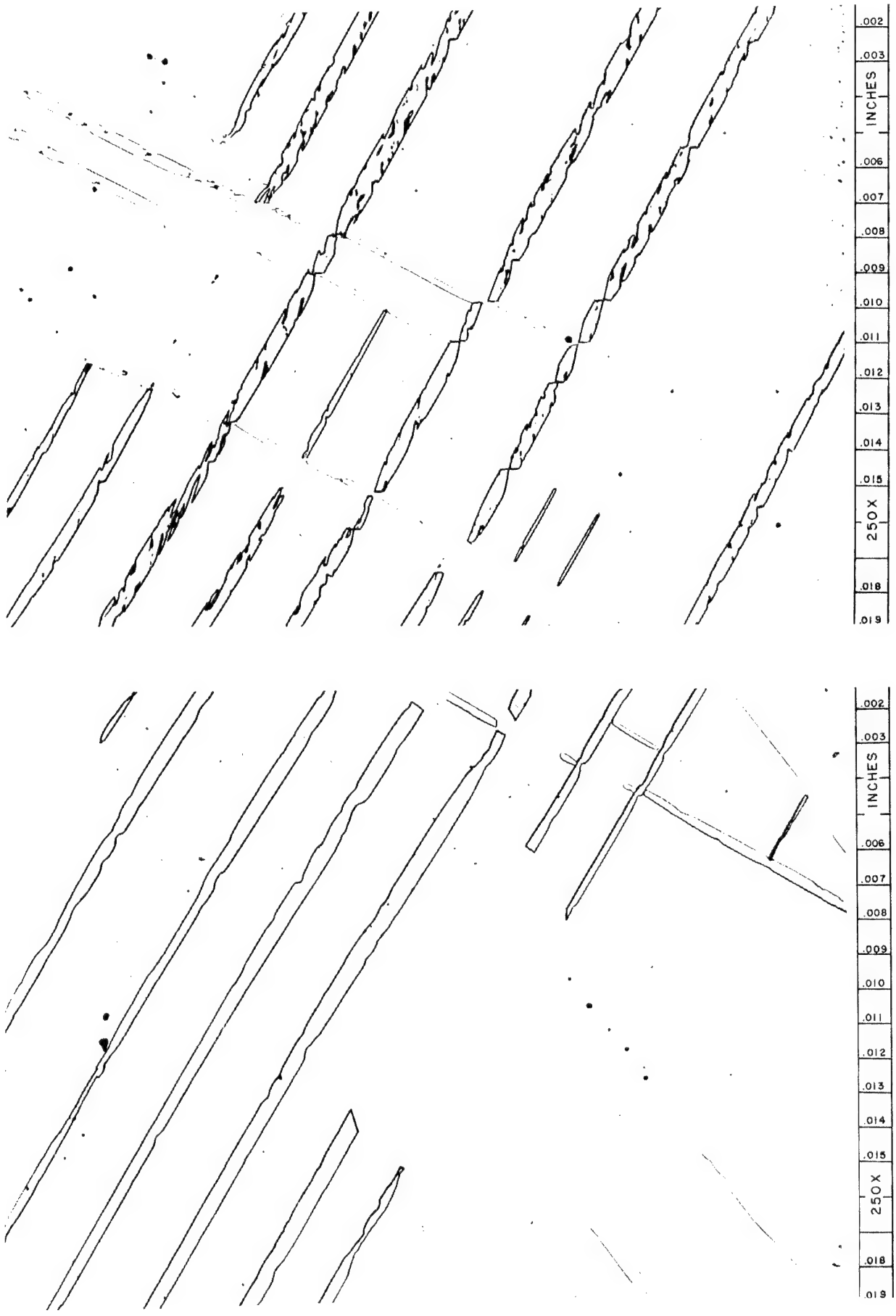

Figure 9. Replicas of a Cb Single Crystal Showing Microstructural Changes Due to Strain and Subsequent Heat Treatment. (a) Compressed at 5000 lbs Maximum Load. Y-50734. (b) Heated at 1000°C for 15 min. at 2×10^{-7} torr. Y-50735.

REPLICATION OF IRRADIATED SPECIMENS WITH ROOM-TEMPERATURE VULCANIZING SILICONES

E.J. Manthos
Oak Ridge National Laboratory

Techniques for the replication of irradiated specimens with room-temperature vulcanizing silicones are described. Both unmounted and metallographically mounted specimens have been replicated. Silicone rubber molds of the specimen surfaces are cast in the hot cells and, after curing, the molds are removed from the specimens and decontaminated. Positive epoxy replicas are then prepared from the silicone rubber molds in a semi-hot area. The replicas may be used for the verification of hot cell observations and are very useful as models for the location of saw cuts during sectioning of metallographic specimens.
Difficulties encountered in the preparation and decontamination of the silicone rubber molds are described, and advantages and disadvantages of the material are discussed.

INTRODUCTION

During hot cell examination of an irradiated specimen, it is often desirable to obtain a replica of the specimen or specimen surface being examined. The replica may be examined in greater detail out-of-cell and used to verify hot cell observations. Standard replication techniques, employing cellulose acetate, are limited to the replication of small areas and essentially flat surfaces and, when applicable, produce a negative replica or mirror image of the original specimen surface. Molds produced from room-temperature vulcanizing silicone rubbers may be back cast with epoxy resin to produce a positive replica. RTV silicone rubbers have been previously utilized for the replication of irradiated specimens.(1)

Mounted metallographic specimens as well as areas of unmounted specimens have been successfully replicated in the hot cells. Entire specimens have also been replicated; however, the technique is involved and not always successful. An RTV mold of a mounted metallographic specimen, that will be resectioned for examination in another orientation, can be used as a record of the specimen. RTV molds of metallographic specimens can be back-cast with an epoxy resin and the positive epoxy replicas, after being vacuum shadowed with aluminum, may be examined microscopically. Defected areas or areas of interest present on an unmounted specimen can be replicated with RTV for a permanent record of the specimen's appearance. Positive, aluminum shadowed, epoxy replicas cast from RTV replicas of mounted and

unmounted specimens may be examined out-of-cell, especially by personnel who are not associated with the hot cells, thus decreasing the amount of cell time spent for the visual examination of a specimen. RTV-epoxy replicas of unmounted specimens can be used as models for the location of saw cuts during the sectioning of metallographic specimens.

DESCRIPTION AND PROPERTIES OF RTV SILICONE RUBBERS

The RTV silicone rubbers used in the hot cells are two part compounds which are viscous liquids before curing. Upon the addition of a catalyst, the compounds cure at room temperature to a flexible, rubbery, solid. In the liquid state, before curing, RTV silicone rubbers are very sticky and adhere to practically everything; as a consequence, the material is messy and difficult to handle. Because of their viscosity the RTV silicone rubbers used in the hot cells are difficult to pour; after curing, RTV has excellent release properties, and does not appear to adhere to anything except RTV. Cured RTV, because of its elasticity and strength, can be flexed and twisted to facilitate the removal of a specimen from a mold. As a rule, parting compounds are not necessary to secure the release of a specimen or epoxy replica from an RTV mold.

Both Dow Corning's Silastic RTV 5363 and 5363 paste catalyst(2) and General Electric's RTV-60 and Thermolite-12 liquid catalyst (3) have been used in the cells. The shelf life of the RTV compounds used in the hot cells is four to six months and the approximate cost of the material with catalyst is $5.00 per lb (approximately 300 cc). Both compounds have similar properties, are red in color, and have a viscosity of 400 to 700 poises. The room-temperature cure time for both compounds, depending upon the amount of catalyst used and depth of RTV cast, may vary from 24 to 48 hr. Four percent catalyst (by weight) is added to the Silastic RTV 5363 to affect a cure. RTV-60 requires from 0.1 to 0.5% (by weight) Thermolite-12 catalyst addition to affect a cure; for hot cell use the 0.1% catalyst addition is used with RTV-60. The Thermolite-12 catalyst may be measured more conveniently with an eye dropper, and a chart is available from General Electric showing the number of drops of catalyst required for a corresponding weight of RTV-60.(4) The viscosity of either RTV may be reduced by the addition of a diluent; RTV-60 and 5% (by weight) General Electric 910 diluent has been used and the resultant mixture pours more readily than undiluted RTV-60. The addition of a diluent slows down the cure rate of catalyzed RTV but has little or no effect on the total cure time; also the tear and tensile strength of the cured RTV is lowered. The linear shrinkage of cured, undiluted RTV is rated at 0.2 to 0.6% and it appears that addition of a diluent may increase the linear shrinkage.

REPLICATION METHODS

The specimen should be clean and free from loose contamination before it is replicated. Clean blotter paper should be spread on the cell floor to prevent contamination of the specimen and mold. The RTV is weighed and mixed out-of-cell. The catalyzed RTV is then poured into the container

which will be used in the cell; the container should be wide-mouthed and pliable, such as a paper cup or plastic beaker. The final container and the catalyzed RTV are then placed in a vacuum desiccator and de-aerated with a mechanical pump until the RTV swells and then collapses. If the RTV is thinned with a diluent, the diluent is added and the mixture is de-aerated. The catalyst is then added and the final mixture is again de-aerated. The amount of catalyst added is determined from the weight of the RTV before the diluent was added. The de-aerated and catalyzed RTV is introduced into the cell as soon as possible, since curing of the RTV begins immediately after the addition of the catalyst. The pot-life of catalyzed RTV is approximately three to five hours and slightly longer for RTV to which diluent has been added. The RTV is allowed to cure at least 24 hours and preferrably 48 hours before the specimen is removed.

Two approaches may be followed in the replication of an unmounted specimen. An attempt can be made to replicate the entire specimen or only the area of the specimen that is of interest can be replicated. Entire specimens have been replicated, but because of inherent handling difficulties associated with hot cell manipulation, the replicas are usually not satisfactory. Positive epoxy replicas cast from RTV molds of entire specimens have not been found to be of sufficient dimensional accuracy for measuring purposes. The probability of air bubbles becoming entrapped between the specimen and the RTV mold surface is greatly increased when an entire specimen is replicated.

In general, it is much less difficult to replicate a portion of a specimen and the resultant replica is of much better quality. If a specimen is cylindrical, 1/2 to 3/4 of the circumference of the specimen can be replicated as shown in Figure 1. A rectangular box is fabricated from cellulose acetate sheet and glued together with household cement. RTV shims are placed in the box to position the specimen and catalyzed RTV is poured around the specimen to the desired depth. After the RTV has cured, the acetate box is stripped from the mold and the mold is twisted and flexed until the specimen pops out. Epoxy resin is then cast in the mold cavity to produce a positive replica. The epoxy replica is then vacuum shadowed with aluminum to render it opaque. A comparison of an aluminum shadowed epoxy replica and the original specimen is shown in Figure 2. If one of the ends of the same specimen is to be replicated, a cylindrical form larger in diameter and shorter in length than the specimen is fabricated from cellulose acetate sheet. An RTV shim is placed in the bottom of the forms and catalyzed RTV is poured in the form to the required depth; the end of the specimen to be replicated is then inserted in the RTV. After the RTV has cured, the specimen is twisted and pulled from the RTV mold.

One surface of a flat or slightly curved plate section can be replicated by placing the specimen face up in a cellulose acetate form and pouring catalyzed RTV over the plate until it is covered to a depth of 1/4 to

1/2 inch. After the RTV has cured, the mold is flexed and the RTV peeled away from the plate. An aluminum shadowed positive replica cast from an RTV mold of the interior of an INOR-8, 5 inch ID pipe section is shown in Figure 3.

A mounted metallographic specimen can be replicated by placing it face up in a cellulose acetate ring; catalyzed RTV is then poured over the face of the specimen to a depth of 1/2 inch. After the RTV has cured, the acetate ring is stripped from the specimen and the RTV peeled away from the mount. The RTV mold is then placed face up in another acetate ring and epoxy resin is poured over the mold. After curing, the epoxy replica is vacuum shadowed with aluminum. A comparison of photomicrographs obtained from an irradiated metallographic specimen and an aluminum shadowed RTV-epoxy replica is shown in Figure 4.

Aluminum shadowed, positive, epoxy replicas cast from an RTV mold of a metallographic specimen can be microscopically examined, with no loss in detail, at a magnification of at least 100 X. If the RTV mold is of good quality, the shadowed epoxy replica can be examined at magnifications as high as 500 X.

DECONTAMINATION OF RTV MOLDS AND PRODUCTION OF POSITIVE EPOXY REPLICAS

After the specimen is removed, the mold is cleaned ultrasonically in a water-detergent solution. The mold is then rinsed with water, dried, placed in a clean plastic bag, removed from the cell, and monitored. If the mold is badly contaminated, a second mold is cast from the original specimen since the first mold probably removed most of the loose surface contamination from the specimen. After the mold is removed from the hot cell, it is again cleaned ultrasonically in a water-detergent solution. If the mold is still contaminated, it can be cleaned ultrasonically in a dilute acid solution. The outer surface of the mold, if badly contaminated, can be cut away with a razor blade. Epoxy resin is then cast into the decontaminated mold to produce a positive epoxy replica. The epoxy replica is monitored and if it is above contamination and/or radiation tolerances, one or two more epoxy replicas are cast from the RTV mold to remove the loose contamination. If the third replica is still above tolerance, a second generation RTV mold is cast from the last positive epoxy replica. Positive epoxy replicas are then cast from the second generation RTV mold and if the epoxy replicas are still above tolerance, a third generation RTV mold is cast from the second generation epoxy replica. The final positive epoxy replica is then shadowed with aluminum. Little or no loss in detail is apparent between the original specimen and second and third generation epoxy replicas, as shown in Figures 5 and 6. At least six epoxy replicas have been cast from a single RTV mold without any apparent deterioration of the mold. Usually the first RTV replica of a metallographic specimen is not badly contaminated and the positive epoxy replicas cast from the mold are of a low containination level.

CONCLUSION

Specimen surfaces may be faithfully reproduced in the hot cells with room-temperature vulcanizing silicone rubbers. RTV molds, because of their flexibility and strength, are especially suited for hot cell use. Positive replicas of the specimen surface may be obtained by back-casting the RTV mold with an epoxy resin. Parting compounds are not necessary to secure the release of a specimen or an epoxy replica from an RTV mold. In general, a portion of an unmounted specimen can be replicated more successfully than the entire specimen. Positive epoxy replicas back-cast from an RTV mold of a metallographic specimen can be viewed microscopically at magnifications of at least 100 X and possibly as high as 500 X. A minimum of six epoxy replicas can be cast from an RTV mold.

RTV in the liquid state is messy and difficult to handle, both in and out of the hot cells. Replicas of entire specimens have not been found to be sufficient dimensional accuracy for measuring purposes. The total time involved in obtaining a positive epoxy replica may be lengthy, up to two to three weeks, especially if the production of second or third generation molds is involved.

REFERENCES

1. R. E. McDonald, B. W. McCollum, G. A. Moore, "Replication of Surface for Hot Cell Application", Proceedings Conference, Hot Lab Equipment Conference, ANS, Chicago, Illinois, 1961.

2. Dow Corning Corporation, Midland, Michigan.

3. General Electric Silicone Products Department, Waterford, New York.

4. Technical Data Book S-3A, General Electric Silicone Department, Waterford, New York.

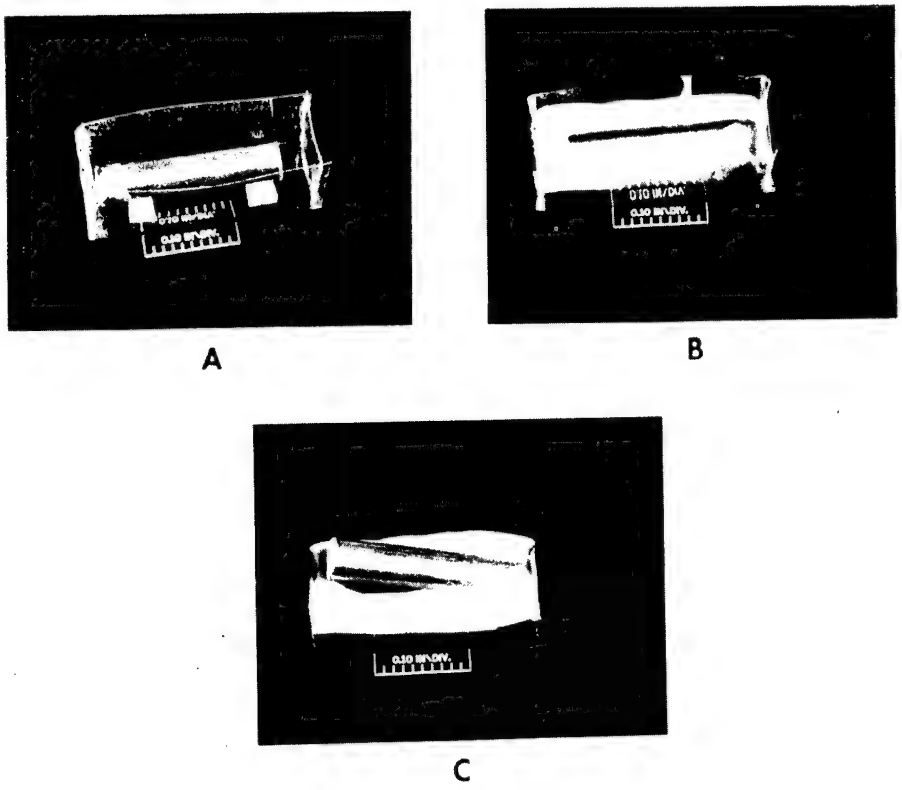

Figure 1. Procedure Followed in the RTV Replication of 1/2 to 3/4 of the Circumference of a Cylindrical Specimen. (a) Cellulose Acetate Form. RTV Shims Are Used to Position the Specimen. (b) RTV Has Been Poured Around the Specimen to the Required Depth. (c) Cured RTV Mold with Specimen Partially Removed. R-14549.

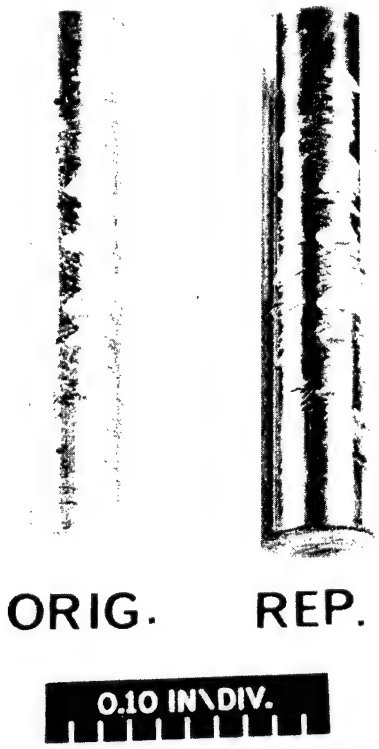

Figure 2. Comparison of Original Specimen Which Was Replicated in Figure 1 and Aluminum Shadowed Epoxy Replica Cast from RTV Mold. R-14557.

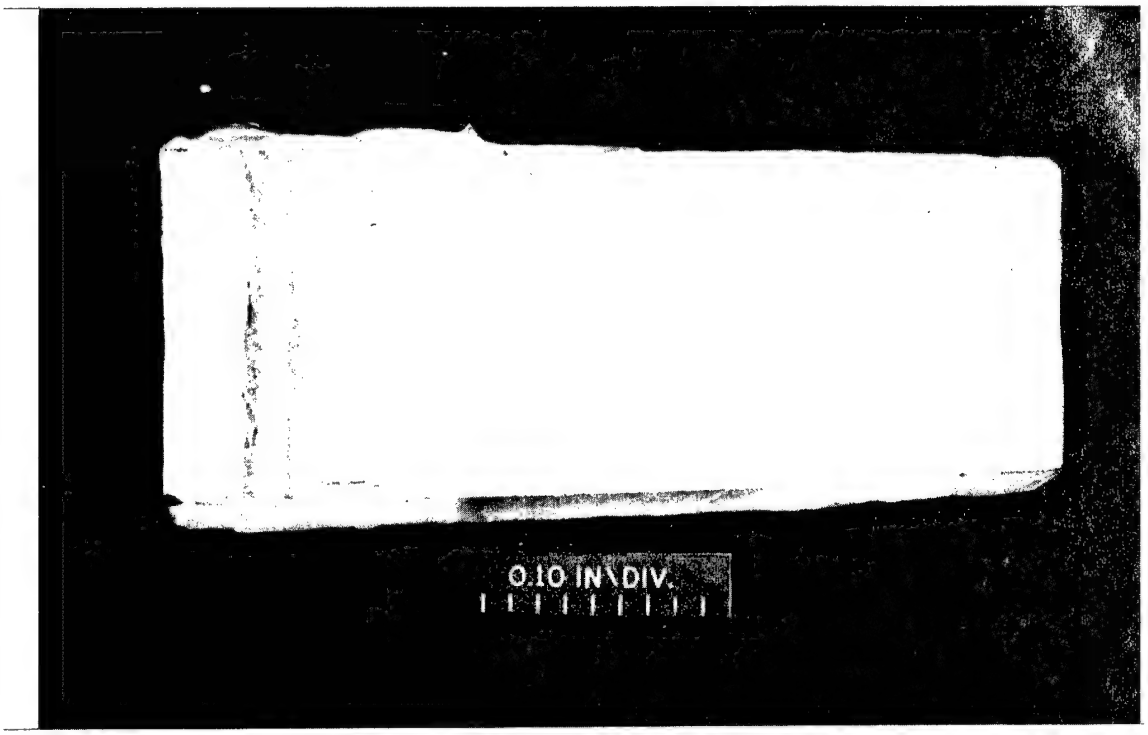

Figure 3. Positive Aluminum Shadowed Epoxy Replica Cast from an RTV Mold of the Interior of an INOR-8, 5 inch ID Pipe Section. R-14136.

ORIGINAL SPECIMEN

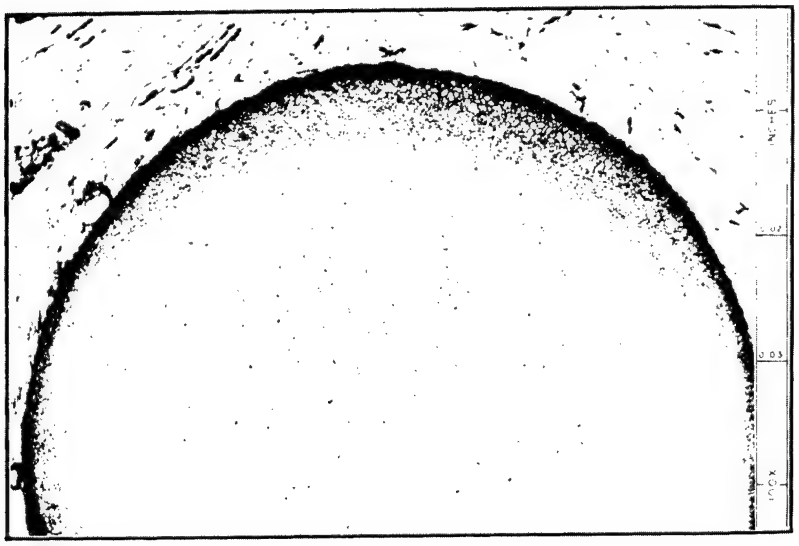

REPLICA

Figure 4. Comparison of Photomicrographs Obtained from Transverse Section of INOR-8 Pin Which Has Been in Contact with Graphite and Aluminum Shadowed Epoxy Replica Cast from an RTV Mold of the Specimen. R-14548.

ORIGINAL SPECIMEN

0.2 in.

SECOND GENERATION REPLICA

THIRD GENERATION REPLICA

0.2 in.

PREPARATION OF THIN FOILS OF URANIUM*

C. L. Angerman
Savannah River Laboratory

Foils of uranium suitable for direct observation in the electron microscope were prepared by electropolishing first in a solution containing phosphoric acid, ethylene glycol, and ethyl alcohol and then in a solution containing sulphuric acid, glycerine, and water. Twins, line dislocations, and dislocation loops were observed in typical samples.

INTRODUCTION

A technique that has received wide attention in recent years is the direct examination of metals in the electron microscope. This is accomplished by thinning the metal sufficiently, usually by electropolishing so that it is transparent to the electron beam. The important feature of this technique is that it permits the direct observation of the configurations and movements of dislocations and other crystallographic defects. Numerous applications of this technique to various metals have been made in studies of deformation mechanisms, precipitation from solid solutions, phase transformations, and irradiation damage.(1) The application of this procedure to the study of deformation and irradiation behavior of uranium appeared to have great potential; therefore, the development of a technique for the thinning of uranium was undertaken.

During the course of these efforts, a number of other techniques were reported in the literature. Hudson, et al,(2) described a technique for thinning irradiated uranium. This procedure consisted of electropolishing first in H_3PO_4 (85%) and then in a solution of H_2SO_4, H_2O, and glycerine. The latter solution removed the anodic layer that formed in the H_3PO_4. Leteurtre used the same solutions in studies of dislocation interactions (3) and precipitation of krypton gas. (4) Azam, et al, (5) used a perchloric acid solution; Douglass and Bronisz (6) employed a chromic-acetic solution in studies of recrystallization.

This paper describes a somewhat different technique and some preliminary observations of the effects of cold deformation and heat treatment on the dislocation structures of uranium.

- - - - - - - - - - -

* The information contained in this article was developed during the course of work under contract AT(07-2)-1 with the U.S. Atomic Energy Commission.

THINNING TECHNIQUE

Our best results were obtained with a solution of 800 cc ethyl alcohol, 500 cc ethylene glycol, and 500 cc H_3PO_4 (85%) with a uranium cathode at 30 ma/cm^2 and room temperature.(7) This solution is used frequently for the electropolishing of standard metallographic samples. The anodic film that formed on the sample surface was removed by electropolishing in a solution composed of 75 cc H_2SO_4 (98%) 7 cc H_2O, and 18 cc glycerine with a platinum cathode at 6 volts and a temperature between 0 and 5°C. While the composition and electrical conditions for the latter solution were the same as those employed at Harwell, the temperature used was lower. Comparison of samples polished in the H_2SO_4 solution for various times and temperatures indicated that the film formed by the H_3PO_4 solution was dissolved concurrently with the formation of a film by the H_2SO_4 solution. Reducing the temperature of the H_2SO_4 solution retarded the formation of that film, but did not appreciably lower the rate of dissolution of the H_3PO_4 film. The peripheries of the samples were painted with "nail polish" to prevent preferential attack at the edges.

These solutions worked equally well on bulk samples and on commercially rolled foils. Bulk specimens were ground initially to a thickness of 5 mils with the aid of a special mount, as shown in Figure 1a. Final thinning by electropolishing was done in the apparatus shown in Figure 1b. The significant feature of this apparatus is the shielded cathodes. This shielding localized the polishing action and resulted in more uniform thinning of the foil. Commercial foils, 3 mils thick, were thinned in the same apparatus.

DISLOCATION STRUCTURES

The effectiveness of this procedure is illustrated in Figures 2 and 3. The samples were taken from uranium foil, 3 mils thick, which was slightly cold worked in the as-received condition. Some samples were annealed for one hour at 600°C to recrystallize the structure; others were beta transformed at 720°C for one hour. Both heat treatments were done in evacuated "Vycor" capsules. Many more dislocations were seen in the beta-transformed foil than in the recrystallized foil. In the beta-transformed foil, many of the dislocations were aligned in "chains" and formed the subgrain boundaries. Somewhat similar configurations have been seen in polygonized aluminum. None of the dislocations moved as a result of the heat produced by the electron beam, although such movement has been observed in aluminum and stainless steel. No stacking faults, such as those seen in stainless steel, were observed in the uranium.

Dislocation loops were present in bulk samples that were beta transformed and deformed at room temperature, as shown in Figure 4. The loops were probably formed when the applied stress forced a dislocation past some obstacles. The formation of loops during deformation has been observed in a number of metals.(8)

ACKNOWLEDGEMENT

The author gratefully acknowledges the work of R.D. Kelsch and W.T. McKettrick in the development of the grinding technique for bulk samples and the design and construction of the thinning apparatus.

REFERENCES

1. Thomas G. Transmission Electron Microscopy of Metals, New York: John Wiley (1962).

2. Hudson, B., K. H. Westmacott, and M. J. Makin. "Dislocation Loops and Irradiation Growth in Alpha Uranium". Philosophical Magazine 7, 377-92 (1962).

3. Leteurtre, J. "Dislocation Reaction in α Uranium". J. Nuclear Materials 6,338-41 (1962).

4. Leteurtre, J. and G. Brebec. "Study by Electron Microscope of Uranium Containing Krypton". J. Nuclear Materials 6, 342-5 (1962).

5. Azam, N., M. Bouleau, and P. A. Jacquet. "Simple Electrolytic Method of Preparing Thin Metallic Foils for Direct Examination by Electron Microscopy". Comptes Rendus 252, 698-700 (1961).

6. Douglass, D. L. and S. E. Bronisz. "Transmission Electron Microscopy of Cold Worked and Recrystallized Alpha Uranium," Trans. AIME (to be published).

7. Angerman, C. L. "Transmission Electron Microscopy of Uranium," J. Nuclear Materials (to be published).

8. Strenthening Mechanisms in Solids. Papers presented at a seminar of the American Society for Metals, October 13 and 14, 1960. Reinhold Pub. Corp. (1962).

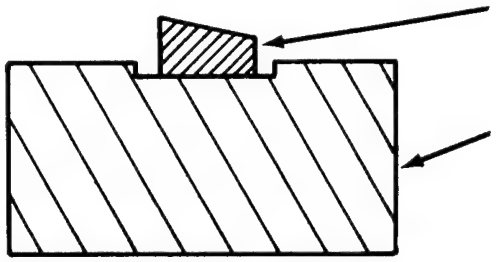

Bulk sample attached to mount with Eastman 910 cement.

Hardened stainless steel mount with groove 5 mils deep machined in one surface.

Sample was ground until steel mount contacted grinding surface. Higher hardness of mount permitted more uniform grinding. Sample was removed from mount by dissolving cement in warm water.

a. Grinding of Bulk Samples.

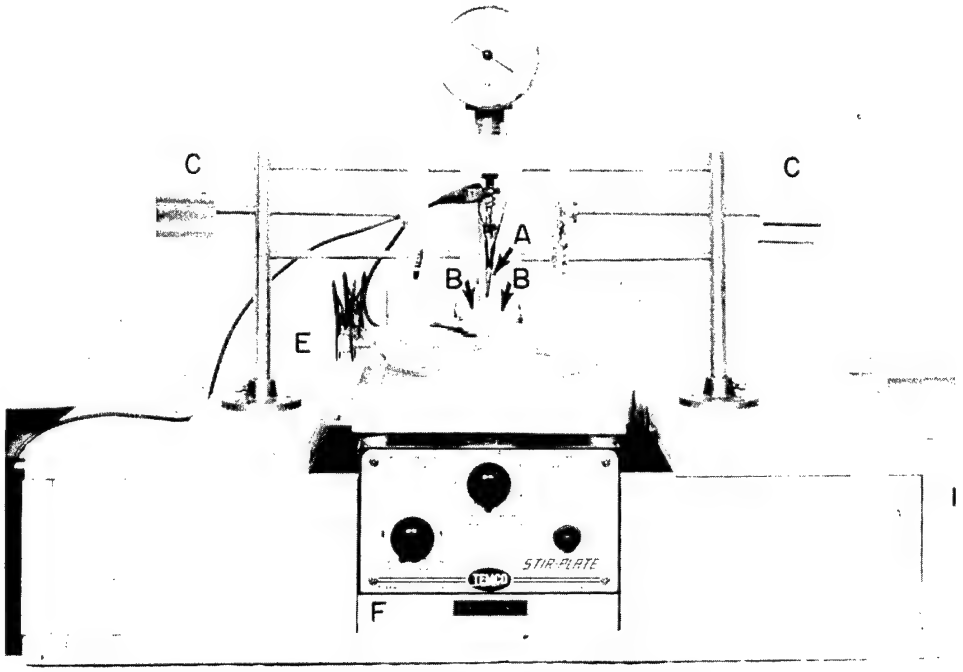

b. Electropolishing Apparatus. A-Specimen strip (anode). B-Glass shielded Cathodes, C-Cathode spacing adjustments. D-Thermometer, E-Cooling coil, F-Stirrer and heater.

Figure 1. Preparation of Foils from Bulk Specimens.

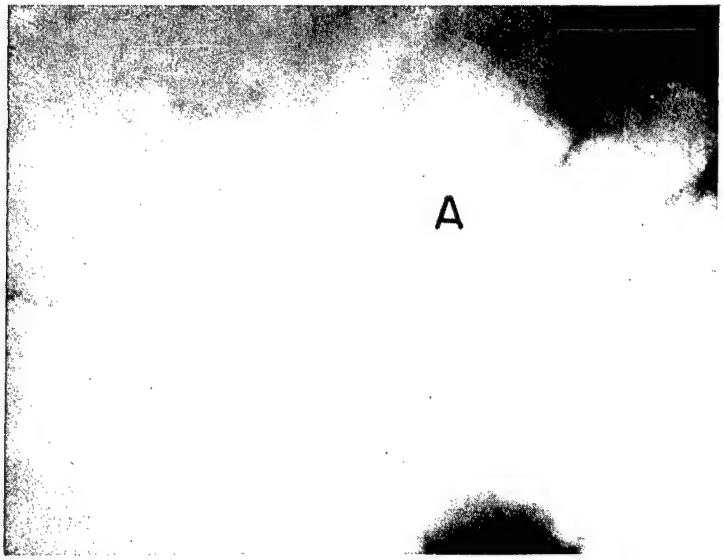

The photograph shows the intersection of three grains.
The short, dark lines near A are dislocations.

Figure 2. Dislocations in Recrystallized Uranium. 30,000X.

(b)

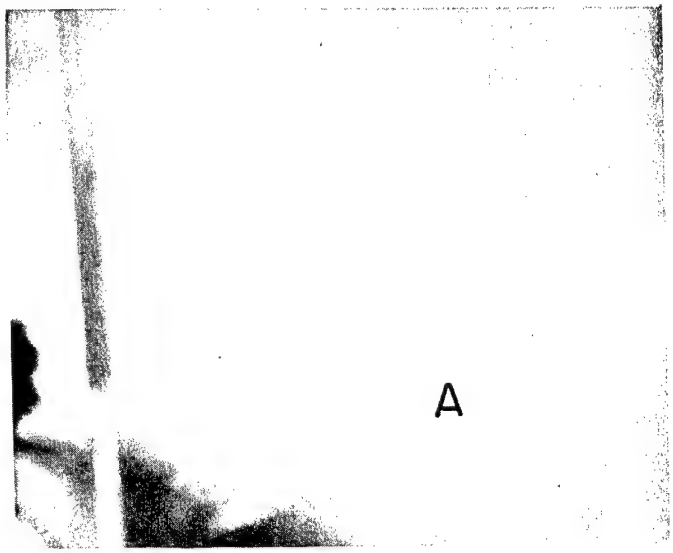

(a)

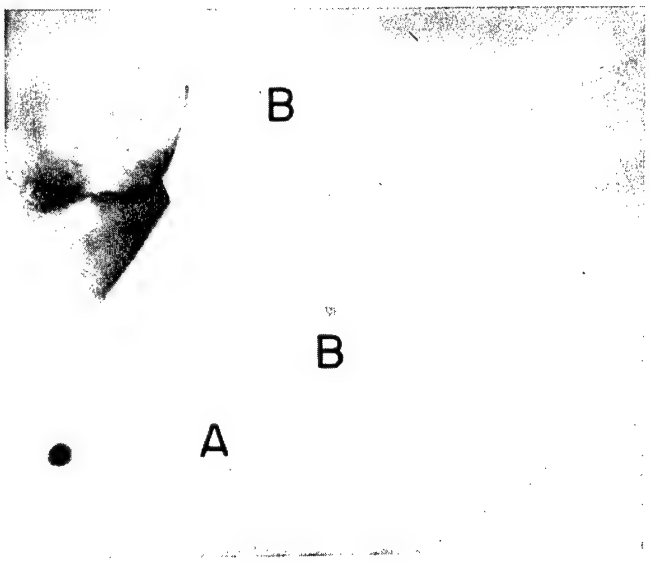

(c)

Figure 3. Dislocations and Twins in Beta-Transformed Uranium. Figure 3a shows the general grain structure. 11,000X. In Figures 3b and 3c, "chains" of dislocations forming subgrain boundaries are at A and twins are at B. 30,000X. 7,000X. Numerous individual dislocations (short, dark lines) are evident in all photographs.

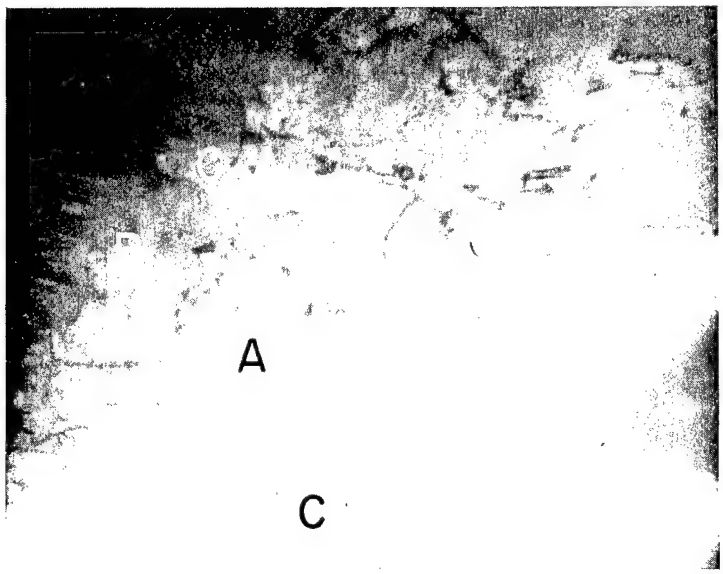

Small dislocation loops are shown at A and an extremely large loop at B. Partially formed loops, as indicated by V-shaped dislocations are shown at C.

Figure 4. Dislocation Loops in Deformed Uranium. 21,000X.

SPECIMEN PREPARATION FOR TRANSMISSION ELECTRON MICROSCOPY OF ALPHA URANIUM*

Dana L. Douglass
Los Alamos Scientific Laboratory

At Los Alamos Scientific Laboratory we have recently completed a transmission electron microscopy study to investigate the effects of cold work and recrystallization on alpha uranium.(1) Our immediate purpose was to gain experience in working with high atomic number materials, but our eventual goal is the thinning and transmission examination of thin films of plutonium.

In preparing thin films of uranium we used an electropolishing bath different from that used by Hudson, Westmacott, and Makin (2) and also different from that just reported by Dr. Angerman. (3) Our electropolishing was performed in a bath composed of 25 g chromic acid, 133 ml glacial acetic acid and 25 ml water. This solution is similar to a standard metallographic electropolishing solution introduced for use on plutonium by K. Johnson, (4) except that it involves the use of 25 ml of water rather than 7 ml. The addition of extra water was suggested to us by T.I. Jones.(5) The standard window technique was used with the edges of the sample masked with a stop-off paint made of polystyrene dissolved in benzene. The electrolytic cell consisted of a cylindrical stainless steel cathode in a beaker containing the chromic-acetic acid solution. The sample, as the anode, was placed in the center of the cell. The electrolyte was cooled below 15°C with liquid N_2 and the bath was stirred constantly with a magnetic stirrer. Under these conditions the current density at 20 v was about 0.2 amp/cm^2. Since the electrolytic thinning produced wedge-shaped specimens, the sample was rotated 90° in its own vertical plane every few minutes to minimize this effect. Upon completion of the thinning, the specimens were rinsed in anhydrous methanol and dried in a warm air stream. (6)

Use of this method reliably produced specimens suitable for viewing in the electron microscope. The time of preparation was conveniently short and, most important, no second electropolishing bath was needed because the surface of an as-polished specimen was relatively inactive and free of a reaction layer. The bath is chemically stable and can be reused repeatedly. Two examples of the thinned foils are shown in Figures 1 and 2.

- - - - - - - - - - - -

*Work performed under the auspices of the United States Atomic Energy Commission.

1. Trans. AIME; to be published.
2. Phil. Mag., 7, 377(1962).
3. "Preparation of Thin Foils of Uranium"; 17th AEC Metallography Group Meeting, Los Alamos, May 21 to 23, 1963.
4. To be published.
5. Private communication.
6. The etchant used for this procedure is described in Appendix A to this publication, page 158.

Figure 1. Annealed Alpha Uranium. 5200X.

Figure 2. Three Percent Cold Rolled Alpha Uranium. 18,000X.

METALLOGRAPHY OF URANIUM NITRIDE

W. Musser, J. Bugl, * and A. A. Bauer
Battelle Memorial Institute

Procedures for the metallographic preparation of UN samples are described. These include cutting, mounting, and grinding procedures as well as chemical, electrochemical, and vacuum-cathodic etching techniques.

INTRODUCTION

The encouraging results recently obtained with UC for fuel elements have opened new prospects for the use of nonoxide refractory ceramics in the field of nuclear fuels. Uranium mononitride is, because of its high uranium density, high thermal conductivity, resistance to deformation at elevated temperatures, and favorable irradiation resistance, most promising as a potential fuel material.

The metallographic procedures described in this paper have been developed to aid in the identification of phases as part of a study of the phase relationships in the uranium-nitrogen system. Metallography also has been used extensively to study the microstructure of UN powder and UN compacts fabricated by isostatic hot pressing and arc melting. Standard techniques have been used in some applications; modified or new techniques have been used in others.

SAMPLE PREPARATION

To select the best method of sample preparation, various cutting techniques were studied. To overcome the problem of specimen fracture encountered in the use of a silicon carbide cutoff wheel, ultrasonic cutting was tested. A minimum disturbance of the cut surface on UN samples was observed using a 1000-w Sheffield cavitron under the following conditions: Frequency - 20 kc; Power setting - 20%; Bias current - 3 amp; Cutting tool - Mild steel; Abrasive slurry - Silicon carbide in kerosene. The average time to cut a UN rod with a diameter of 3/8 in. was 45 min. To cut material in which free uranium was present took as much as 4 hr.

In most cases, however, a metallurgical cutoff machine was satisfactory. The specimen was rotated at a low speed against a high-speed, rotating silicon carbide cutoff wheel. In all cases kerosene was used as a lubricant. To cut a 3/8 in. rod of UN by this means took 3 to 5 min. The mounting of uranium nitride compacts was accomplished by conventional means. At other times UN powder as well as UN compacts with a number of open pores were prepared by impregnation mounting, using "Epon Resin 828" in vacuum. By this method, pores and cracks in the structure are filled with hard plastic and specimens can be ground and polished very easily.

* Euratom

An optimum polish was obtained by a two-step sequence.

(1) Specimens were rough polished to remove grinding scratches on a fast speed wheel covered with a nylon or silk cloth and a slurry of 200 cm^2 water, 4 grams of chromium trioxide and 25 grams of "Linde A" polishing abrasive.

(2) A final polish was obtained on a wheel covered with Gamal cloth and operated at a lower speed (650 rpm). A slurry of 20 grams chromium trioxide and 20 grams of ferric oxide in 200 cm^2 water was applied to the cloth.

To prevent water stains the specimens were washed after each step with ethyl alcohol.

Figures 1,2,3, and 4 show as-polished UN compacts which contain various phases. The higher nitride phase can be readily identified in the as-polished condition.

ETCHING TECHNIQUES

UN can be etched either chemically, electrochemically, or by vacuum cathodic etching.

The most widely employed method was the chemical etch which involved two steps. First the specimen was swabbed for 30 sec. with a solution of 50 cm^3 lactic acid and 50 cm^3 nitric acid. This etch delineated the second phases, either higher nitride or uranium, in the UN matrix. Figures 5,6, and 7 illustrate this delineation of the U_2N_3 and uranium phases. Next the specimen was swabbed for 30 to 60 sec. with a solution of 50 cm^3 lactic acid, 50 cm^3 HNO_3, and 7 drops of HF. This etch does not attack the UN grain boundaries but rather oxidizes the UN grains preferentially to reveal the UN grains. Figures 8,9, and 10 illustrate this effect.

To aid in the identification of free uranium another swab etch consisting 1 part each of hydrogen peroxide and ammonium hydroxide was employed. The oxidized uranium phase could be identified as a result of a yellow discoloration. This etch was also used to study the reaction of UN with tungsten, as shown in Figure 11.

Electrolytic etching has been used sucessfully in several uses. A solution of 18 parts acetic acid and 1 part chromium trioxide applied at 40 dc volts for 5 secs. was used to define the grain boundaries in the higher nitride phase as shown in Figure 12. To study UN precipitated in a uranium matrix an etchant of 8 parts ethyl alcohol, 5 parts orthophosphoric acid, and 5 parts ethylene glycol was applied at 40 dc volts for 1 sec. The specimens were mechanically polished before etching first on Forstmann's cloth using 1 micron diamond with a kerosene lubricant and then on Gamal cloth using 5 cc gamma alumina and 95 cc hydrogen peroxide. A resulting structure is shown in Figure 13.

Cathodic vacuum etching enjoys several advantages as compared with chemical etching techniques. It produces a surface free of stain and results in excellent relief delineation of the phases which is necessary for electron microscopy replication techniques. It also delineates structural details within the various phases. Etching was performed under the following conditions: Voltage - 300 v; Current - 15 milliamps; Atmosphere - Argon; Pressure - 40 micron Hg; Time - 30 min. Figures 14, 15, and 16 illustrate the structures developed using this method.

SUMMARY

Techniques have been developed for the preparation of metallographic samples of uranium nitride. Various etching techniques were found to be required for optimum phase delineation and identification, depending upon the phases present and type of microstructural detail desired.

Figure 1. UN Compact, 96 Percent Dense. As polished. 250X. RM-24505.

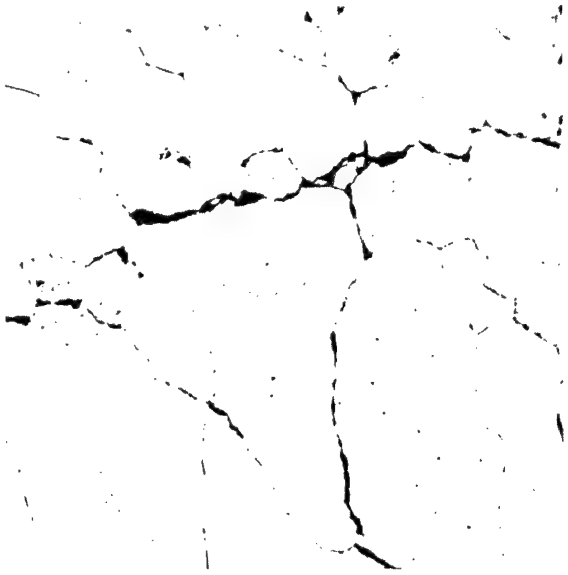

Figure 2. Cast UN Compact. U_2N_3 formed at cracks. As polished. 250X. RM-24499.

Figure 3. Particle in UN Matrix. Light gray phase in particle is U_2N_3 and dark grey phase is believed to be complex carbonitride. As polished. 500X. RM-24496.

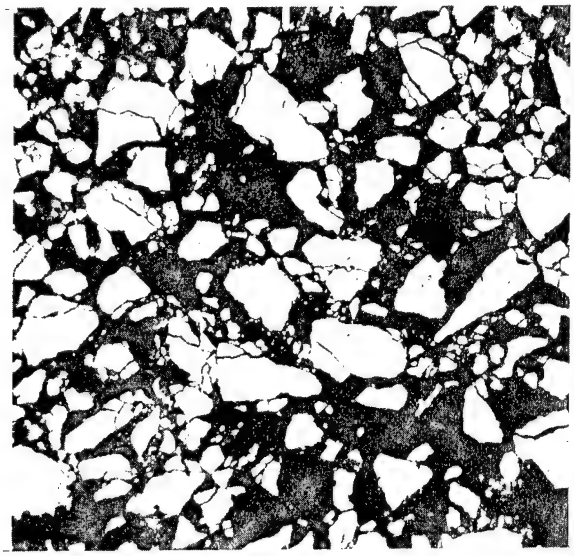

Figure 4. UN Powder. As polished 250X. RM-24512.

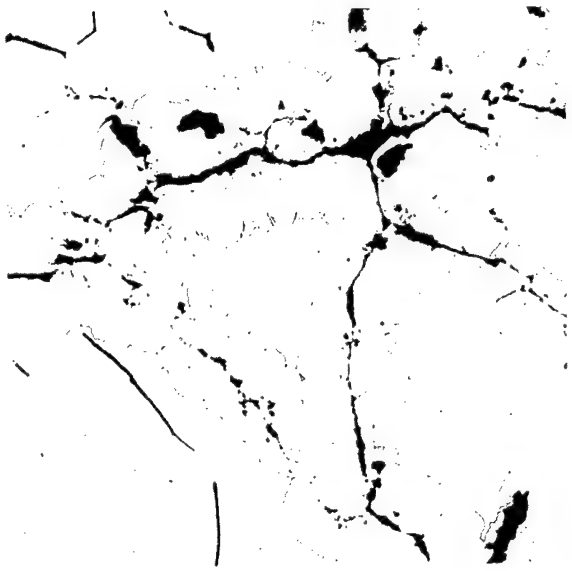

Figure 5. U_2N_3 Formed at Cracks in an UN Compact. 250X. RM-24501.

Figure 6. Free Uranium in the Grain Boundaries of UN and Intergranular Precipitated. 250X. RM-24498.

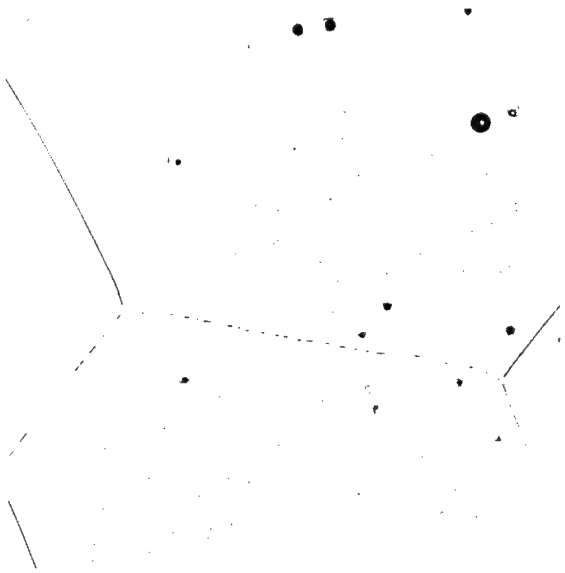

Figure 7. Intergranular Precipitated Uranium. 250X. RM-24511.

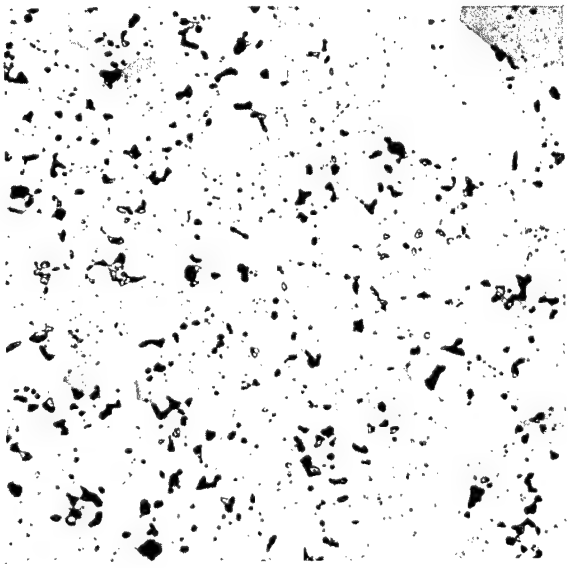

Figure 8. UN Compact Fabricated by Isostatic Hot Pressing. 250X. RM-24497.

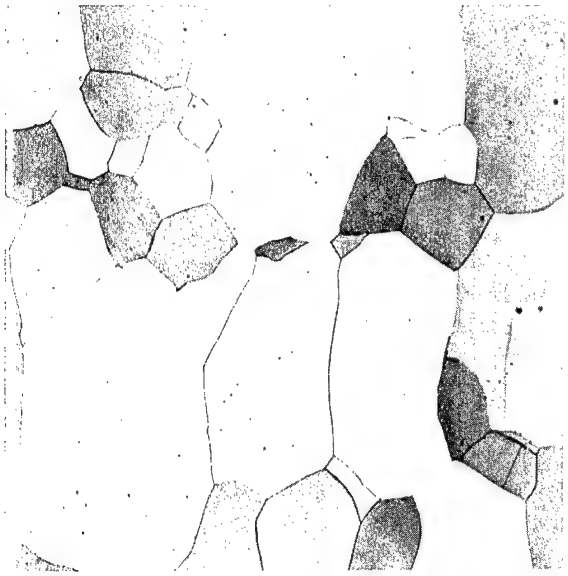

Figure 9. UN Compact Fabricated by Arc Melting. 250X. RM-19096.

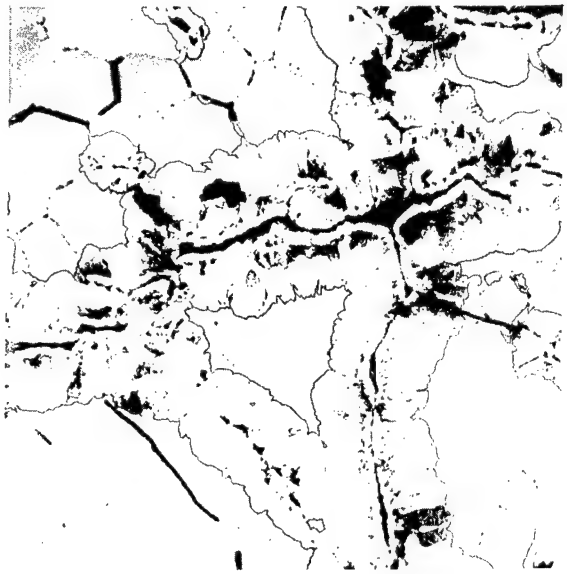

Figure 10. U_2N_3 Formed at Cracks in an UN Compact. 250X. RM-24500.

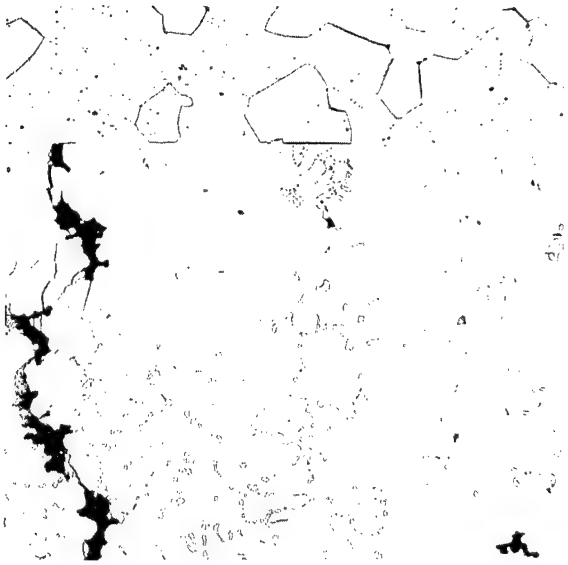

Figure 11. Reaction Zone Between Tungsten and UN + Free Uranium. 100X. RM-24508.

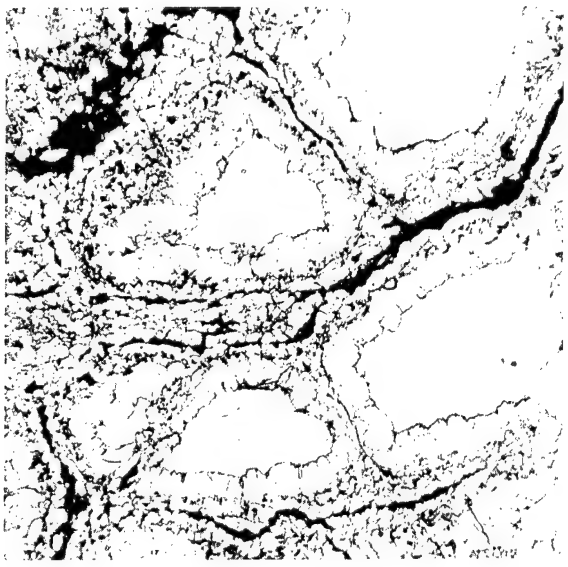

Figure 12. U_2N_3 Formed at Cracks in an UN Compact. RM-24503.

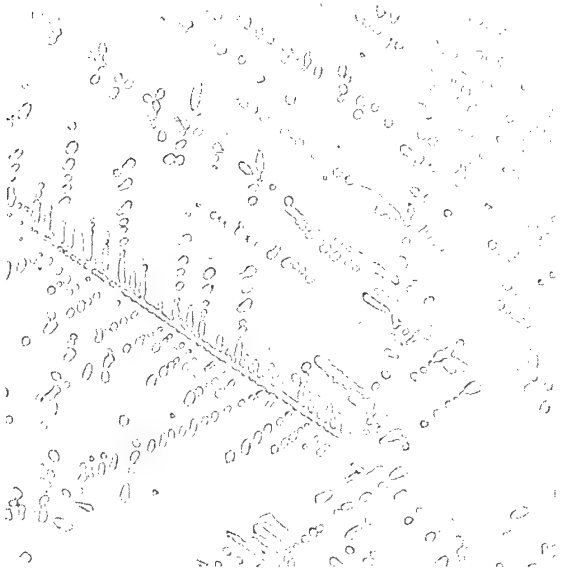

Figure 13. UN Precipitated in Uranium. 250X. RM-24510.

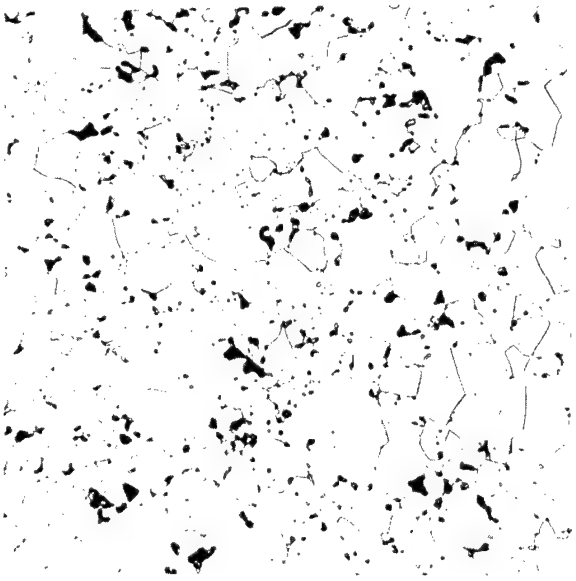

Figure 14. UN Compact Fabricated by Isostatic Hot Pressing. 250X. RM-24504.

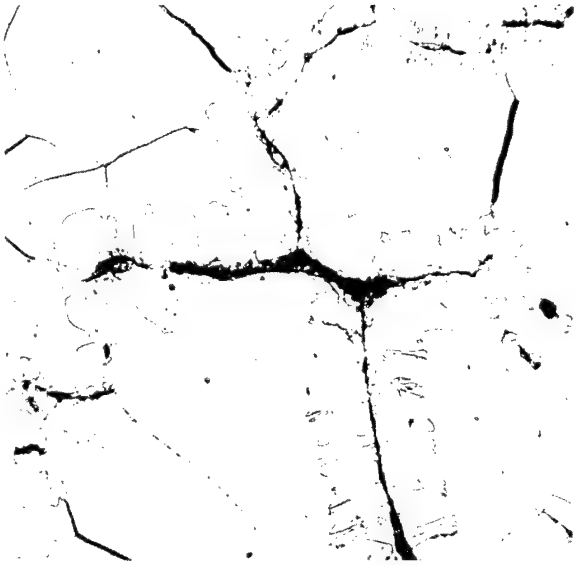

Figure 15. U_2N_3 Formed at Cracks in an UN Compact. 250X. RM-24502.

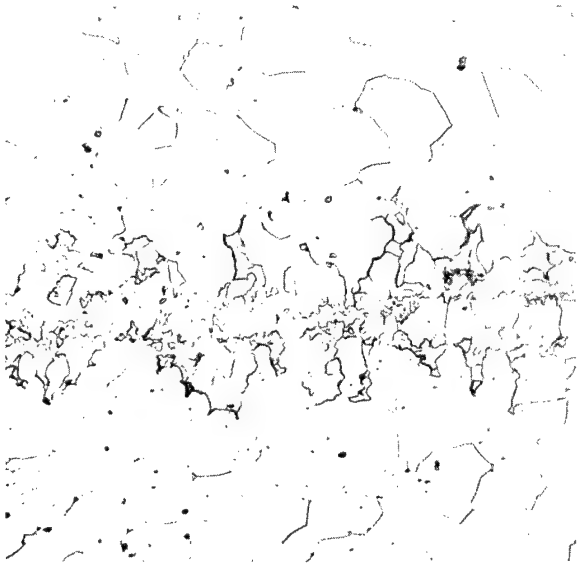

Figure 16. UN to UN Bond. 250X. RM-24028.

METALLOGRAPHY OF URANIUM CONTAINING SMALL ADDITIONS OF IRON, SILICON, OR ALUMINUM*

C. L. Angerman and M. R. Louthan, Jr.
Savannah River Laboratory

In uranium with alloying additions of up to 400 ppm Fe and up to 800 ppm of either Si or Al, the various U-containing phases were examined with the electron microscope. These phases were also extracted chemically and identified by electron diffraction. During γ-phase heat treatments, the alloying additions, as well as impurity atoms, segregate into networks of "incipient" precipitates that can be seen only after certain etching treatments.

INTRODUCTION

Additions of up to 400 ppm iron and up to 800 ppm of either silicon or aluminum are used to promote grain refinement during beta transformation(1) and to improve irradiation stability (2) of uranium fuel. Characterization of the phases that are produced by these additions and the effects of heat treatments on their distributions is necessary for a complete understanding of the properties of the alloys. Existing phase diagrams indicate the compounds that might be expected in binary systems, but data on the ternary and quaternary systems are not available.

This paper describes the metallographic appearance and the identification of the phases present and the effects of heat treatment on a few of the possible ternary and quaternary alloys. Since the intermetallic particles were small, electron microscopy was used extensively in the examinations of the structures. Typical heat treatments were either 30 minutes at 830°C or 10 minutes at 720°C followed by quenching in either water or oil. Annealing after quenching was done at 550°C for 30 minutes. Some samples were alpha annealed at these same conditions prior to the beta treatment.

SUMMARY

In each alloy, the additions were dissolved completely at gamma-phase temperature. The solubility limits at beta-phase temperatures were greater than 400 ppm Fe and 800 ppm Si, but the limit for Al was between 150 and 250 ppm. Annealing at alpha-phase temperatures after quenching from the beta or gamma phases precipitated U_6Fe, U_3Si, or UAl_2, either singly or in combinations, depending on the alloy. However, Si was soluble in both

- - - - - - - - - - -

* The information contained in this article was developed during the course of work under contract AT(07-2)-1 with the U.S. Atomic Energy Commission.

U_6Fe and UAl_2 and caused a decrease in the c/a ratio of U_6Fe of 0.014 and a decrease in the a_o value of UAl_2 of about 0.05 to 0.12 Å. Metallographic examination indicated that Fe was also soluble in UAl_2, but no change in the lattice parameter was detected within the accuracy of the measurements.

Although no discrete precipitates were observed after quenching from the gamma phase, indicating that the alloying additions were dissolved completely, networks of "incipient" precipitates were revealed by certain etchants. These incipient precipitates are believed to be the result of a segregation of the solute atoms to the grain and subgrain boundaries of the beta phase that existed during cooling. As the cooling rate increased, the degree of segregation to the boundaries decreased, and a more severe etch was required to reveal the networks.

DISCUSSION

METALLOGRAPHIC TECHNIQUES

The minor phases resulting from the alloying additions were distinguishable after electropolishing in the standard phosphoric acid-ethylene glycol-ethyl alcohol solution. For examination with the electron microscope, "Formvar" replicas were dry-stripped from the electropolished surface and shadowed with uranium at an angle of 18 degrees. The electropolish left the intermetallic phases in relief, but attacked the nonmetallic compounds, such as UC, UN, UH_3, and UO_2.

An extraction replica technique was employed to identify the intermetallic phases. Samples were electropolished in the same manner as previously described. A "Formvar" film was cast on the surface and scribed to form squares suitable for insertion into the electron microscope. Prolonged electropolishing (approximately 20 minutes) through this "Formvar" film freed the film in which the particles were imbedded.

IDENTIFICATION OF PHASES

Three phases, U_6Fe, UAl_2, and U_3Si, that were extracted in the manner described above, were identified by selected area electron diffraction. The lattice constants calculated from these patterns indicated that Si was soluble in both U_6Fe and UAl_2. The c/a ratio for U_6Fe decreased from 0.500 for an alloy containing 30 ppm Si to 0.486 for an alloy containing 330 ppm Si. The value of a_o for UAl_2 decreased from 7.74 Å for an alloy with 30 ppm Si to 7.69 and 7.62 Å for alloys containing 310 and 340 ppm Si, respectively. Iron had no significant effect on the lattice parameter of UAl_2. However, the metallographic examinations showed that some Fe was soluble in UAl_2. No changes were observed in the lattice parameter of U_3Si when either Fe or Al was present in the alloy.

Each phase had a characteristic appearance after electropolishing that permitted a tentative identification on the basis of metallographic appearance (see Figure 1). The U_6Fe [or $U_6(Fe, Si)$] particles were in relief with somewhat rounded interfaces. Frequently they were elliptical when the particle lay in a grain boundary, or triangular when the particle was at an intersection of three grains. Although the UAl_2 [or $U(Al, Si)_2$] particles were also in relief, they had a more rounded shape than the U_6Fe and had more vertical interfaces. Additionally, the UAl_2 particles were smaller than the U_6Fe particles. The U_3Si had a characteristically striated surface that made identification relatively easy.

EFFECT OF HEAT TREATMENT

In the as-cast condition all the alloys contained an eutectoid structure, as illustrated in Figure 2. The eutectoid was composed of a mixture of either U_6Fe, U_3Si, UAl_2, or a phase tentatively identified as UC; the relative amounts of each phase depended upon the composition and the cooling rate during solidification.

Gamma Treatment

At least 400 ppm of Fe and 800 ppm each of Si and Al were soluble in the gamma phase. The standard electropolish did not reveal any minor phases in small samples that were water quenched after 30 minutes at 830°C. Trace amounts of UAl_2 were observed in more massive pieces of alloy (240 or 800 ppm Al) that were oil quenched.

In contrast, electrolytic etching in a 50 vol % HNO_3 solution at 1 v (open circuit) for 15 to 30 seconds revealed a network structure in all of the gamma-quenched alloys, as illustrated in Figure 3. Examination of this structure with the electron microscope indicated that the lines were rows of shallow pits. These lines are believed to be the result of segregation of some alloying or impurity atoms to the grain and subgrain boundaries of the beta phase during cooling and are called incipient precipitates. The white bands are believed to be "ghosts" of the gamma grain boundaries. These hypotheses are supported by the similarities in sizes of the beta and gamma grains, as observed by hot-stage metallography,(3) and the sizes of the networks formed by the black lines and the white bands, respectively. Similar structures were observed with the same etch by Mathews (4) and with a chromic-acetic acid etch by Robillard. (5)Althaus and Cook (6) also observed these structures, but concluded they were artifacts after a study of the etching conditions.

The nature of the particles comprising these networks and the ability to reveal the networks with etchants other than the HNO_3 etch were dependent on the cooling rate from the gamma phase. Samples of unalloyed ingot uranium were annealed 30 minutes at 950°C to dissolve some of the carbon, then air cooled or quenched in either water at 22°C, brine at -2°C, or a 50% $CaCl_2$ solution at -50°C. The networks in the air cooled sample were composed of discrete precipitates of UC that could be revealed by electropolishing (Figures 4, a and b). In contrast, the networks in the quenched samples were composed of incipient precipitates that could be revealed only by a "pitting" type etch (Figure 4, c and d). As the cooling rate increased a more severe etch was required to reveal the networks, as indicated in the Table. The exact nature of the incipient precipitates is not known at this time.

TABLE I

CONDITIONS FOR REVEALING NETWORKS

	Networks revealed by		
Cooling Conditions	HNO_3 Etch	Chromic-Acetic Etch	H_3PO_4 Electropolish
Air cool	Yes	Yes	Yes
Water quench	Yes	Yes	No
Brine quench	Yes	No	No
$CaCl_2$ quench	Yes	No	No

Any segregation of the solute atoms to the beta grain boundaries should increase the chemical reactivity in the localized area in proportion to the degree of segregation. When only a portion of the solute atoms were segregated, as in a rapid quench, a more reactive etchant was required to reveal these areas. When more, or essentially all of the atoms, as in the case of a discrete precipitate, were segregated, the less severe etchants or polishes could be used.

Beta Treatment

The examination of samples containing up to 400 ppm Fe, 800 ppm Si, and 800 ppm Al in the beta-quenched condition indicated that the solubility limit in beta uranium was greater than 400 ppm for iron, greater than 800 ppm for Si, and between 150 and 250 ppm for Al. In general, U_6Fe or U_3Si precipitates were observed in alloys containing up to 400 ppm Fe or 800 ppm Si. UAl_2 was not observable in alloys containing approximately 25 ppm Al but was present in trace amounts in a sample containing 110 ppm Al and was readily observable in samples containing 250 ppm Al or more. The alloys containing more than 700 ppm Al contained a network of UAl_2 precipitates similar to the networks of incipient precipitates observed in the gamma-quenched samples.

In some instances trace amounts of U_6Fe and U_3Si were observed after beta quenching. This slight precipitation may have resulted from local nonuniformities during cooling or to incomplete dissolution of any pre-existing particles. The U_3Si was observed in only one of 25 samples examined, while $U_6(Fe, Si)$ was present in five samples. The alloy content appeared to have little or no effect on whether or not U_6Fe was precipitated since trace amounts of precipitation were observable in a sample with 63 ppm Fe and no precipitation was observable in a sample with 400 ppm Fe.

Alpha Annealing

The structures produced by alpha annealing at 550°C after either beta or gamma quenching corroborated the interactions indicated in the diffraction patterns. This treatment precipitated U_6Fe, U_3Si, and UAl_2, depending upon the composition. The U_6Fe precipitated as networks in alloys containing 25 ppm Al and as random precipitates in alloys containing greater than 250 ppm Al (Figure 5). The U_3Si was always present as random precipitates regardless of Al content. U_3Si was not observed in samples containing up to 350 ppm Si if Fe was present in at least equal concentrations. In samples containing two or three times more Si than Fe, the concentrations of U_3Si and U_6Fe were approximately equal. These observations corroborate the selected area diffraction work, showing that Si was highly soluble in U_6Fe. Alloys with 800 ppm Al in addition to the Fe and Si contained less U_6Fe and U_3Si than corresponding alloys with 25 ppm Al, indicating that Fe and Si were soluble in UAl_2.

One alloy, containing 250 ppm Fe and 25 ppm Si, had a microstructure radically different from any of the other alloys examined. Networks of U_6Fe precipitates were present after beta quenching, and alpha annealing caused additional precipitation of U_6Fe in a Widmanstatten pattern (Figure 6). No explanation can be given for this unusual behavior since the chemical analyses did not indicate an abnormally high Fe content.

REFERENCES

1. Boland, J. F., H. C. Kloepper, Jr., and N. F. Neumann. "The Alloying Influence or Iron and Silicon on the Grain Size of Beta Heat-Treated Dingot Uranium". Process Development Quarterly Progress Report. MCW-1465 (August 1961).

2. Bellamy, R. G. "The Swelling of Alpha-Uranium under Neutron Irradiation to 0.7 at .% Burnup". Symposium on Uranium and Graphite. Institute of Metals. (1962).

3. Angerman, C.L. "High-Temperature Metallography of Uranium". Presented at the 15th Meeting of the AEC Metallography Group. E. I. du Pont de Nemours and Co., Savannah River Laboratory, Aiken, S. C. (1961), NMI-4996.

4. Mathews, C.O. "The Precipitation of Impurities in Commercial and High-Purity Uranium". Technical Papers of the Tenth Metallographic Group Meeting Held at Knolls Atomic Power Laboratory, October 24, 1955. TID-7523 (Pt. 2) (declassified September 30, 1960).

5. Robillard, A. Influence of Heat Treatment in β and γ Phases on the Microscopic Structure of Uranium. Commissariat a l'Energie Atomique, Paris, France. CEA-1057 (1959).

6. Althaus, W. A. and M. M. Cook. "An Anomalous Structure Produced by Etching Polished Uranium Surfaces with 1:1 Nitric Acid". Summary Technical Report for the Period April 1, 1962 to June 30, 1962. NLCO-855 (1962).

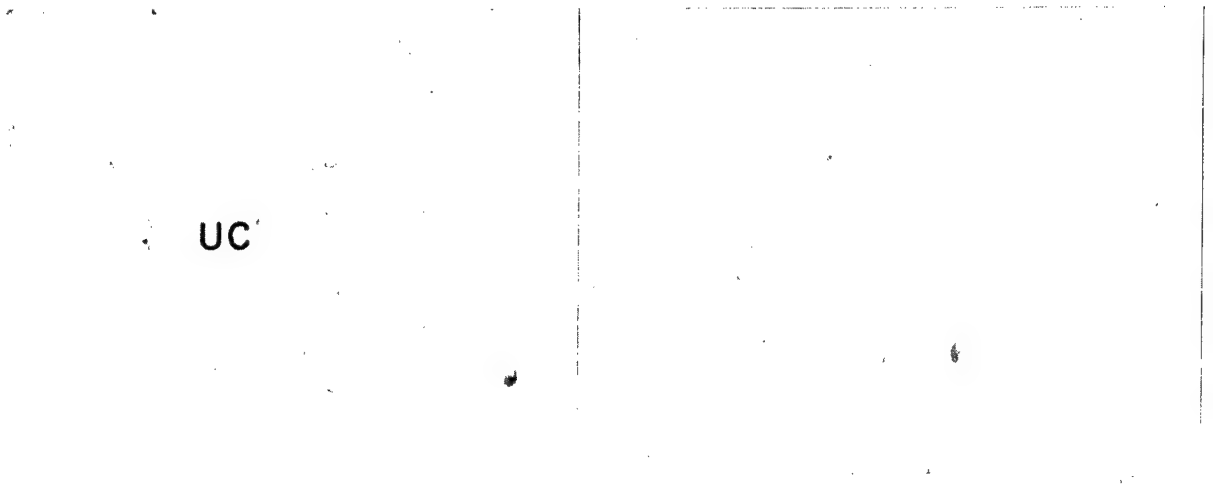

a. U_6Fe Particles. Both triangular and round shapes, rounded interfaces. 4000X. 1268A.

b. U_3Si Particles. Striated surface. 7800X. 1090A.

c. UAl_2 Particles. Round shape, interfaces. 7800X. 1110B.

Figure 1. Typical Appearances of Precipitate Particles.

a. Alloy: 150 ppm Fe - 100 ppm Si - 10 ppm Al. 2000X. 1000A.

b. Alloy: 350 ppm Fe - 30 ppm Si - 800 ppm Al. 5400X. 1097D.

Figure 2. Eutectoid Structures in As-Cast Alloys.

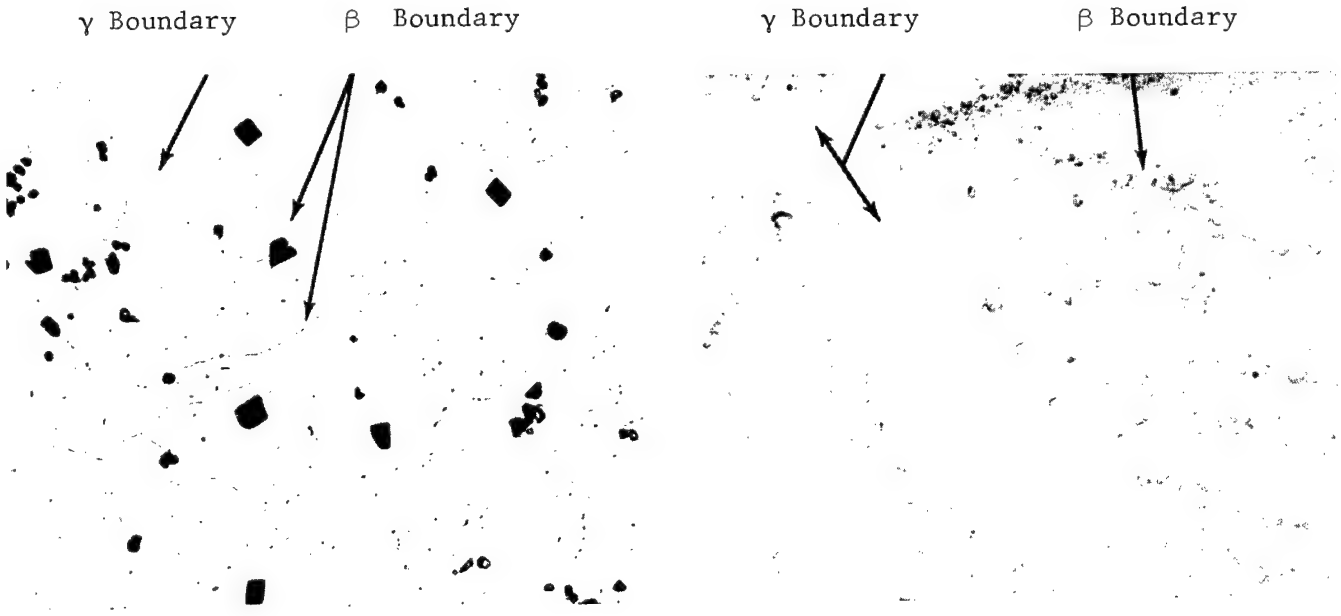

a. Network Revealed by Electrolytic Nitric Acid Etch. 250X. 44540.

b. Rows of Pits Which Form the Lines Shown in Figure 3a. 7800X. 1156B.

Figure 3. Networks of Incipient Precipitates in Gamma Quenched Alloys.

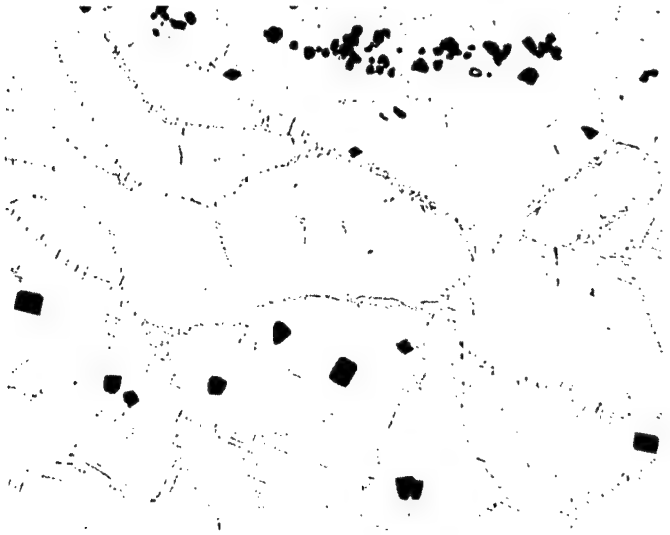

a. Electrolytic Nitric Acid Etch.
250X. 46936.

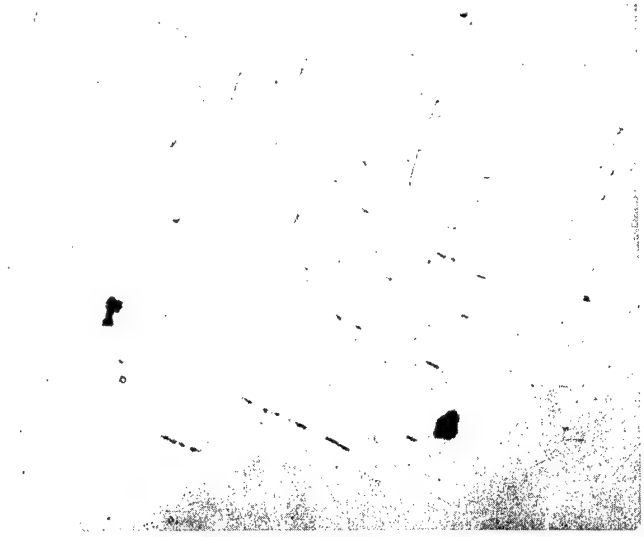

b. Phosphoric Acid Electropolish.
7800X. 1166A.

Figures 4a and 4b show networks of discrete UC precipitates formed during air cooling.

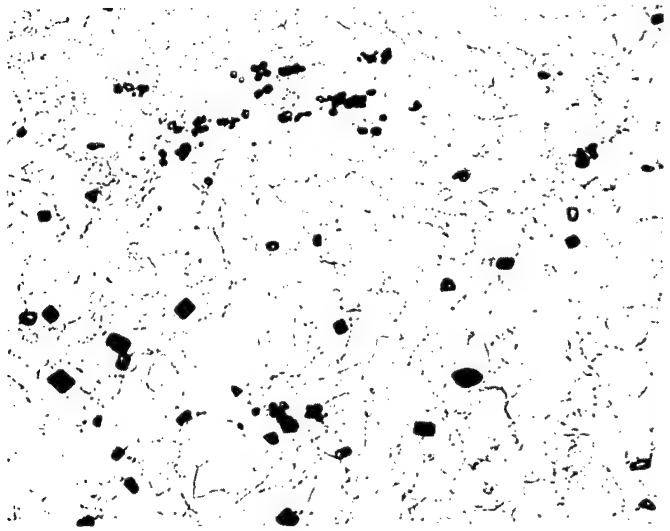

c. Electrolytic Nitric Acid Etch.
250X. 50982.

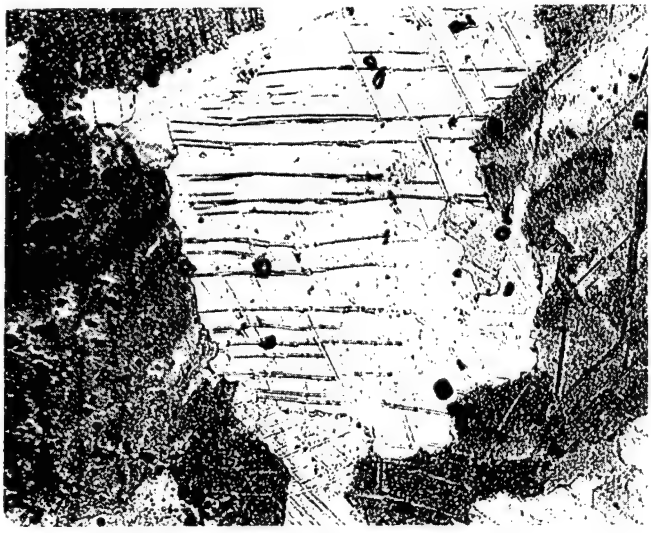

d. Chromic-Acetic Acid Etch.
250X. 51020.

Comparison of Figures 4c and 4d shows the necessity for more severe nitric acid etch to reveal incipient precipitates in samples quenched in 50% $CaCl_2$ at -50°C. Structure in Figure 4d was etched more severely than in Figure 4c to insure that if networks were present they would be revealed.

Figure 4. Effect of Cooling Rate from Gamma Temperatures on Network Structures.

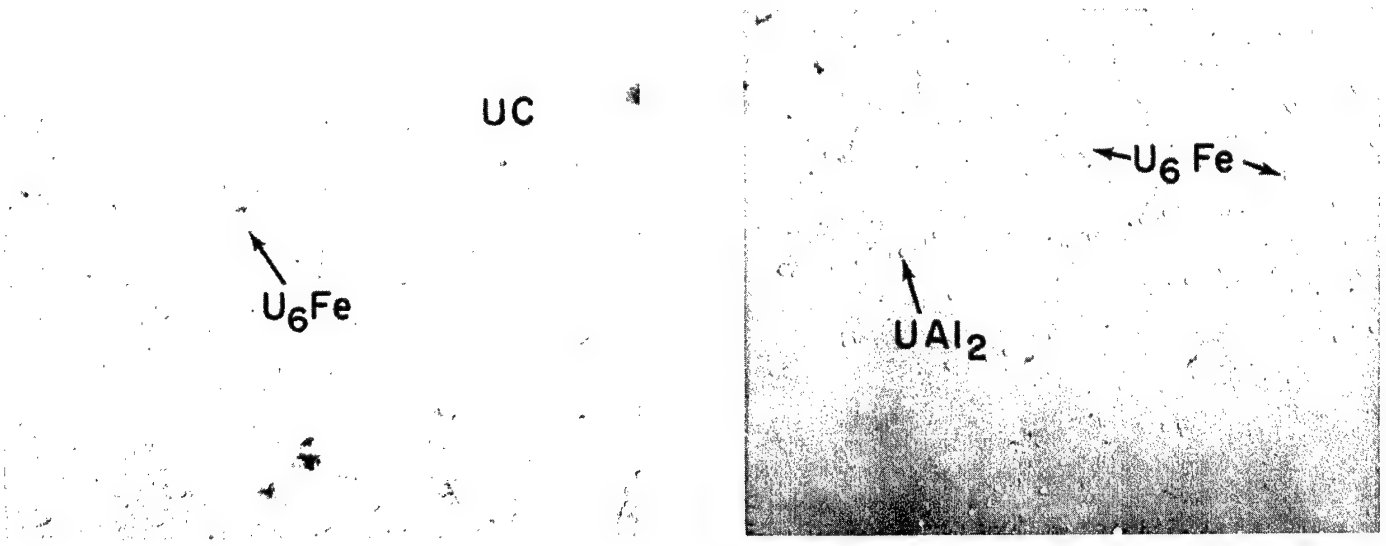

a. U_6Fe Precipitated in Networks. 7800X. 1238C.

b. U_6Fe Precipitated Randomly. 4000X. 1235C.

Figure 5. U_6FE Distributions Produced by Alpha Annealing.

This pattern was observed in only one sample.

Figure 6. U_6Fe Precipitated in a Widmanstätten Pattern. 4000X. 1268B.

PLUTONIUM METALLOGRAPHIC PRACTICES AT BATTELLE

R.H. Snider, V.W. Storhok, and M.S. Farkas
Battelle Memorial Institute

A wide variety of plutonium-bearing materials have been prepared for metallographic examination at the Battelle Plutonium Laboratory. Operating philosophy, equipment, general metallographic procedures as well as specific techniques for such materials as oxides, nitrides, and several metallic alloys are described.

Extreme toxicity necessitates stringent handling requirements to prevent ingestion of even minute quantities of plutonium by laboratory personnel. In order to minimize the chances of accidental ingestion, Battelle has adopted a policy of complete containment of plutonium during all metallurgical and most other operations. This policy has proved to be very successful. In three years of operation, no internal plutonium ingestion has occurred.

The Battelle Plutonium Facility is located at the Battelle Nuclear Center near West Jefferson, Ohio, and is a separate building designed specifically for plutonium work. A floor plan of the building is shown in Figure 1.

Most of the laboratory equipment is housed in mild steel or stainless steel glove boxes built at Battelle and generally designed for the equipment involved. These boxes are all kept at a negative pressure of 1/2 to 1 inch water, so that any leakage is into the box. A dry, inert gas is employed as an atmosphere in boxes where oxidation of specimens may be a problem. Nitrogen from a liquid nitrogen source is generally used for glove box atmospheres although helium or argon can also be supplied if necessary. A constant flow of about 6 to 10 cubic feet of gas per hour is enough to keep the oxygen content in the box below 2 percent. This is supplemented by a solenoid valve which opens and introduces a surge of gas whenever box pressure becomes too negative, as when gloves are pulled out rapidly. Both inlet and exhaust lines are filtered to prevent contamination of gas and ventilating ducts. Glove box gloves are made of neoprene impregnated with lead to attenuate the soft gammas emitted by plutonium. To date, finger and body badges have indicated that personnel gamma exposures have been far below tolerance levels.

Most of the metallography equipment is housed in the three interconnected boxes circled in Figure 1 and shown in Figure 2. The box partially visible in the right rear of the photograph is used for grinding and polishing; the center box is for etching; and the plexiglass box contains a microscope, camera, and microhardness tester. Mounting equipment is in a separate box along with equipment for cutting and filing specimens.

Metallographic specimens are generally cut with a hand hacksaw and one face is filed flat. The specimen is then set face down in a Lucite ring which has the bottom side covered with an adhesive aluminum tape. The ring is then filled with a room-temperature setting plastic. In order to minimize bubble formation in the plastic, the mount is placed under a pressure of 2 to 3 psi nitrogen while the plastic is setting. A shallow pressure cooker has been modified to serve as the pressure vessel.

After the plastic has set, the tape is removed, the specimen and mount surfaces are evened by filing, and then hand ground through 600 silicon carbide paper. Polishing proceeds on 6 micron and 1 micron diamond wheels. Since space is at a premium, one polishing drive unit is used with several different polishing wheels. Final polishing is generally accomplished with 1/2 micron diamond on a vibratory polisher. Chemically pure carbon tetrachloride is used as a lubricant in most grinding and polishing operations. In addition to filling the requirements of being free of moisture and being non-reactive with the specimens, carbon tetrachloride is readily disposable through evaporation. If possible, use of polishing media other than diamond paste is avoided as they tend to cake when the carbon tetrachloride lubricant evaporates. Since all the grinding and polishing equipment is confined to a relatively small enclosed area and it is easy for abrasives to be inadvertently spread, cleanliness is of utmost importance. Consequently, the area is cleaned frequently and most equipment is covered when not in use.

The etching box contains facilities for both chemical and electroetching. Some of the greatest difficulties encountered in metallographic examination of plutonium materials have been associated with etching. These difficulties have largely stemmed from etchants behaving differently on the same material in different conditions of heat treatment. However, it was generally possible to develop satisfactory etchants for all specimens. Some examples of microstructures obtained from materials studied are shown in Figures 3 through 8.

All metallographic examination and photography is done with an A.O. Spencer metallurgical microscope fitted with a tri-nocular head to permit use of a camera attachment. The eyepiece and camera tubes come out of the box through a neoprene diaphragm. The inside of each tube has a glass contamination barrier sealed to the tube with a rubber compound. Although the microscope and camera are not as sophisticated and versatile as a metallograph, the results have been generally satisfactory.

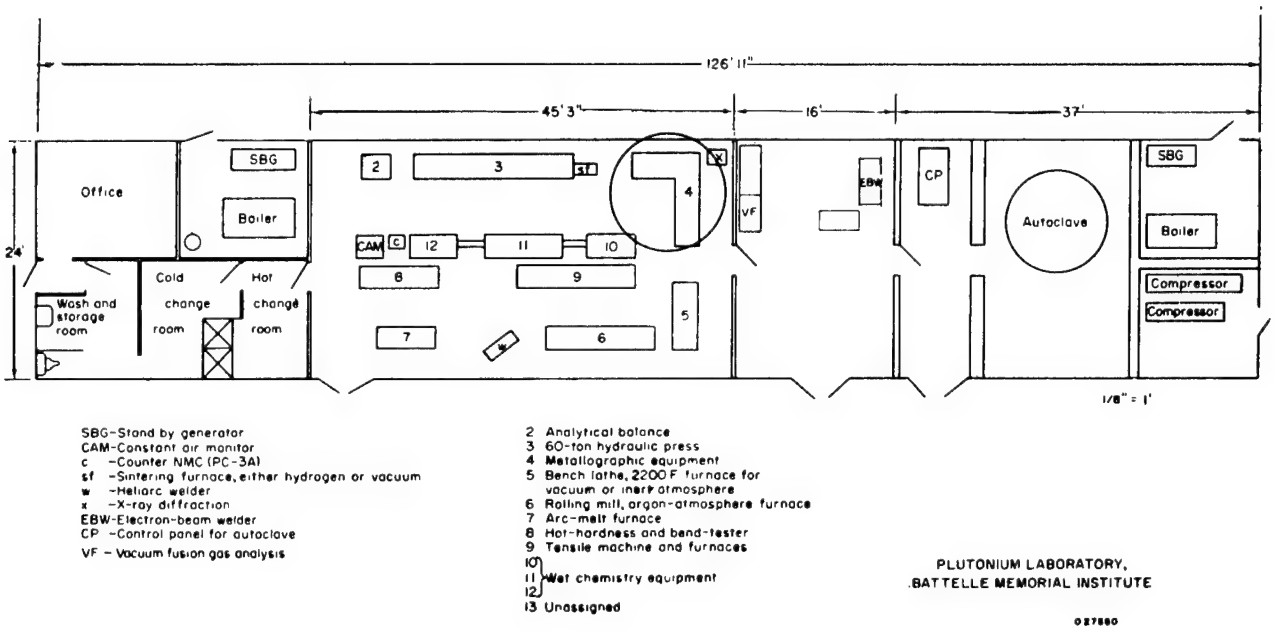

Figure 1. Floor Plan of Battelle Plutonium Facility.

Figure 2. Metallography Boxes at Battelle Plutonium Facility.

Figure 3. Th-5 $^{w}/_{o}$ Pu. Cold reduced 90% and heat treated one minute at 650°C. Etch: 100cc ethyl alcohol, 10cc perchloric acid 2 sec. at 40v. 400X. PL98.

Figure 4. Nb-25.6 ^{w}/o Pu-6.1 ^{w}/o Si (Nb-30 vol % $PuSi_2$), as cast. Etch: 50cc lactic acid, 20cc HNO_3, 3cc HF-swab. 200X. PL160.

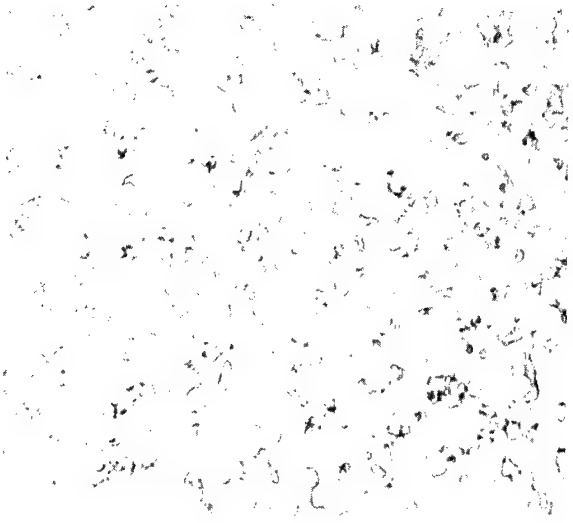

Figure 5. Fe-27.6 ^{w}/o Pu-11.9 ^{w}/o Cr (Fe/20Cr-30 vol % $PuFe_2$), pack rolled to 80% reduction at 900-950°C. Etch: 80cc ethyl alcohol, 20cc HNO_3, 3d. HF, 40-60v. 800X. PL533.

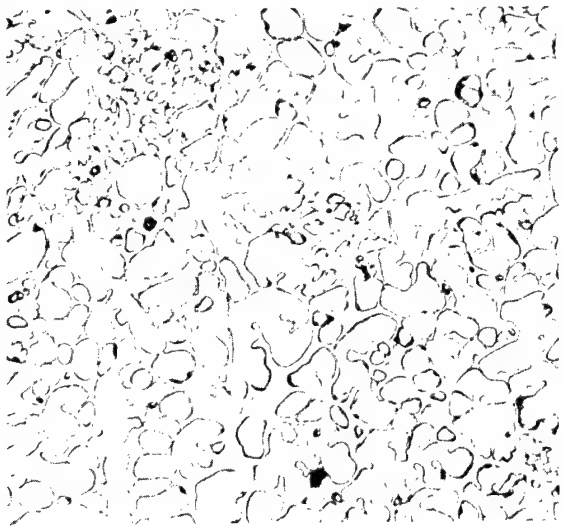

Figure 6. U-10 w/o Nb-5 w/o Pu, 26 Hrs. 900°C, Oil Quenched. Etch: 80cc ethyl alcohol, 20cc HNO_3, 4d. HF, 60v. 200X. PL581.

Figure 7. Arc Melted PuN. Etch: 80cc ethyl alcohol, 20cc HNO_3, 6d. HF, 25v. 200X. PL448.

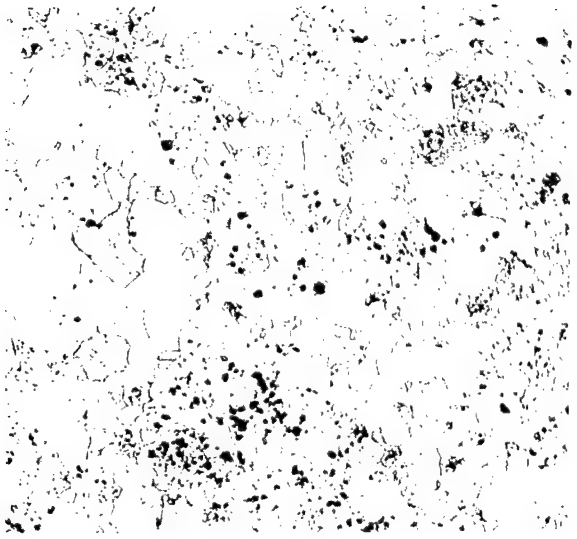

Figure 8. Powder Produced PuN. Etch: 80cc ethyl alcohol, 20cc HNO_3, 3d. HF, 20-60v. 200X. PL513.

A NEW MICROHARDNESS TECHNIQUE

T.M. Kegley, Jr. and B.C. Leslie
Oak Ridge National Laboratory

Conventional microhardness tests using Kentron and Tukon hardness testers are not adequate for resilient materials such as pyrolytic carbon and pyrolytic graphite, since hardness indentations made on such materials vanish upon removal of the test load. However, if a thin pyroxylin film is placed on the specimen before making the microhardness test, then an image of the indentation is retained on the film.
The technique that was developed for coating the pyroxylin film on the specimen so as to record the hardness indentations and some of the test results are described.

INTRODUCTION

In connection with fueled graphite development work at Oak Ridge National Laboratory a request was made of the Metallography Group for a determination of the microhardness of the pyrolytic carbon coatings deposited on uranium carbide fuel particles. A microhardness test was attempted using a conventional microhardness tester but the indentation in the pyrolytic carbon coating could not be found. Indeed, it was found that due to the almost perfect elasticity displayed by the pyrolytic carbon, the indentation had vanished. Thus it became apparent that a different technique would have to be developed for determining the hardness of the pyrolytic carbon coatings.

Direct Measurement

Perhaps the best measurement of the microhardness of an elastic material would be a measurement of the actual penetration of the indenter into the material under a given test load. The Rockwell hardness test accomplishes this for ordinary hardness measurements, but as yet there is no readily available means for measuring the penetration on a microhardness scale.

Indirect Measurements Using Coating Techniques

Indirect measurements of the microhardness of elastic materials can be made by coating either the indenter or the specimen with a coating material which records the indentation made by the indenter in the elastic material.

Two materials used by others for coating* the indenter are graphite and ammonium chloride.(1,2) In one method the diamond indenter was coated with water suspension of graphite; while in the other method

- - - - - - - - - - -

* The coating used for this procedure is described in Appendix A to this publication, page 158.

the diamond indenter was coated with ammonium chloride by allowing ammonium chloride to sublimate and deposit on the diamond. Use of a coated indenter is somewhat awkward because the indenter must be removed from the hardness tester after each indentation in order to observe and measure the indentation trace left on the indenter.

Two materials used by Grodzinski for coating the specimen were silver and flame-deposited carbon soot.(3) For silver he found that a correction had to be made for the load taken up by the silver layer as well as for the thickness(0.01μ) of the silver layer. When flame-deposited carbon soot was used as the material coating the specimen, he stated that no correction was necessary.

At Oak Ridge National Laboratory a technique was developed for coating the specimen with a thin pyroxylin film so as to record the hardness indentations. Using this technique, microhardness measurements were made of the pyrolytic carbon deposited on nuclear fuel particles. For comparison with the measurements obtained for pyrolytic carbon, microhardness measurements were also made of pyrolytic graphite sheet and polycrystalline natural graphite.

For metals the diamond pyramid hardness is essentially an unrecovered hardness since the length of the diagonals is little affected by elastic recovery.(4) With pyrolytic carbon and pyrolytic graphite, however, there is almost complete recovery and the hardness measured is an elastic hardness. To indicate that the microhardness values are for an elastic hardness, we report the DPH values as DPH-G and the Knoop values as KHN-G.

SPECIMEN PREPARATION

The specimens of pyrolytic carbon coated uranium carbide fuel particles were prepared by mounting and vibratory polishing procedures described by DuBose and Gray.(5) In brief, these procedures consisted of mounting the coated particles in epoxy resin, grinding the resulting specimen mount through 600 grit silicon carbide paper, and vibratory polishing the specimen mount 6 hr on a nylon cloth using a slurry consisting of 10 g Linde A alumina and 100 ml of silicone oil.

The pyrolytic graphite and natural graphite specimens were prepared by grinding through 600 grit silicon carbide paper and then vibratory polishing in two stages. First the specimens were vibratory polished 6 hr on a nylon cloth using a slurry which consisted of 75 g Linde A alumina and 300 ml water. Finally the specimens were vibratory polished 1/2 hr on microcloth with a slurry which consisted of 75 g Linde B alumina and 300 ml water.

COATING TECHNIQUE FOR MICROHARDNESS TESTING

Film Materials Investigated

Various materials were coated on specimens in the search for one which would produce the best image of a hardness indentation. Metals were investigated by vacuum evaporating a metallic film on the polished surface. The results from two films, aluminum and chromium, were unsatisfactory since each film frequently stuck to the indenter when the test load was lifted, and left a jagged image of the indentation. Figure 1 shows a jagged indentation made in an aluminum film which was vacuum evaporated on a specimen mount containing coated particles. Carbon which was vacuum evaporated was also unsatisfactory since a usuable image of the indentation was not obtained. Several organic materials, used in replication for electron microscopy, were also coated on the specimens. Each of these materials were dissolved in a suitable solvent and placed on the surface of the polished specimen. A film of the organic material was then left on the polished surface upon the evaporation of the solvent. The organic replica materials indluded:

(1) 10% Saran, methyl ethyl ketone solvent
(2) Cellulose acetate (Fac film), acetone solvent
(3) 1-1/4, 2, 2-1/2, 5% pyroxylin (Parlodion), amyl acetate solvent.

Of the organic replica materials, pyroxylin gave the most consistent results and was the material finally selected.

Effect of Pyroxylin Film on Microhardness Values

The effect of the pyroxylin film upon the determined microhardness values had to be considered. Diamond pyramid hardness measurements were made of a nickel specimen both in the coated and uncoated conditions. The pyroxylin film was applied to the nickel specimen by two methods.

(1) A drop of the 5% pyroxylin amyl acetate solution was placed on the specimen and the specimen turned vertically so as to drain excess toward the edge.
(2) A drop of the same solution was placed on the specimen and spread evenly over the polished surface with a cotton swab.

Table I shows the effect of the pyroxylin film on the microhardness values determined. In method 1 the film apparently was thick enough to enlarge the apparent indentation and subsequently lower the numerical diamond pyramid hardness values by 10 points or more. When method 2 was used there was no significant difference between the microhardness values obtained with and without the pryoxylin film.

TABLE I

EFFECT OF PYROXYLIN FILM ON THE MICROHARDNESS VALUE DETERMINED

	Range DPH 100 g load	Average DPH 100 g load
Nickel, uncoated	90.6 - 100.2	96.5
Nickel, coated by method 1: a drop of solution is placed on specimen and specimen turned vertically	80.0 - 89.8	83.4
Nickel, coated by method 2: a drop of solution is placed on specimen and spread evenly with cotton swab	90.6 - 98.7	95.0

Procedure for Coating with Pyroxylin Film

The pyroxylin film is placed on the specimen, for which the microhardness is to be determined, by placing on the polished surface a drop of the coating solution which consists of 5% pyroxylin dissolved in amyl acetate. Upon evaporation of the amyl acetate solvent the pyroxylin film is in place and the specimen is ready for microhardness testing.

If desired the pyroxylin film can be removed by washing the specimen with ethyl alcohol or amyl acetate.

MICROHARDNESS RESULTS

Microhardness measurements were made with a Kentron microhardness tester using both 136^{o} diamond pyramid and Knoop indenters under 100 g load.

Microhardness of Pyrolytic Carbon Coatings

Pyrolytic carbon is deposited on the fuel particles by the decomposition of a carbonaceous gas under proper conditions of gas composition, flow rate, temperature and pressure. Depending on process conditions, one or both of two types of pyrolytic carbon may be deposited. Figure 2 illustrates the laminar and columnar types of coatings deposited on uranium carbide fuel particles.

Figure 3a shows four diamond pyramid hardness indentations made on a laminar type coating. After removal of the pyroxylin film by washing the specimen with amyl acetate, the indentation images have vanished and the area of the indentations appears as in Figure 3b. Figure 4 shows two diamond pyramid hardness indentations made on a columnar type coating.

Microhardness was determined with the indenter direction parallel to the fuel particle surface and also with the indenter direction perpendicular to the fuel particle surface as indicated in Figure 5. Microhardness values obtained for the pyrolytic carbon coatings are given in Table II. For the indenter direction parallel with the fuel particle surface the average microhardness for the laminar coatings of four specimens varied from 126 to 199 DPH-G, while the average microhardness for this direction for the columnar coatings varied from 59 to 76 DPH-G. For the indenter direction perpendicular to the fuel particle surface the average microhardness for the laminar coatings of four specimens varied from 109 to 192 DPH-G, while the average microhardness for this direction for the columnar coatings varied from 30 to 80 DPH-G. Thus all the laminar coatings were harder than the columnar coatings.

TABLE II

MICROHARDNESS OF PYROLYTIC CARBON COATINGS DEPOSITED ON URANIUM CARBIDE FUEL PARTICLES

Indenter Direction

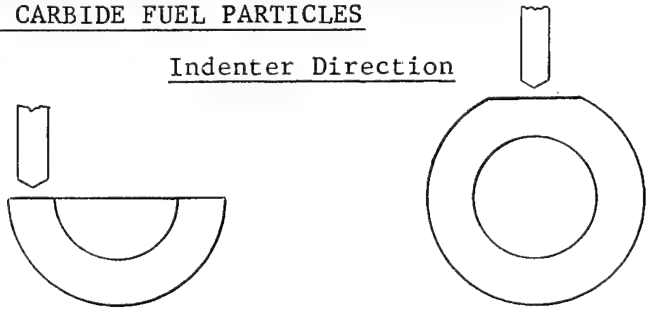

Specimen	Type of Coating	Parallel to Fuel Particle Surface		Perpendicular to Fuel Particle Surface	
		Range DPH-G 100 g load	Average DPH-G 100 g load	Range DPH-G 100 g load	Average DPH-G 100 g load
A	Laminar	186 - 204	197	183 - 198	192
B	Laminar	184 - 207	199	169 - 191	179
C	Laminar	161 - 187	173	139 - 160	152
D	Laminar	115 - 150	126	97 - 122	109
E	Columnar*	70 - 81	76	78 - 85	80
F	Columnar*	51 - 63	59	38 - 48	43
G	Columnar	67 - 78	73	32 - 46	39
H	Columnar	64.5 - 75	70	69 - 76	73

* Actually duplex coating, but hardness indentations were made in columnar portion.

Microhardness of Pyrolytic Graphite Sheet

Pyrolytic graphite consists of layers of carbon atoms which are arranged in a hexagonal pattern, the layers being randomly oriented with respect to each other. The "c" direction is considered to be the direction perpendicular to the layers or the direction perpendicular to the surface of deposition.

The anisotropy of the pyrolytic graphite sheet was particularly evident in its microhardness behavior. Figure 6, which shows 136° diamond pyramid and Knoop indentations made at 100 g test loads on a section of pyrolytic graphite taken parallel to the "c" direction, illustrates this anisotropic behavior. In Figure 7 the Knoop indentations with the long diagonal essentially parallel to the layers appear almost as lines, while those with the long diagonal in the "c" direction appear more like the usual Knoop indentations.

Microhardness was determined with the indentor direction parallel to the layers and also with the indenter direction parallel to the "c" direction as shown in Figure 5. Microhardness measurements for the pyrolytic graphite sheet are summarized in Table III.

TABLE III

MICROHARDNESS OF PYROLYTIC GRAPHITE SHEET

	Indenter Direction			
	Parallel to Layers		Parallel to "c" Direction	
	Range	Average	Range	Average
Diamond Pyramid, Hardness-G, 100 g load	50 - 56	53	44 - 52	49
Knoop Hardness Number-G, 100 g load			44 - 50	46
Long diagonal in "c" direction	90 - 100	97		
Long diagonal parallel to layers	31 - 35	34		

For the indenter direction parallel to the layers the average microhardness was 53 DPH-G, while for the indenter direction parallel to the "c" direction the average microhardness was 49 DPH-G. The Knoop hardness for the indenter direction parallel with the layers depended on the orientation of the indenter. For the indenter direction parallel with the layers but with the long diagonal parallel to the layers, the average hardness was 34 KHN-G. For the indenter direction parallel with the layers but with the long diagonal parallel to the "c" direction, the average hardness was 97 KHN-G.

Microhardness of Natural Graphite Specimen

An effort was made to measure the microhardness of a natural graphite specimen from Ceylon using the same technique used for the pyrolytic carbon coatings and the pyrolytic graphite sheet. The natural graphite specimen when tested did not display the resiliency observed for the pyrolytic carbon coatings and the pyrolytic graphite sheet. Figure 7 shows the appearance of a diamond pyramid indentation in the natural graphite specimen. Although the indentation was made with the same 100 g test load used for the other specimens, the size of the indentation in the natural graphite specimen was very much greater.

Rough measurements of indentations made in the natural graphite specimen yielded a hardness of 6 or 8 DPH, which is much lower than the average values of 53 and 49 DPH-G found for the pyrolytic graphite.

DISCUSSION

In the discussion which follows three aspects concerning the behavior of the specimens, as brought out by the hardness tests, will be mentioned briefly.

Hardness Variation

Some variation was observed in the hardness values obtained from different indentations in pyrolytic carbon coatings of the same specimen. This variation may be due in part to differences in the thickness of the pyroxylin film since it was found that a thick pyroxylin film on a nickel specimen resulted in significantly lower hardness values. More probably the variation is due to other factors since care was taken to use as thin pyroxylin film as possible. The hardness variation may be associated with such factors as the position of the plane of sectioning of the coated particle, actual differences existing between particles of the same batch, and experimental scatter in the hardness test.

Anisotropic Behavior of Pyrolytic Graphite

The anisotropic nature of pyrolytic graphite is reflected strongly in the microhardness tests, particularly when the Knoop indenter is used. With the indenter direction in each case parallel to the layers, the Knoop hardness was 34 KHN-G when the long diagonal was parallel to the layers and 97 KHN-G when the long diagonal was parallel to the "c" direction. A similar anisotropic behavior is observed in pyrolytic graphite's elastic properties. Along the layers Young's modulus is 4,500,000 psi, while across the layers it is 1,500,000 psi.(6)

Behavior of Natural Graphite

The low hardness exhibited by the natural graphite specimen was somewhat surprising. Yet the natural graphite specimen differs from the pyrolytic graphite sheet in several important respects and would not be expected to behave exactly as pyrolytic graphite. The natural graphite specimen consisted of randomly oriented crystals, while the pyrolytic graphite specimen consisted of highly oriented crystals. The natural graphite specimen may have been more porous and this would have resulted in a low hardness.

Grisdale et al.,(7) have observed a Moh's hardness of about 9.8 for pyrolytic carbon produced at 1000°C and a Moh's hardness of 1.0 to 1.5 for polycrystal graphite. Their measurements were made by scratch hardness and rocking pendulum methods and thus measure somewhat different characteristics than do indentations microhardness tests. Nevertheless, their results show pyrolytic carbon to be much harder than polycrystal graphite, which is in agreement with the results reported here.

SUMMARY

A technique has been developed to measure the indentation microhardness of elastic materials such as pyrolytic carbon coatings deposited on nuclear fuel particles and pyrolytic graphite. The technique, through the use of a thin transparent pyroxylin film, allows conventional tests to be run on microhardness testers such as Kentron and Tukon hardness testers.

The hardness measurements showed the laminar type of pyrolytic carbon coating to be harder than the columnar type, 97-207 DPH-G for the laminar as opposed to 32-81 DPH-G for the columnar. The columnar coating was found in some instances to be harder and in other instances to be softer than the pyrolytic graphite sheet, which varied in hardness from 44 to 56 DPH-G. Rough measurements of a polycrystalline natural graphite specimen indicated a hardness of 6 to 8 DPH.

REFERENCES

1. C. B. Brodie and R. Smoluchowski, discussion of D. R. Tate's paper, "A Comparison of Microhardness Indentation Tests", ASM Transactions, 35, 388 (1945).

2. E. B. Bergsman, "Some Recent Observations in Microhardness Testing", ASTM Bulletin, 176, 37-43 (1951).

3. P. Grodzinski, "Elastic and Plastic Hardness of Hard Materials", Nature, 169, 925-26, (1952).

4. H. Bückle, "Progress in Micro-Indentation Hardness Testing", Metallurgical Reviews, 4 (13), 49-100 (1959).

5. C.K.H. DuBose and R. J. Gray, Metallography of Pyrolytic Carbon Coated and Uncoated Uranium Carbide Spheres, ORNL-TM-91 (Mar. 21, 1962).

6. R. J. Diefendork and E. R. Stover, "Pyrolytic Graphite. . . How Structure Affects Properties", Metal Progress, 81 (5), 103-108, May 1962.

7. R.O. Grisdale, A. C. Pfister, and W. Van Roosbroeck, "Pyrolytic Film Resistors: Carbon and Borocarbon", Bell System Tech. J., 30, 271-314 (1951).

Figure 1. Diamond Pyramid Hardness Indentations Made in Aluminum Film Which Was Deposited on Polished Section of Pyrolytic Carbon Coated Fuel Particles. Y-50428.

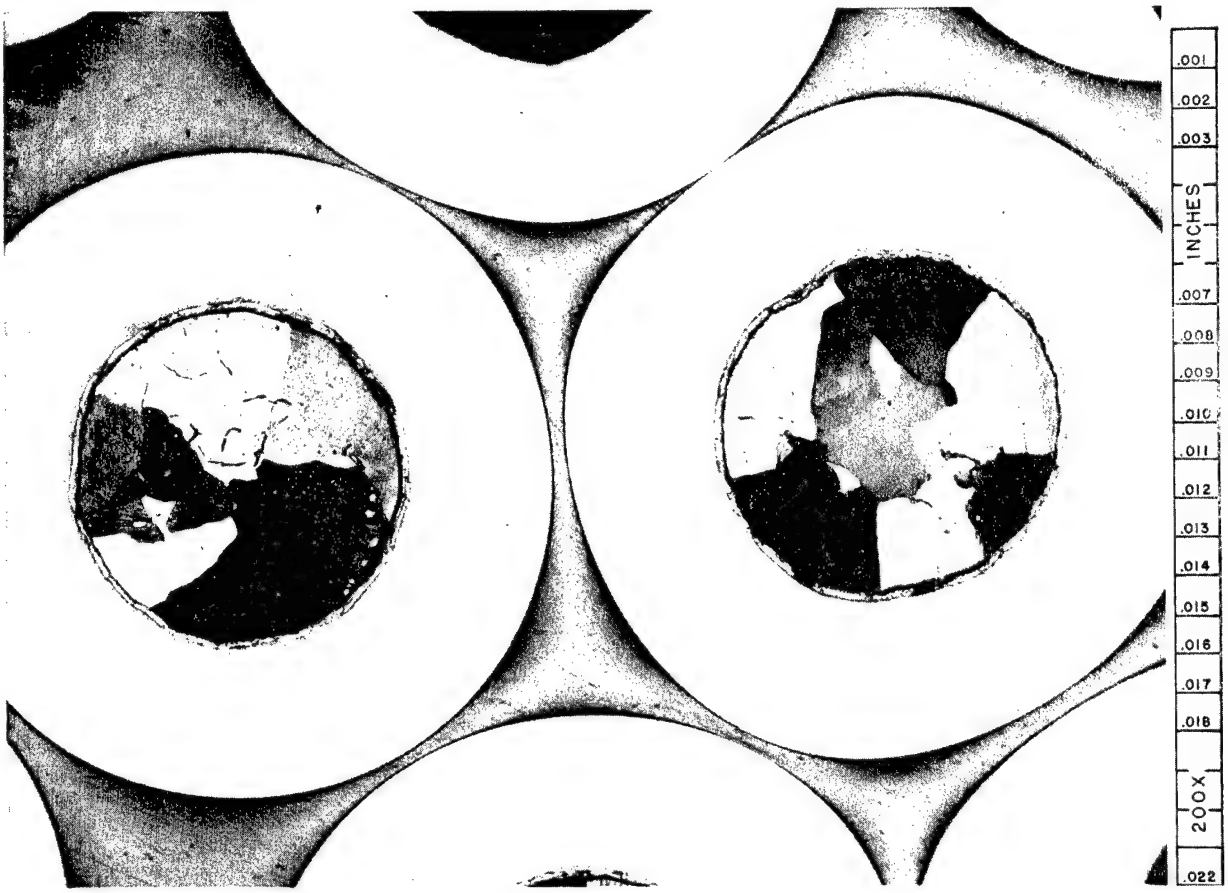

Figure 2. Pyrolytic Carbon Coatings on Uranium Carbide Fuel Particles. (a) Laminar Type Coating, Bright Field Illumination. Y-27296. (b) Columnar Type Coating, Polarized Light Illumination. Y-39525.

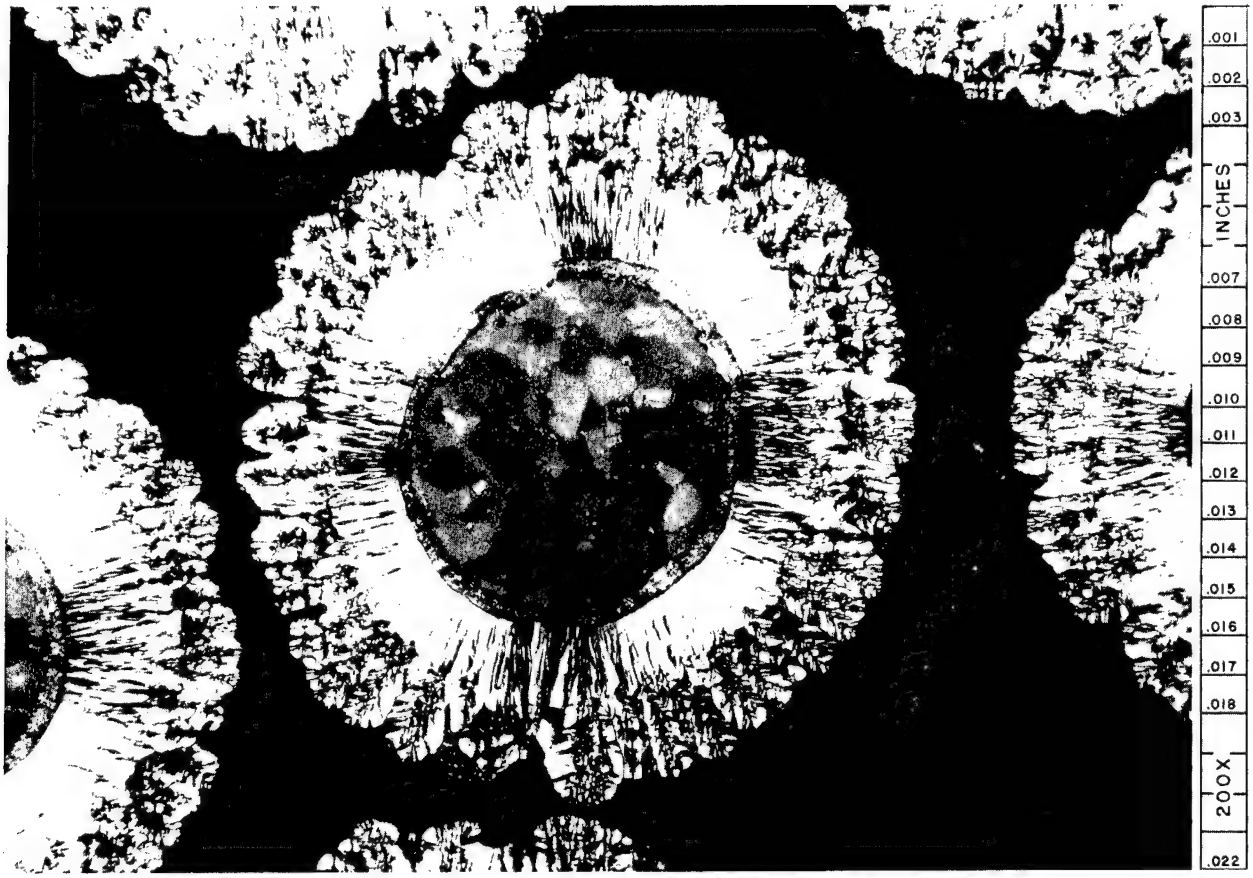

Figure 2. (Continued).

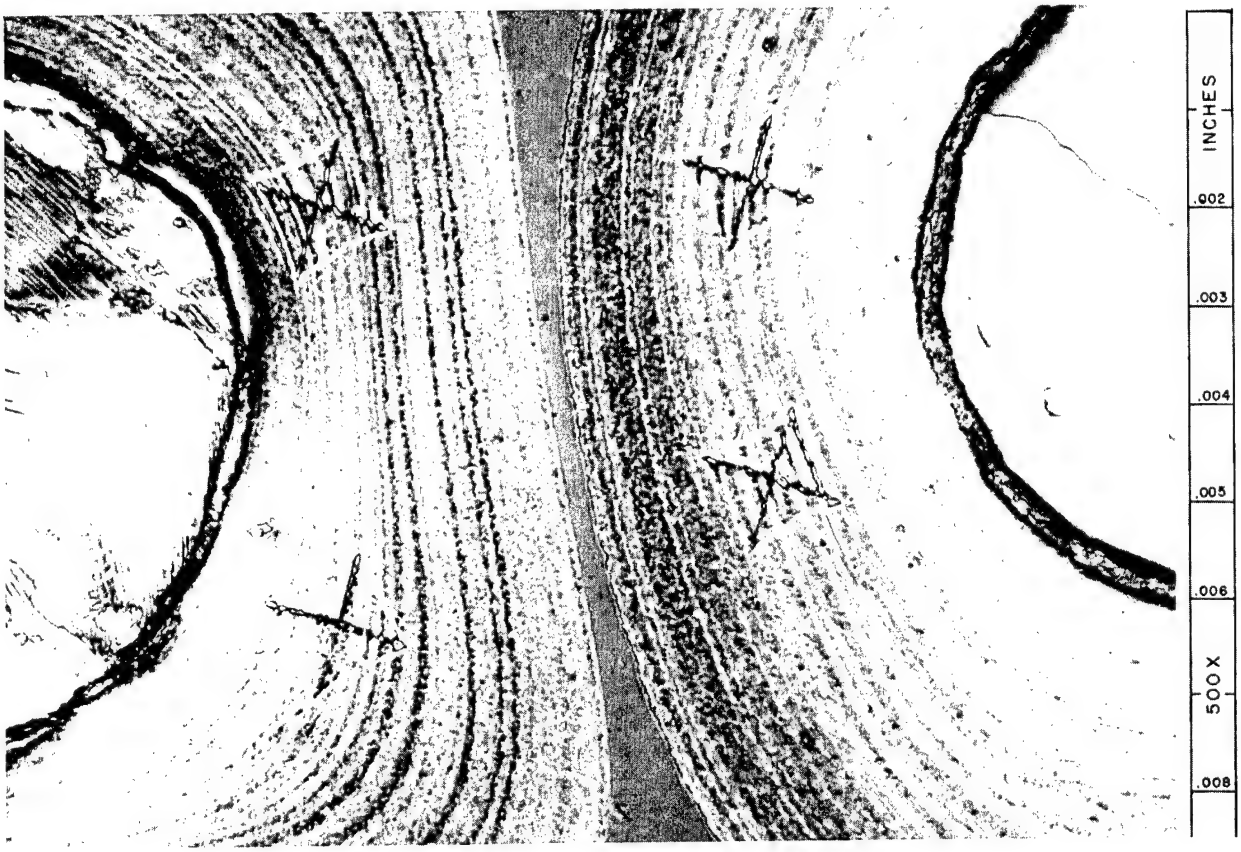

(3a)

Figure 3. Diamond Pyramid Hardness Indentations in Laminar Type Pyrolytic Carbon Coating of Uranium Fuel Particles. Uranium carbide fuel particles have been etched with HNO_3-CH_3COOH-H_2O, but particles appear brighter because of reflection from pyroxylin film. (a) Before Removal of Pyroxylin Film. Y-48435. (b) After Removal of Pyroxylin Film. Y-48676.

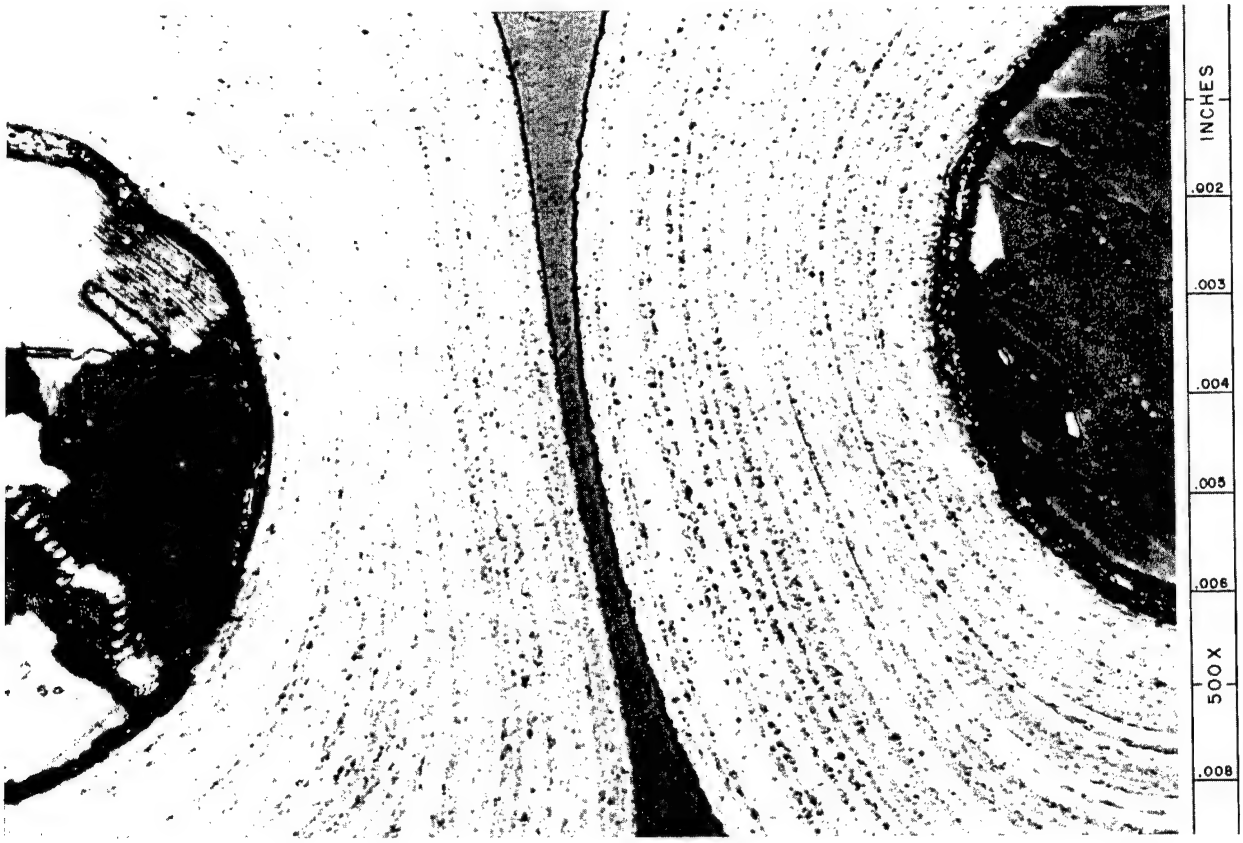

(3b)

Figure 3. (Continued).

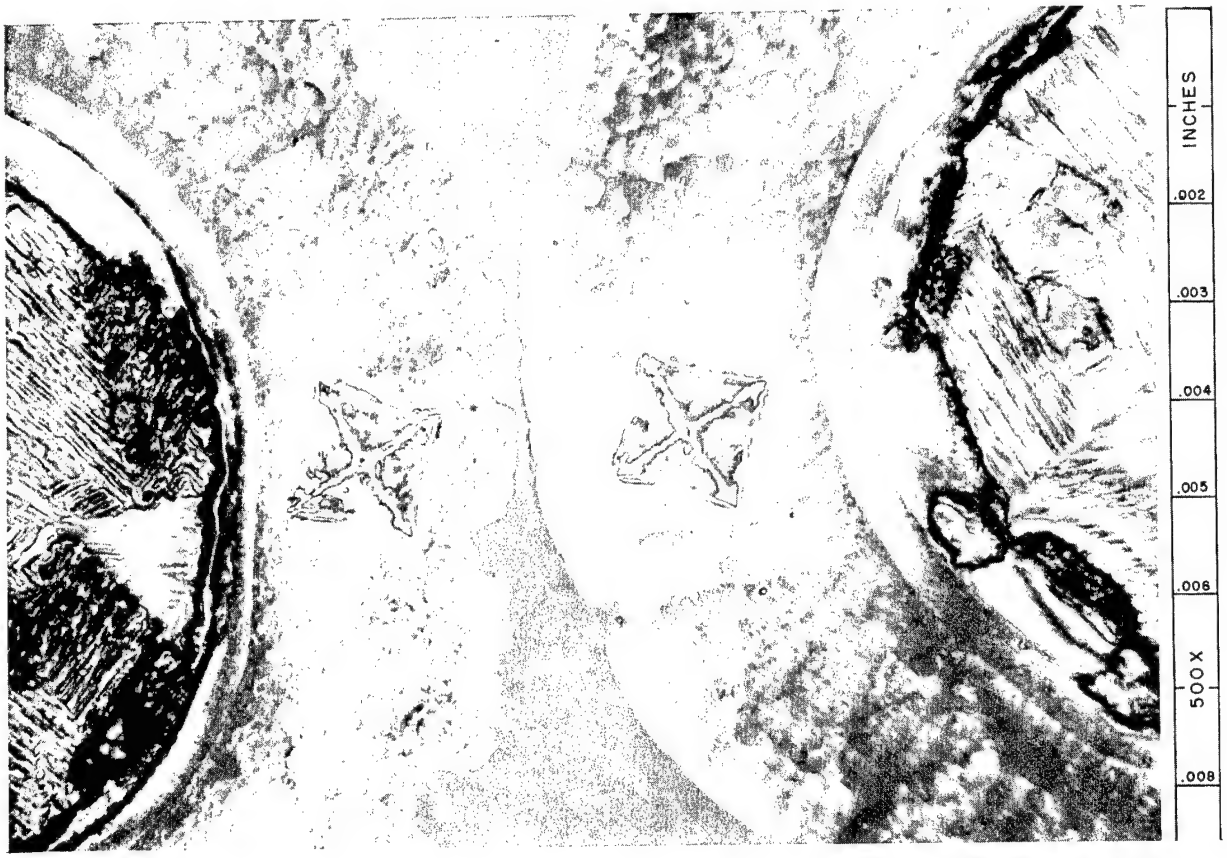

Figure 4. Diamond Pyramid Hardness Indentations Made in Columnar Type Pyrolytic Carbon Coating of Uranium Fuel Particles. Specimen coated with pyroxylin film to record indentations. Y-48685.

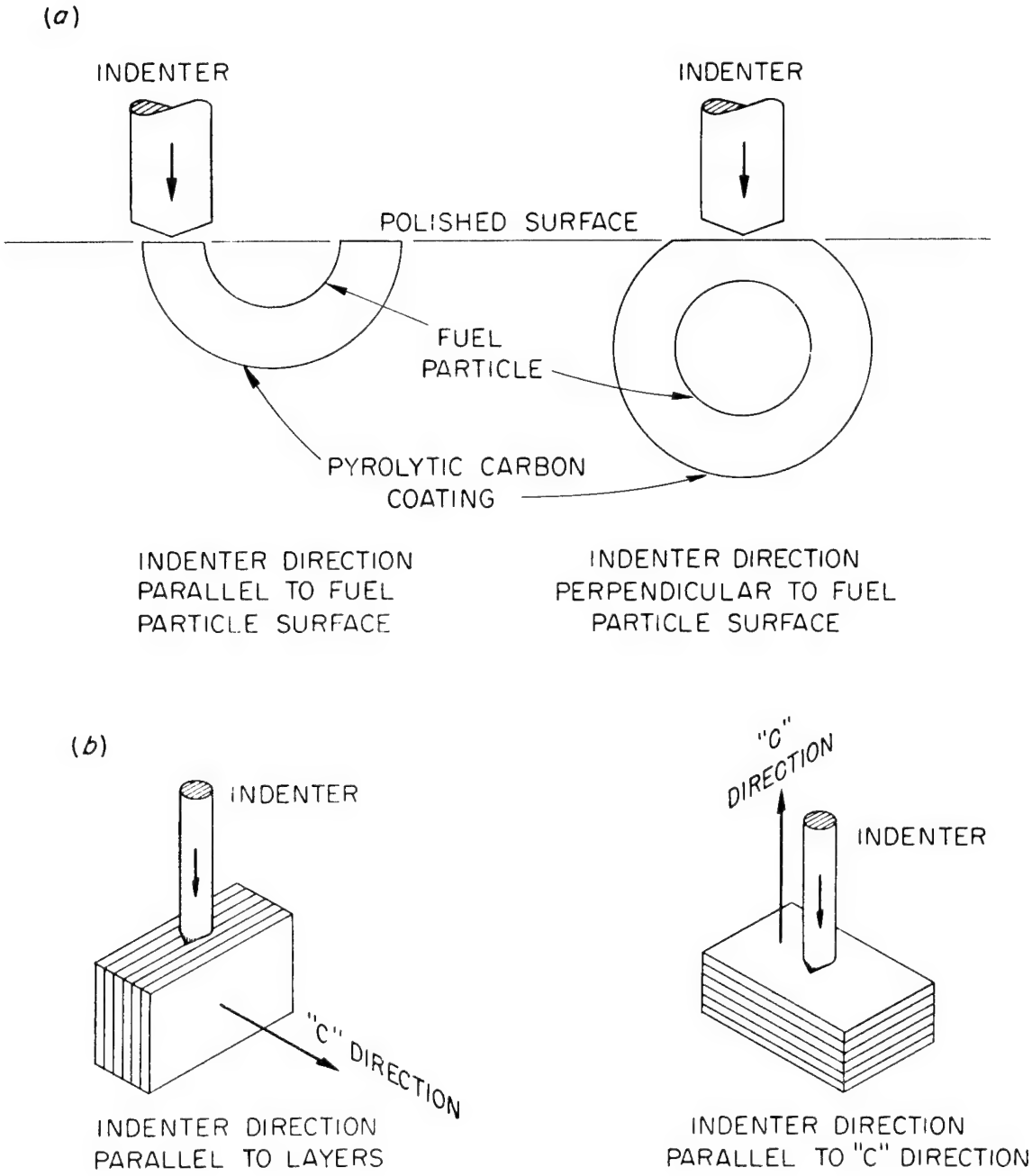

Figure 5. Indenter Directions or the Directions of Movement of the Indenter for (a) Pyrolytic Carbon Coating on Fuel Particles and (b) Pyrolytic Graphite Sheet.

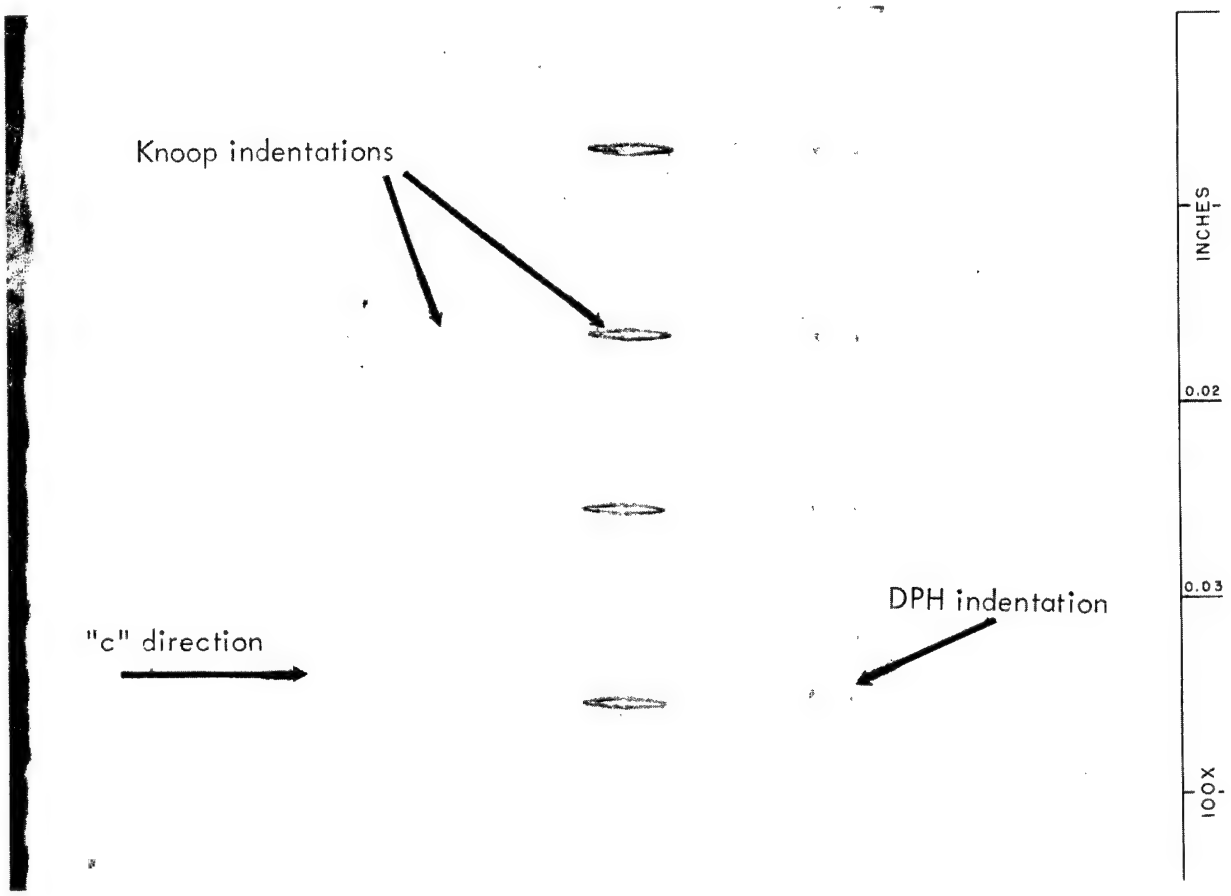

Figure 6. Diamond Pyramid and Knoop Hardness Indentations Made at 100g Load in Pyrolytic Graphite Sheet. Specimen coated with a pyroxylin film to record indentations. Sensitive tint illumination. 100X. Y-38528.

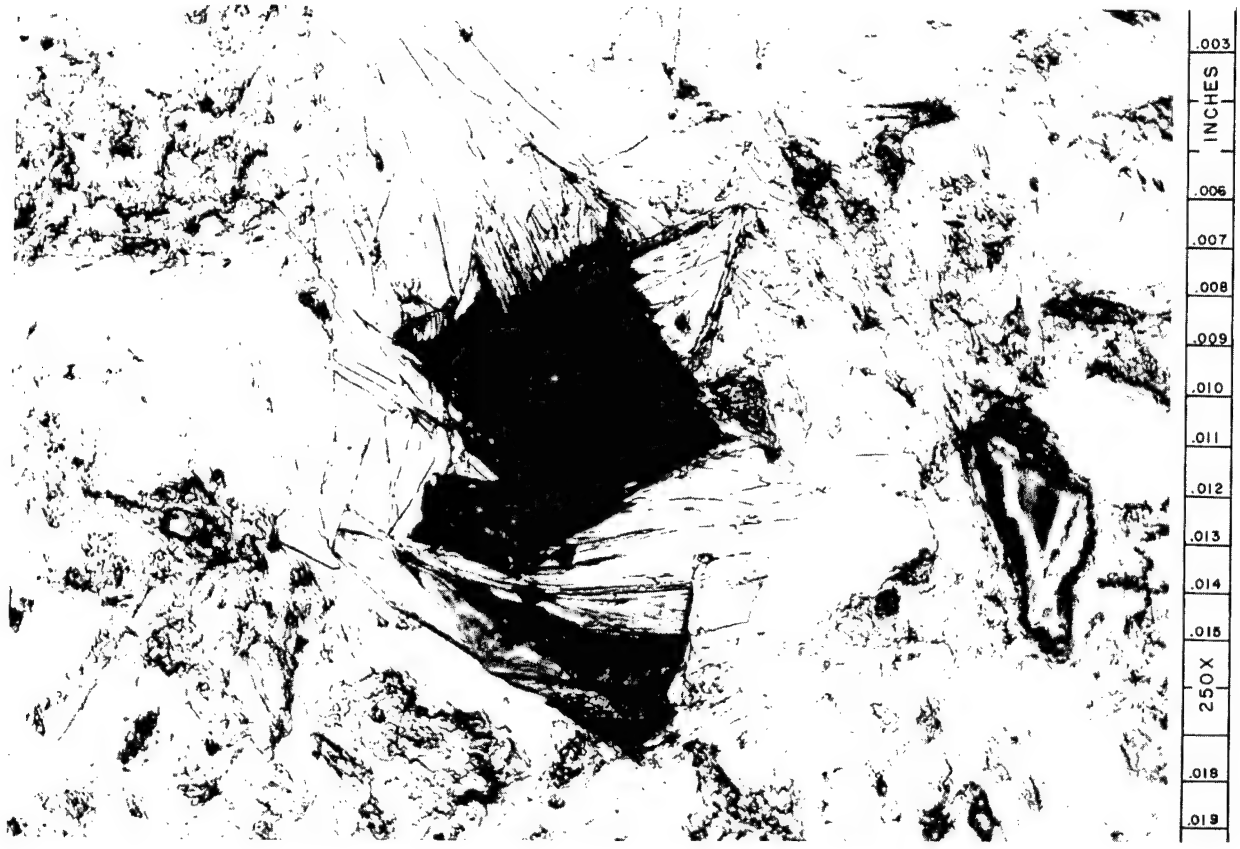

Figure 7. Diamond Pyramid Hardness Indentation at 100g Load in Natural Graphite Specimen. No pyroxylin film was used. Y-48828.

A PORTABLE METALLOGRAPHY LABORATORY

R.S. Crouse
Oak Ridge National Laboratory

During the fabrication of large reactor components in the Oak Ridge National Laboratory and other local area shops, need for on-the-spot metallographic examination became apparent. The components were bulky and difficult to move to a central metallography lab. Although they were too valuable to be cut into small sections, it was permissible for specific areas to be ground and polished in situ for examination. These restrictions on standard metallographic procedures required that some means of polishing, etching and examining be devised to cope with these situations. This report deals with two specific instances, the ways in which they were handled, and the portable kit which evolved.

DEVELOPMENT OF THE KIT

Presentation of the Problem

While the pump housing for the Molten Salt Reactor Experiment was being heat treated at one of the plant sites in Oak Ridge, salt from a nearby heat treating pot spattered on one of the sections. The spatter resulted in some rather unsightly looking pits that disturbed the personnel working on the unit. Before attempts to grind out the pits were started, the shop foreman wished to know if any cracks had occurred in conjunction with the pits. The section was a single casting of INOR-8 weighing about three hundred pounds. A similar section is shown in Figure 1. At that time no means of doing examination in the field was available, so by considerable effort the piece was transported to the Metals and Ceramics Division's Metallography Lab.

Procedure

Once the piece was sitting on the floor of the lab it was possible to grind and polish a spot in the pitted area by hand. Microscopic examination at this point became quite a problem because of the unwieldiness of the specimen and the rather restricted limits of the metallurgical microscope. It was suggested that several cellulose acetate replicas be taken in selected areas, metallized and examined under a microscope. This proved to be quite an effective means of looking at the surface of interest. Figure 2 is a picture of such a replica taken at a pit. This technique enabled the author to assure the shop foreman that no cracks could be found associated with the pits.

The experience with the pump section pointed up a need for some means of taking metallography to the specimen rather than the normal procedure. Recognizing that preparing a metallographic specimen is merely a refined means of removing material from a metal surface, some portable hand grinder was sought. Since a heavy duty orbital sander was available, this was pressed into service. It was found that, although the time-honored uni-directional grinding was impossible with this tool, a very satisfactory ground surface could be obtained. Metallographic grinding paper was used in the normal sequence; 320, 400 and 600 grit, being careful to completely remove all vestiges of previous grinding. Water lubricant was provided from plastic wash bottles.

Once the grinding was completed, polishing was done with the same orbital sander. Strips of Buehler microcloth were cut to fit the sander pad and polishing abrasive slurry was applied from a plastic wash bottle. The sections were first polished with 0.5 micron alumina (Linde A), then followed with 0.1 micron alumina (Linde B) for the final polish. Here it became apparent that a fortunate choice of tools had been made. The orbital motion of the sander tended to keep polishing abrasive fairly well in place where a rotary motion would have flung it away. Etching was done chemically in the conventional manner using cotton swabs. Liquids were allowed to drain onto blotter paper spread on the floor.

Consideration of all these aspects of the problem resulted in the kit shown in Figures 3 and 4. The kit contains all the equipment and materials necessary in most cases to obtain a satisfactory microstructure in the field. An effort was made to use plastic containers, graduates and etching dishes to eliminate breakage. Figure 4 shows only a few of the possible chemical reagents one might need. Before going into the field one would of necessity need to know with what metals he would be dealing so the proper chemicals could be obtained.

Practical Application

Shortly after the materials for the portable lab were assembled, the opportunity arose to put it to use. A large flange of INOR-8 was being machined in the ORNL shops when one of the periodic dye check inspections showed defects in the rim. The piece was about thirty inches in diameter, one and one-half inches thick and quite heavy. Using the procedure given above, suspect areas were polished, etched and replicated. Figures 5 and 6 are typical aluminized replicas of the type of cracks found.

These microcracks turned out not to be serious since they were in an area outside the bolt holes in the flange. The rim of the flange had been built up with weld metal to bring it up to proper outside dimensions and the cracks were fairly typical of some types of INOR-8 weld metal. The performance of the flange would not be affected.

Figure 7 is a photomicrograph of a replica at 750 X to show something of the fidelity one can get. It also demonstrates one of the drawbacks of this type of replication. It is extremely difficult to find a flat field. The acetate sheet tends to buckle and twist after removal from the polished surface if not allowed to completely dry in place. Since time is usually short when using the portable lab, it is necessary to strip the replica as soon as possible. If the replica can be left in place for several hours, buckling is minimized. It is also possible to reduce unevenness by pressing it onto a piece of "double sticky" tape mounted on a glass microscope slide. In this case it is best to use the thinnest acetate available. Heavy film will produce a relatively flat replica if the very minimum amount of solvent is used. However, it becomes most difficult to handle if buckling does occur.

Development of this portable lab has opened a new area of service for the metallographer. It is possible to augment such inspection methods as X-ray, dye penetrant, and ultrasonic with a semi-nondestructive test performed on the spot.

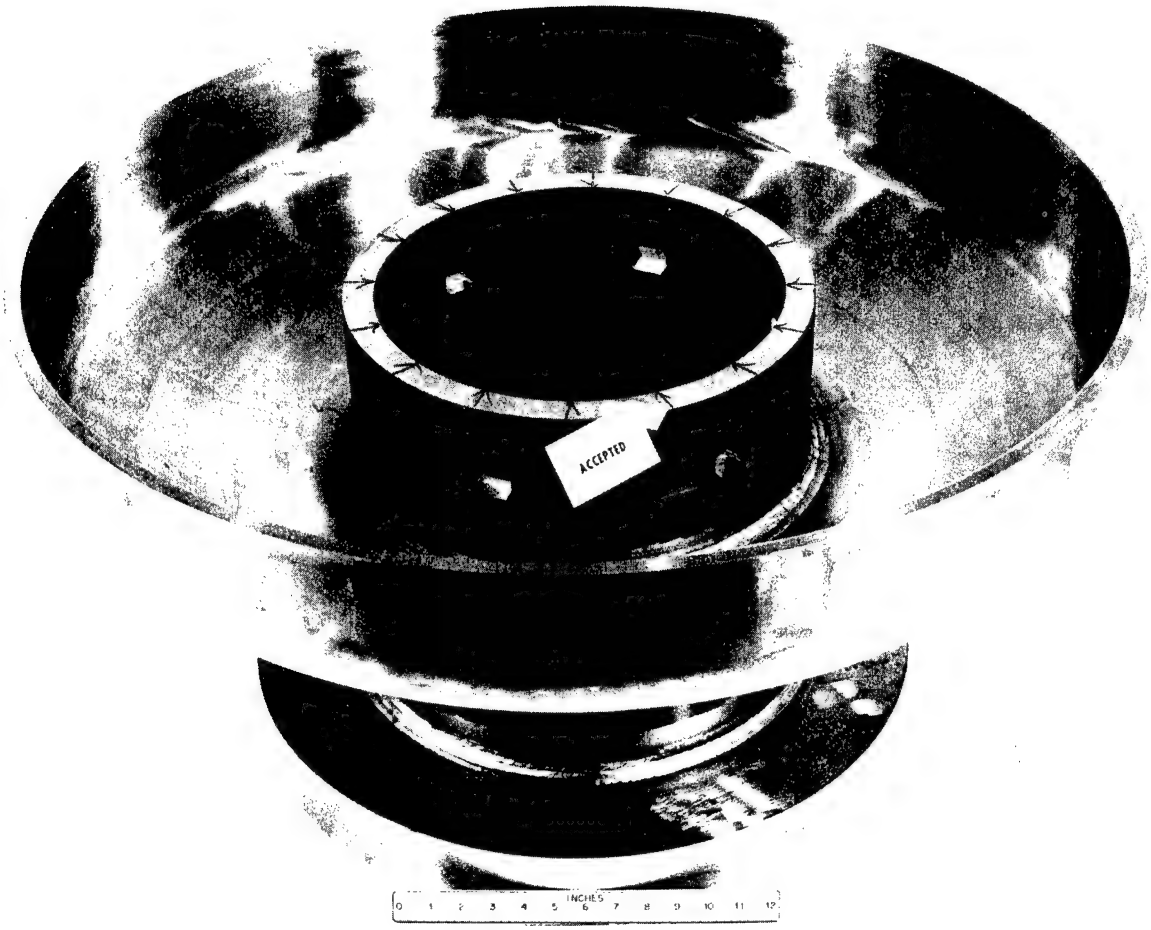

Figure 1. Pump Bowl Similar to the One Examined for Suspected Cracks. ORNL Photo 38672.

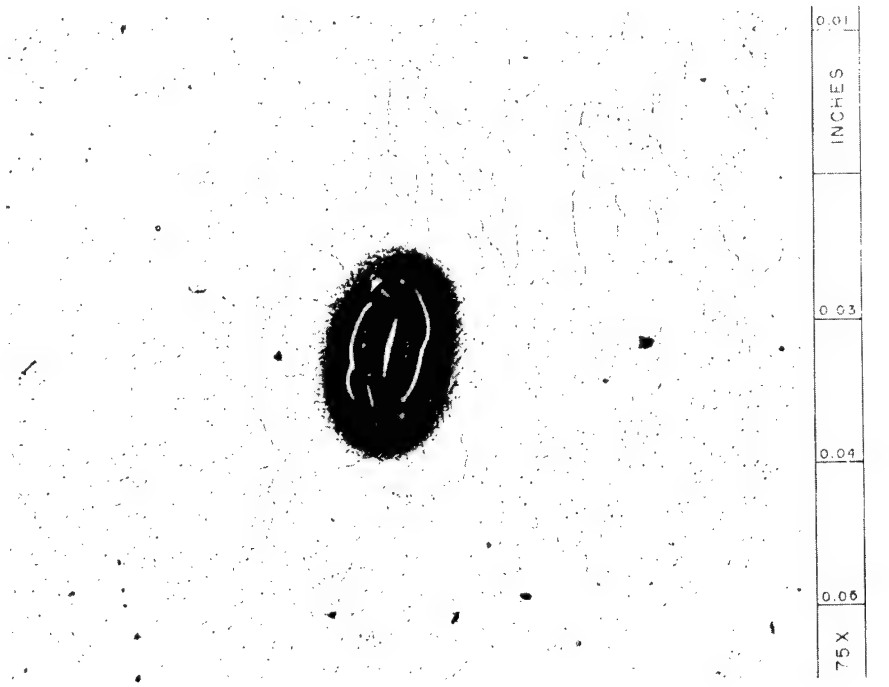

Figure 2. Photomicrograph of a Replica of a Pit and Surrounding Area from INOR-8 Pump Bowl. 75X. Y-39891.

Figure 3. Metallography Field Kit in Closed Position. Y-50251.

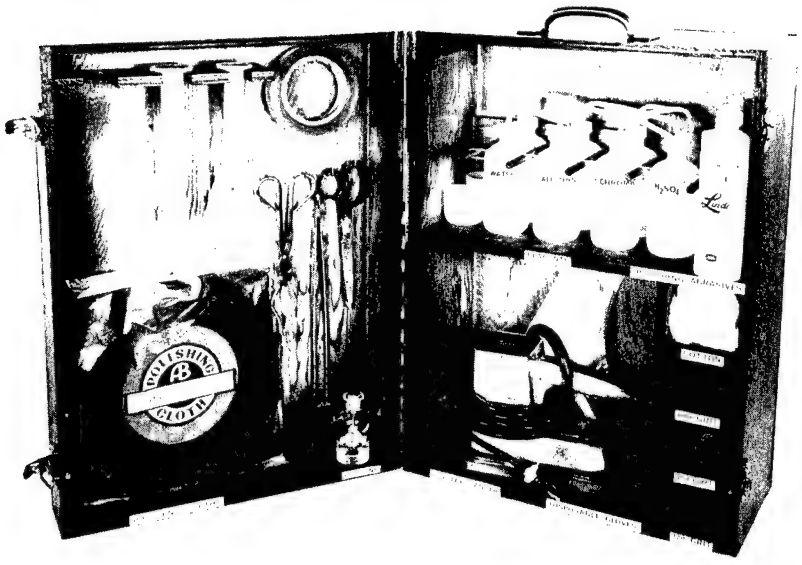

Figure 4. Metallography Field Kit in Open Position Showing Arrangement of Materials and Equipment. Y-50252.

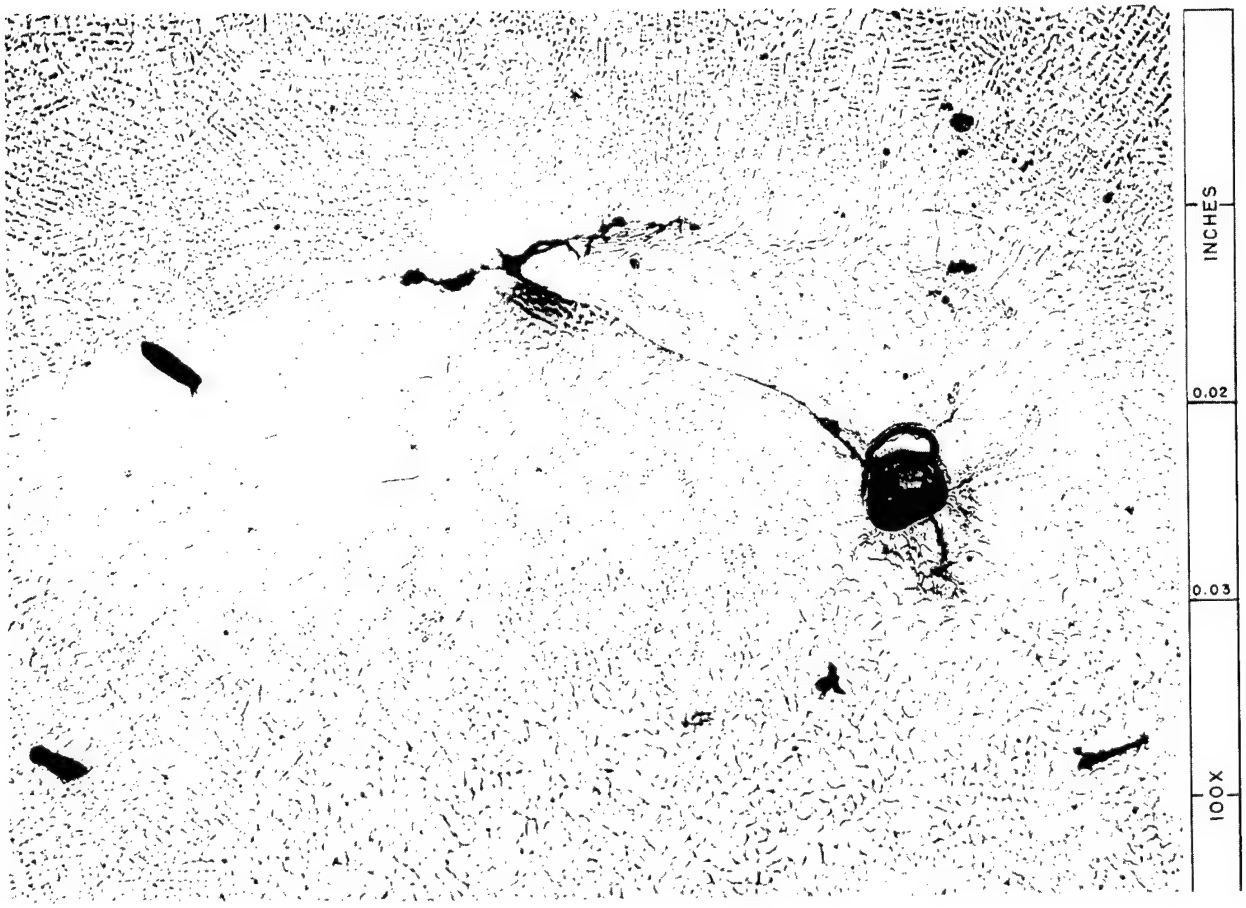

Figure 5. Photomicrograph of Aluminized Replica of Microcrack Found in Rim of MSRE Flange. 100X. Y-47909.

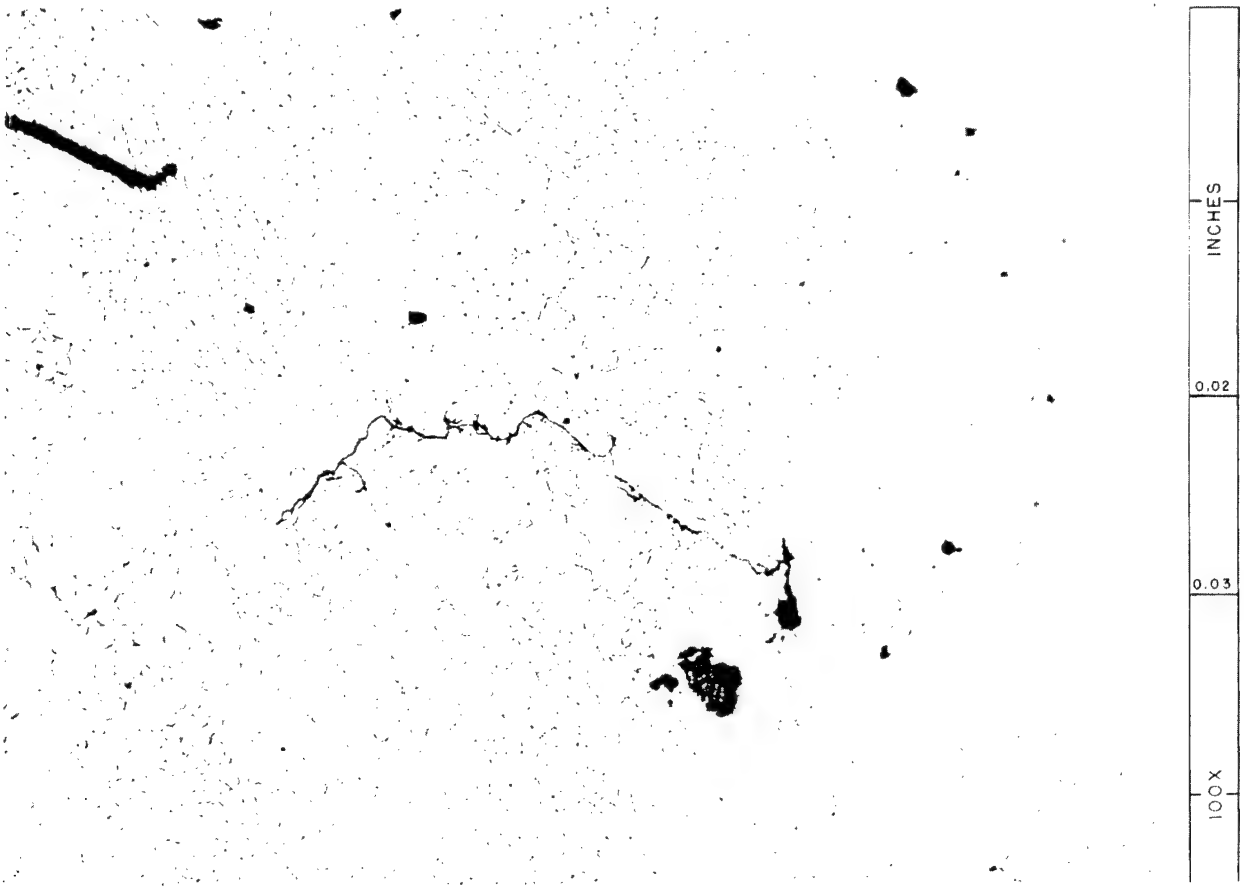

Figure 6. Photomicrograph of Aluminized Replica of Microcrack Found in Rim of MSRE Flange. 100X. Y-47911.

Figure 7. High Magnification Photomicrograph to Illustrate Resolution Possible by Acetate Replication. 750X. Y-49892.

METALLOGRAPHY OF POWDER MATERIALS*

T. I. Jones
Los Alamos Scientific Laboratory, Los Alamos, New Mexico

Metallography has proven to be a useful technique for the evaluation of powder materials. In many instances, re-evaluation of particle size measurements and chemical and X-ray data results from metallographic examinations.

INTRODUCTION

The production of a variety of complex-shaped parts by use of powder materials has demanded that the Powder Metallurgy and Ceramic disciplines exercise careful control over several characteristics of the starting materials. The chemistry of the starting materials is one vital characteristic. Often, however, impurities may be lower than detectable limits. In some cases a second phase may not lend itself to detection by chemical or X-ray analysis. The density of powder particles is an important property and is a critical factor in the measurement of particle sizes. In analyzing for density by gas flow, closed porosity is not detected. For some control purposes, other characteristics are of utmost concern. Three such characteristics which must be determined are: particle size, size distribution, and particle shape. In general, the measurement of size properties involves the use of both direct and indirect methods. The direct methods measure the coarser size particles by use of standard screens and microscopic techniques. The indirect methods measure the finer size particles and depend upon the use of sedimentation, elutriation and centrifuging. Most of these measurements are time consuming, tedious to perform, and individually will not yield all three characteristics desired.

METALLOGRAPHIC PREPARATION

This paper presents a brief description of a metallographic method for examination of powder materials. This method has been used principally for the initial evaluation of particle size, relative size distribution, particle shape, density, the degree of agglomeration, and the presence of extraneous phases. Basically, this method involves the mixing of a small quantity of powder in an epoxy-filled metal cylinder which after the resin hardens is remounted in a longitudinal direction and the section polished.

---

* This research was done under the auspices of the Atomic Energy Commission.

Several preparatory steps are involved prior to mixing the powder and epoxy resin. Figure 1 shows an Al foil which is placed over the brass plate and held smooth on the plate by the brass retaining ring.

A steel tube, 5/8 inch diameter by 0.030 inch wall thickness, is cut into 1/2-inch lengths to act as the molds for the initial mounting operation. The ends of the 1/2-inch long tubes are ground flat and the tubes cleaned in a dilute HNO_3 solution. These tubes are then cemented to the Al foil with Silastic 731 adhesive. Figure 2 shows four such tubes cemented to the Al foil. Care should be taken so that scarcely any adhesive is forced into the inside diameter.

A plastic scoop is used to extract a measured volume of powder from the powder reservoir. The volume of powder in this scoop is poured into a plastic bottle for transfer to the mounting area. The transfer bottles may be loaded in an argon atmosphere and the caps sealed to the bottle with Scotch electrical tape. Figure 3 shows a plastic scoop, a measured quantity of powder and two transfer bottles. The scoops are used only once for each powder to prevent cross contamination. When several contaminated scoops are collected, they are cleaned and inspected before reuse. The plastic scoop will hold about 1/3 cc of powder.

The epoxy resin used for this operation was Shell Chemical Company's Epon 828. This resin has a high viscosity at room temperature and is heated to 60°C before using to increase its fluidity. The hardener, D.E.A. (diethanolamine), is also heated before mixing with the 828 resin. After the 828 resin and D.E.A. hardener have been mixed, the fluid is poured into the heated molds. The molds are filled only half full to allow space for the powder and for stirring. Figure 4 shows the hot plate used for maintaining the molds at 60°C. The contents of the transfer bottle are poured into the half-filled mold and stirred with the glass stirring rod. The stirring rod is used for only one mold. This contaminated stirring rod is placed on the separate Al foil shown in the figure for subsequent disposal.

This entire mounting operation is conducted in an argon-filled, dry box whenever pyrophoric powders or powders involving health hazards are mounted. Figure 5 shows the dry box unit. Argon is supplied to the bottom of the box forcing the air out the oil-trapped vent in the top. Argon is flowed into the box at a rate of 16 cfm for about 40 minutes in order to displace the air. The rather long pot life of over two hours for this resin is adequate to accommodate the atmosphere flushing, powder-epoxy mixing, and settling operations.

The Al foil on which the powder and epoxy-filled cylinders are cemented is transferred to an oven for curing at 75°C overnight.

The hardened mounts are removed from the Al foil by cutting off the Al foil and adhesive from the outside diameter. It has been found desirable to leave the foil cemented onto the base of the tube in those mounts containing pyrophoric powders to prevent possible reaction with air and to insure bubble-free mounts. The tubes are laid on their sides and remounted in 1-1/4 inch diameter mounts again using epoxy resin. Generally, the standard 1-1/4 inch diameter mounts are ground and polished using the Buehler Automet system and a diamond abrasive. Occasionally a vibratory polisher is used for soft metal powders, such as Sn and Cd, after the preliminary polishing on the Automet apparatus.

Figure 6 shows a typical polished cross-section in which the large well graded metal powders settled uniformly to the bottom of the tube. Figure 7 shows a more normal instance in which the small particles did not completely settle before the epoxy hardened.

A great many materials have been examined by this technique. Frequently, the metallographic examination has revealed a situation not in agreement with manufacturers' claims or even with chemical and X-ray analyses. Often a revised interpretation of the data from the Fisher sub-sieve sizer or the Sedibal particle size tests results from the metallographic examination of powders. The Fisher sub-sieve sizer measures resistance to gas flow through a tamped powder; the Sedibal particle size tester weighs the sedimentation on a balance pan hung in a liquid. The following figures will illustrate some of the materials which have been examined.

RESULTS

Figure 8 shows an Al powder. This spherical powder has an average particle size of 28μ. All measured particle sizes referred to in this paper were made using a Fisher sub-sieve sizer. The spherical shape of this powder would please the theoreticians and enhance the results of their mathematical calculations.

Figure 9 shows a second Al powder. The shape and range of particle size would not aid in the accuracy of calculations. This powder had an average particle size of 42μ.

Figure 10 shows an Al powder made by an intensive milling process. These flakes are quite useful in the production of pigments and paints but by themselves would be relatively poor for producing high-density Al pressings.

Figure 11 shows an Fe powder having a 26μ average particle size. Note the variety of particle shapes and sizes. Figure 12 shows a higher magnification view of this powder. Note that the gray inclusions in this material are similar to the inclusions in Armco Fe. This powder might have undesirable chemical composition if an ultra-high purity Fe were required for a pressing.

Figure 13 shows a Cu powder of 19μ average particle size which was described as having been "atomized". Evidently this process involved heating the Cu particles in a stream of gas to give spherical shapes. Figure 14 shows a higher magnification view of this powder. A matrix network can be seen in these as-polished particles which was presumed to contain an oxide phase. Several dark particles were observed and were thought to be CuS. A number of brassy-appearing particles were also observed. Discounting the effect of the impurities in this powder, it was thought that by using suitable pressing techniques the powder would have been excellent for producing a Cu filter in which the control of pore size would be important.

Figure 15 shows a Cu powder of 6μ average particle size. By using suitable pressing techniques, it was thought that this powder most likely would have produced a relatively high-density, sintered part. Again the dark gray particles were noted in this powder.

Figure 16 shows a bronze powder of 27μ size. The particles appeared to be dense and had a uniform appearance indicating a solid solution.

Figure 17 shows a purported brass powder of +44μ size. Figure 18 shows that this powder was, instead of brass, actually Cu spheroids with a presumed Zn coating. In some areas a brassy or golden color was observed between the Cu and Zn indicating some diffusion had occurred. Note that CuO in the grain boundaries and the CuS in the grains of Cu.

Figure 19 shows a Mo powder of 6μ average size. It was estimated that this powder was roughly typical of many Mo powders examined. Some very small particles have apparently been retained. The roundish voids in the epoxy matrix were thought to have represented cavities left by pulled-out Mo particles.

Figure 20 shows a Mo powder having a 9μ average particle size as measured by the Fisher sub-sieve sizer. Comparing this powder with that of the previous figure, one can observe the misleading measurement by the Fisher unit. Actually the individual particles here are smaller than the others previously shown but have agglomerated into these large shapes. The porosity of these agglomerates was probably responsible for the 9μ size measured rather than a more massive agglomerate size. Before a metallographic analysis could be made, this powder was chosen for an experiment in spheroidization. The powder was selected because of its supposed relatively large size, 9μ average particle size. Figure 21 shows the results of spraying this powder through a flame gun and quenching in a water curtain. Some spherical shapes were produced but showed a matrix structure assumed to contain an oxide phase. Many of the particles showed only partial reaction and some appeared unchanged. This powder would not have been used had it been examined first by metallography.

Figure 22 shows a typical W powder of 1μ average particle size. The darker, unresolved mass in this figure was believed to have been sub-micron W powder which had agglomerated into this shape.

Figure 23 shows a W powder which originally had a 2 to 4μ particle size. This powder had been subsequently Ni plated with the resulting structure shown in the figure.

Figure 24 shows a W powder which was claimed to yield and did yield a very high pressed density. This 35μ powder did contain an estimated 10% of a Cu-colored phase and about 15% of an unidentified dark gray phase.

Figure 25 shows a Ta powder ordered with specifications of -50 +200 mesh particles. This figure shows the +50μ powder having annealed Ta particles, particles showing a rolled texture and fragments showing a high degree of cold work similar to chips from a lathe operation. It is to be imagined that the grain size of a pressing made from this powder would be very difficult to control.

Figure 26 shows at higher magnification a Ta particle with small inclusions. A similar pattern of inclusions has been observed in both Ta-W alloys and Ta metal with high interstitial content.

Figure 27 shows another Ta powder ordered with specifications requiring -40 +150 mesh powder. This powder was measured on the Fisher sub-sieve sizer as having a 10μ average particle size. The figure shows that the longitudinal direction of these particles would probably not pass through a 150-mesh screen. The lower average Fisher particle size of this Ta powder compared to that of the previous Ta was probably caused by its lower density. Erratic results would occur if it were assumed that this powder contained dense 10μ equiaxed particles.

Figure 28 shows a Re powder of 2μ average particle size. The wire-like particles seen in this figure have appeared in all four Re powders examined. The wire-like structures observed could have resulted from cornflake-like particles.

Two very soft metal powders were successfully polished by this technique. Figure 29 shows a 20μ Sn powder. This powder had dense particles and probably would have pressed to a high density because of the range of particle sizes present. Figure 30 shows a Cd powder of a -100 mesh size. This powder had some low density particles and a much wider range of particle shapes and sizes.

In contrast to these soft metal powders, very hard carbide powders were polished using the Automet apparatus and a diamond abrasive. Figure 31 shows a 4.5μ TaC powder. The larger particles had a fair amount of open porosity which may have influenced the measurement of particle size.

Figure 32 shows a 10μ TiC powder. This powder had been etched and three particles are shown which have multiple grains. Because the great majority of particles do not show internal grains, it was presumed that this material must have fractured along grain boundaries. It seems unusual that although no scratches were observed on the as-polished particles many particles showed scratches after etching. This would lead to an initial assumption that a flowed layer had been built up during the polishing operation. With a hardness of 3100 DPH for TiC, the idea of plastic flow would seem remote.

Figure 33 shows a 7μ average particle size for ZrB_2. The second phase shown in one particle was presumed to be ZrB.

Figure 34 shows a B powder. Boron has been reported to have a slightly higher hardness than TiC. The darker phase shown in some particles was presumed to be a carbide of boron. The metallic-appearing flakes were thought to have been abraided from the hardened steel hammers of the hammer mill used to crush this hot-pressed boron. Figure 35 shows a boron particle with a non-metallic white side. Although positive identification could not be made, it was assumed that this was part of the BN liner used to separate the B from the graphite die in the hot-pressing operation.

Figure 36 shows a closely graded 10μ UO_2 powder. The individual particles were quite dense.

Figure 37 shows a commercial, spherical UO_2 powder. The porosity shown for these particles was thought to be real rather than caused by insufficient polishing.

Figure 38 shows another commerical UO2 powder of 22μ average particle size. This powder contained white, metallic-appearing phases, golden phases, and some purplish phases. The white and golden phases were presumed to be high U alloys. The purplish phase was thought to be a reaction product between UO_2 and TiO_2. TiO_2 had been present in the UO_2 as an additive.

Figure 39 shows a "snowflake"-type UO2 of 5μ average particle size. The "rosette" particles had too low a density for powder rolling or for a cold-pressing and sintering operation.

Figure 40 shows a typical graphite powder used by the Powder Metallurgy Section for reaction with metals and metal hydrides.

Figure 41 shows a 5μ UC_2 powder made by arc-melting U and C and then crushing the button to this size. No UC was detected by etching with HNO_3.

Figure 42 shows a UC powder in the polished condition. No UC_2 was detected after etching with HNO_3.

Figure 43 shows UC-ZrC solid solution powder. This powder was made by reacting the metal hydrides with carbon then crushing the material to this size. No second phase was observed when the powder was etched with a HNO_3 solution. ZrC powder had a similar structure to this.

Figure 44 shows a UC-ZrC powder which contained a UC_2 phase.

Figure 45 shows individual particles of UC_2 in another UC-ZrC powder. These particles were unusual in that possibly four phases were present: UC_2 with UC precipitated along preferential planes and UO_2 and U_2C_3 mixtures in the gray areas.

Figure 46 shows a UC-ZrC powder made by crushing an arc-melted button. The button was made by arc-melted U, Zr and C. This figure shows some particles which had an air-oxidizing phase thought to be unreacted U metal.

Figure 47 shows a two-phase particle which was believed to have contained a Zr core with ZrC on the exterior.

Figure 48 shows UC-ZrC particles made by crushing commercial, spherical UC-ZrC. It seemed obvious from the cored structure of this material that it had been arc-melted. Very little UC_2 was detected in the microstructure.

CONCLUSIONS

The preceding photomicrographs have illustrated a few of the advantages of a metallographic method of powder material evaluation compared with conventional techniques. This method permits an estimation to be made in a single test of the particle size, size distribution, particle shape, relative density, and existence of extraneous phases.

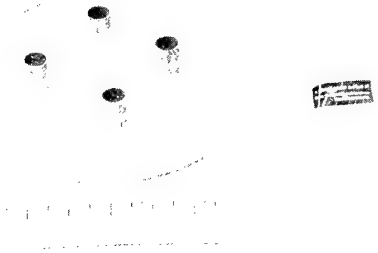

Figure 3

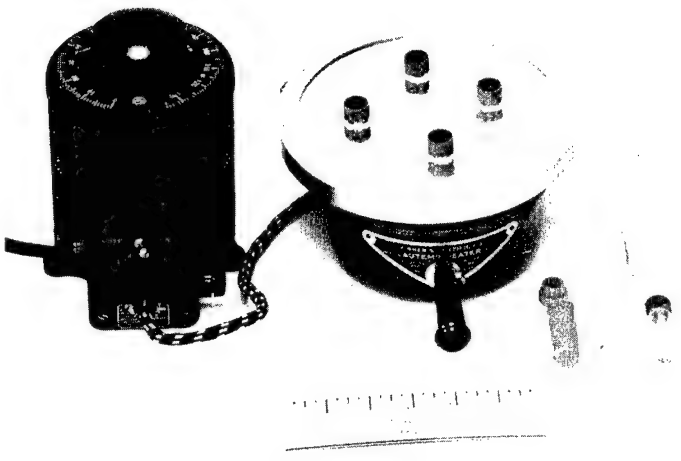

Figure 4

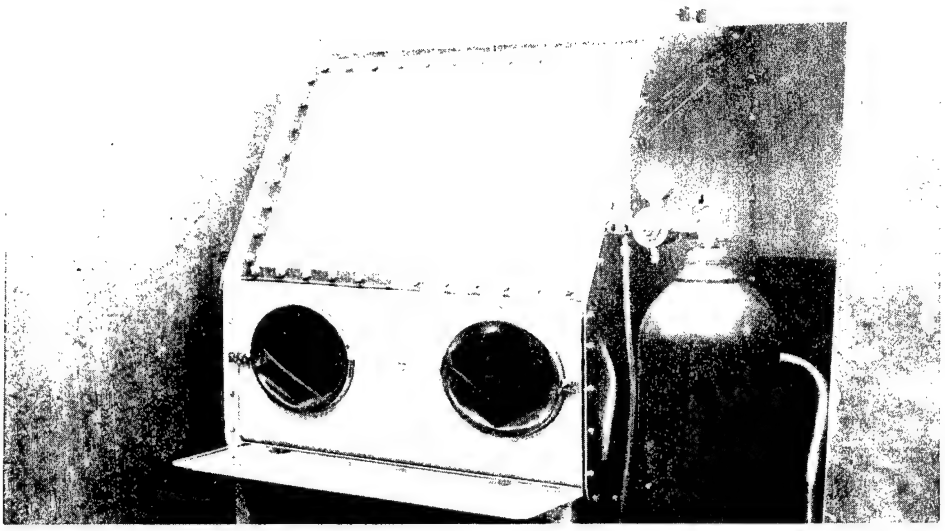

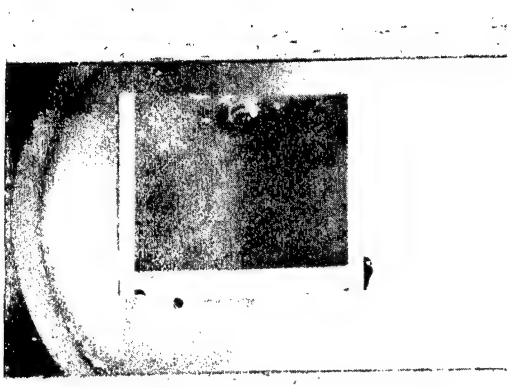

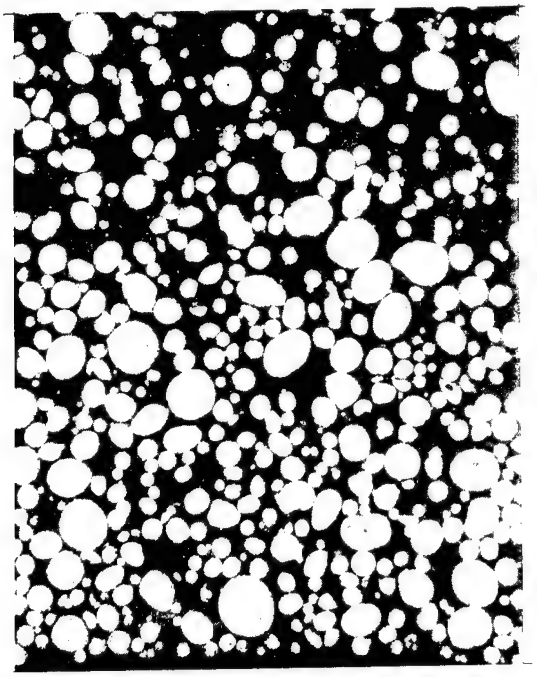

Figure 8 100X

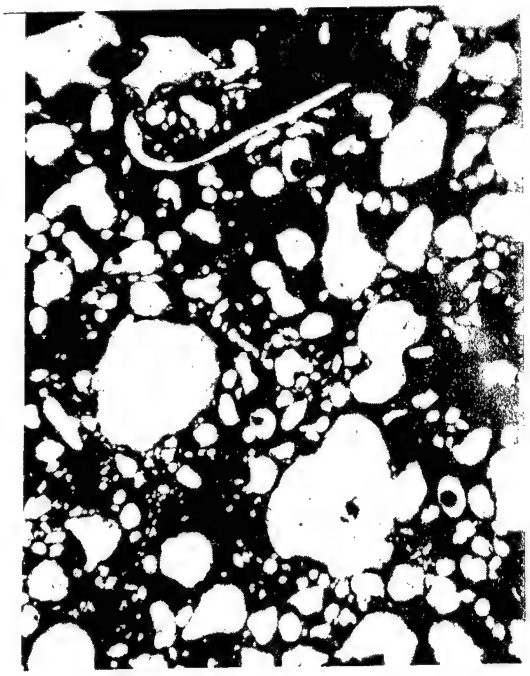

Figure 9 100X

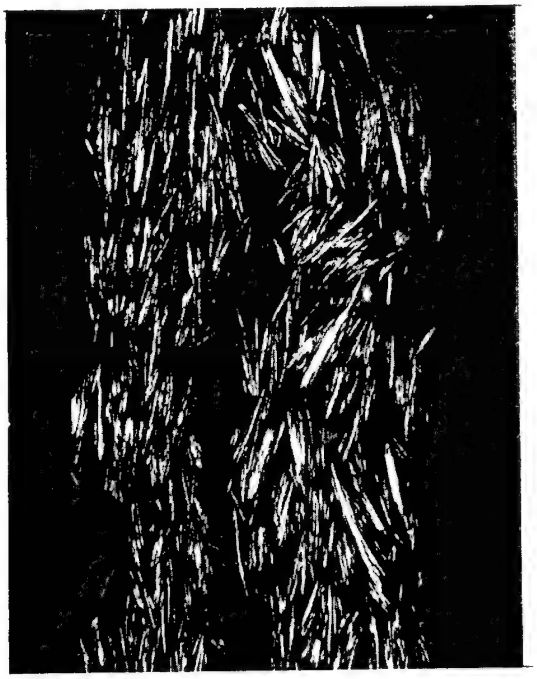

Figure 10 250X

Figure 11 100X

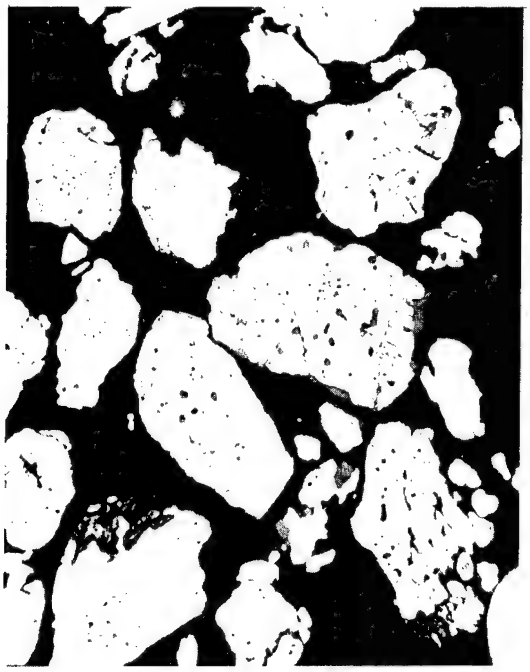

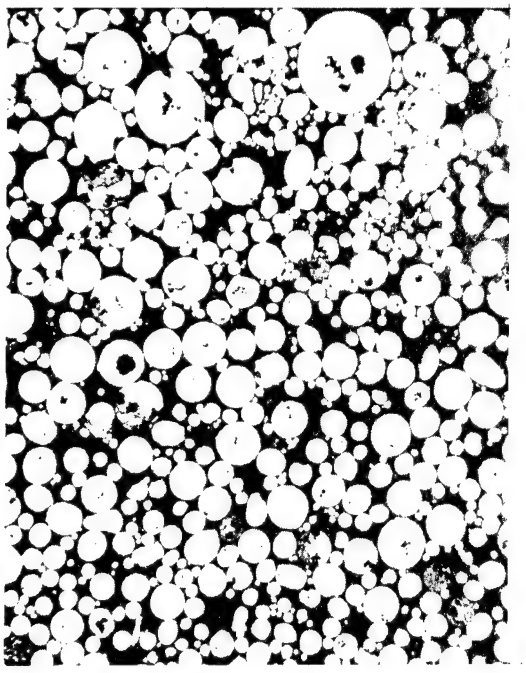

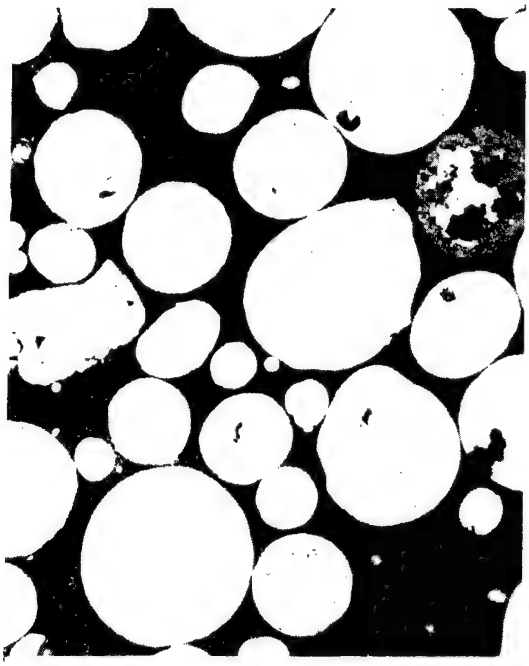

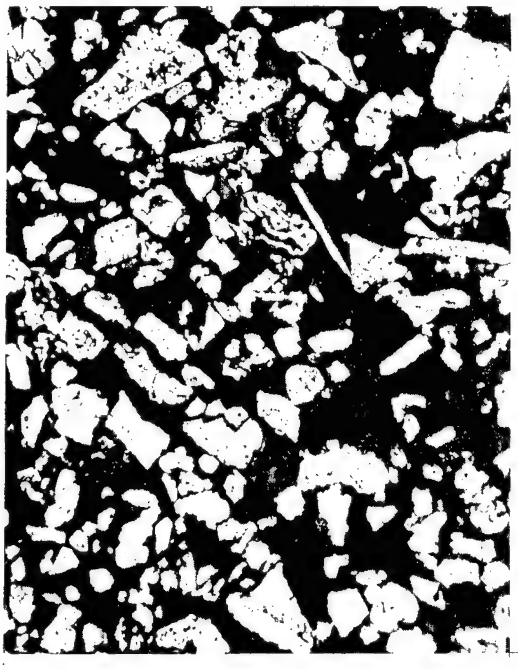

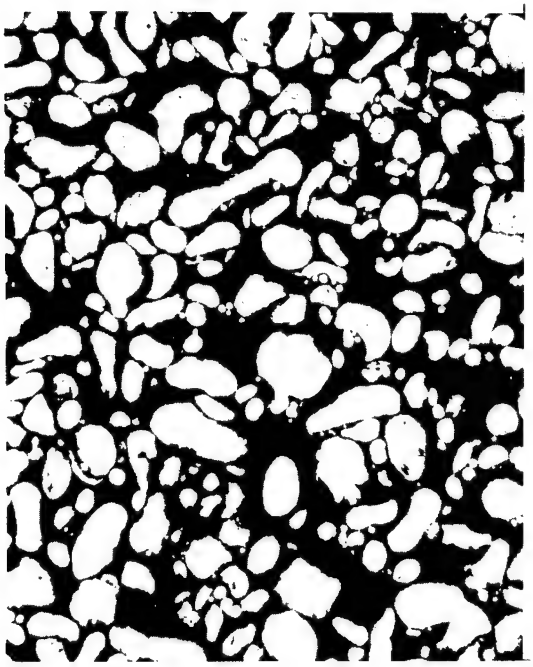

Figure 16 100X

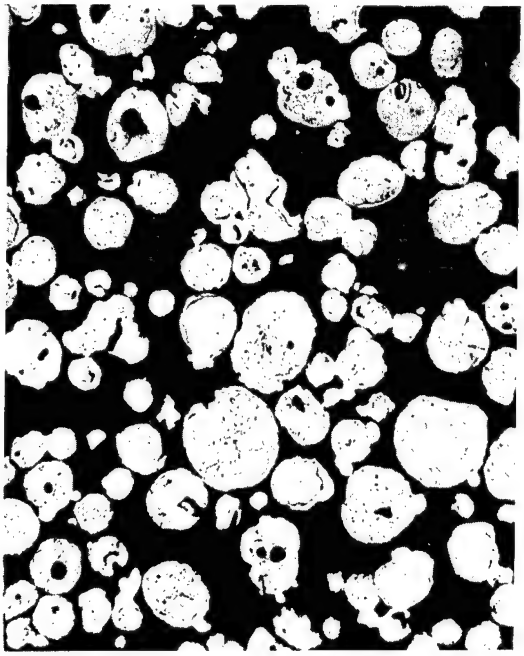

Figure 17 100X

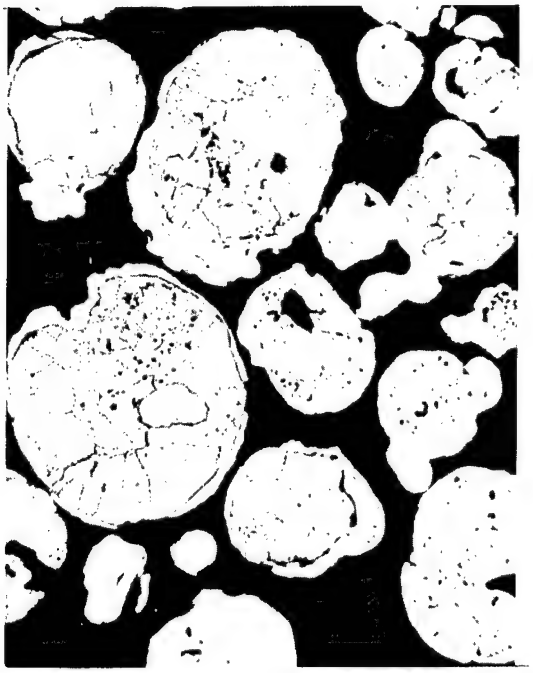

Figure 18 250X

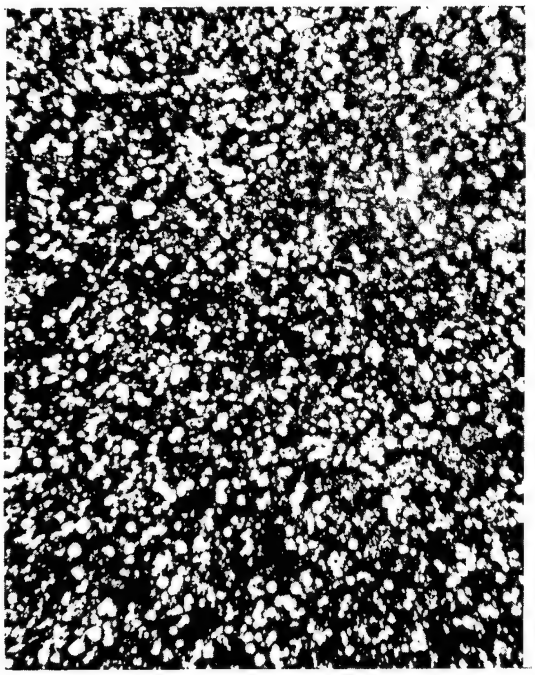

Figure 19 100X

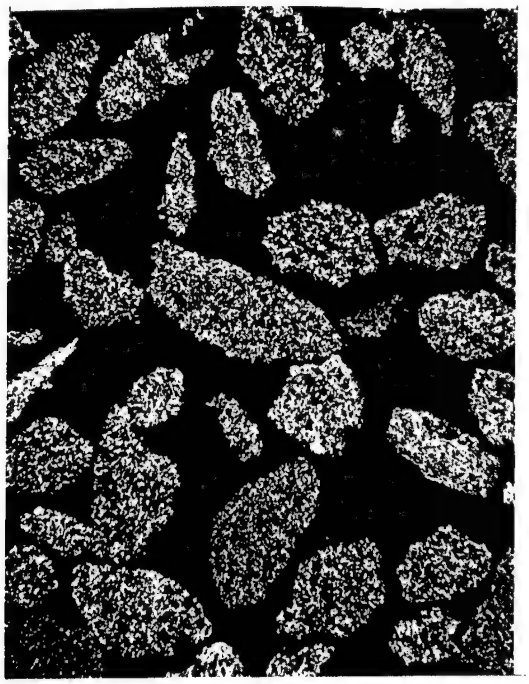

Figure 20 100X

Figure 21 250X

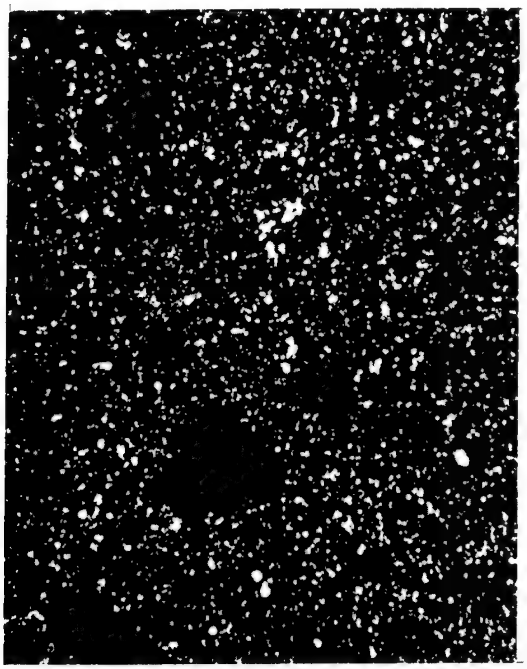

Figure 22 500X

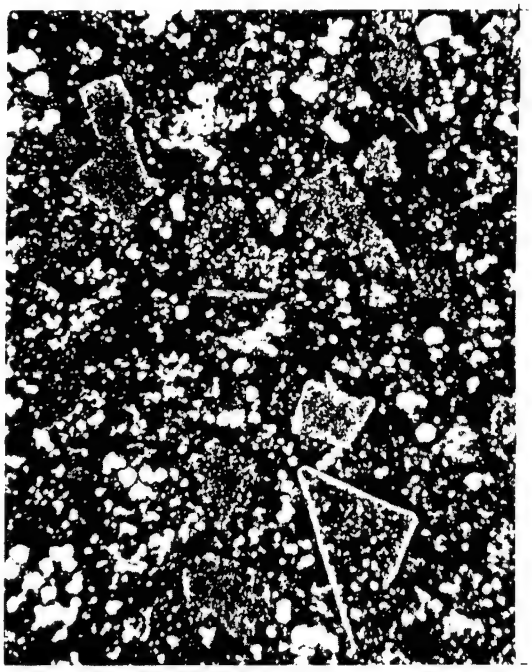

Figure 23 250X

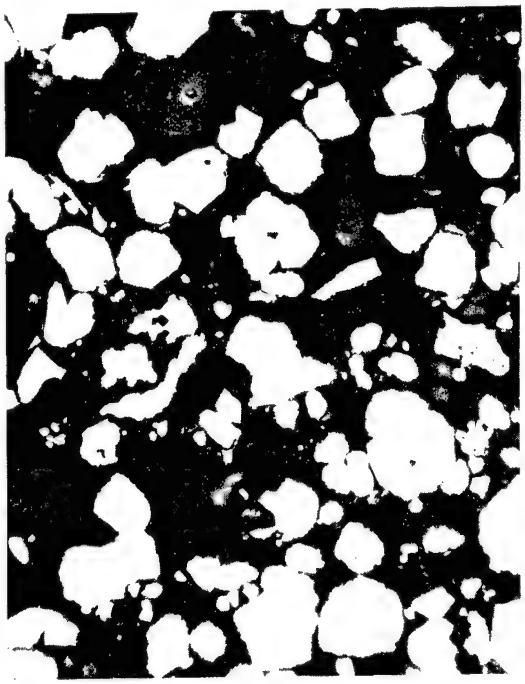

Figure 24 250X

Figure 25 100X

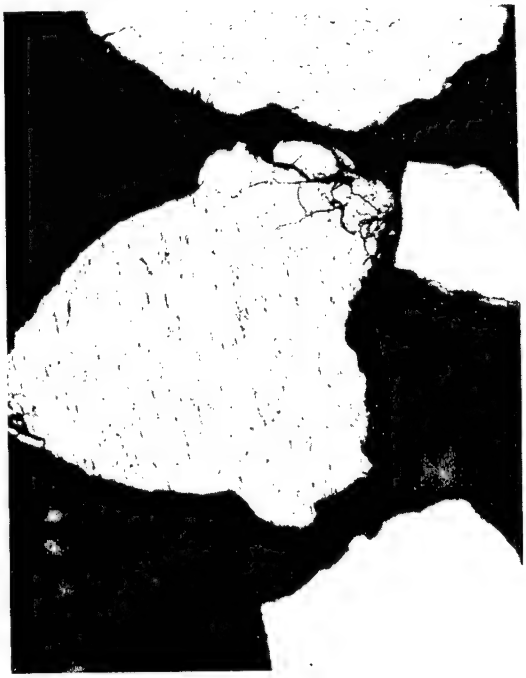

Figure 26 250X

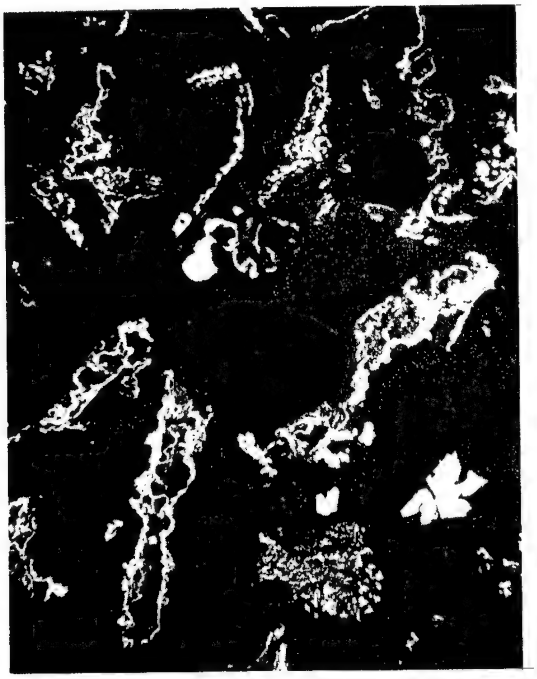

Figure 27 100X

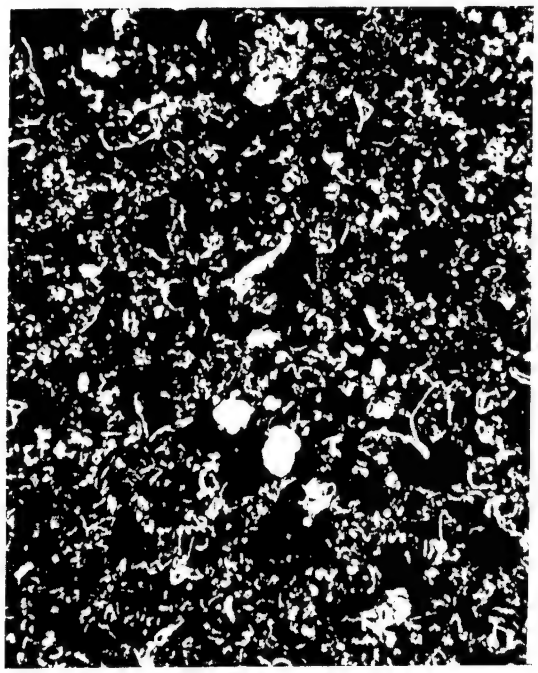

Figure 28 250X

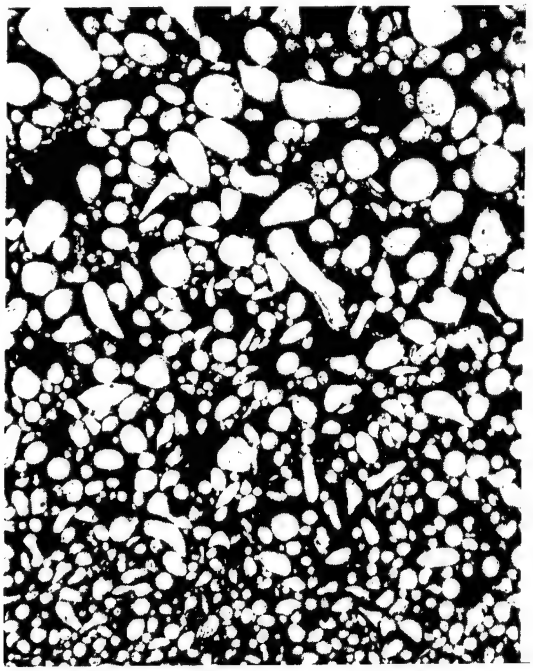

Figure 29 100X

Figure 30 100X

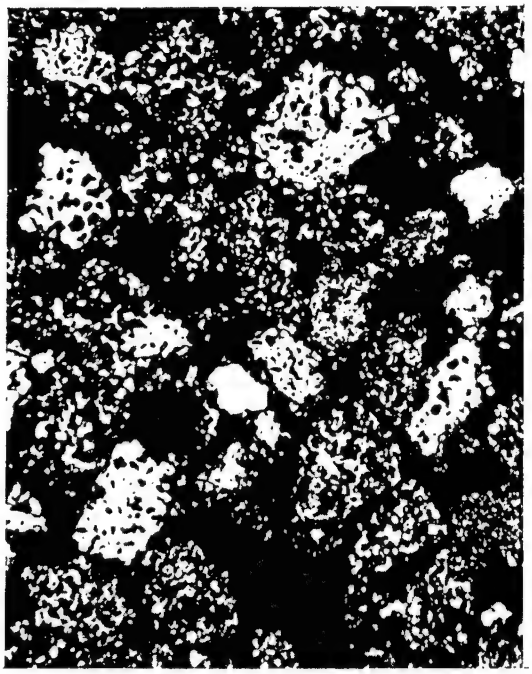

Figure 31 250X

Figure 32 250X

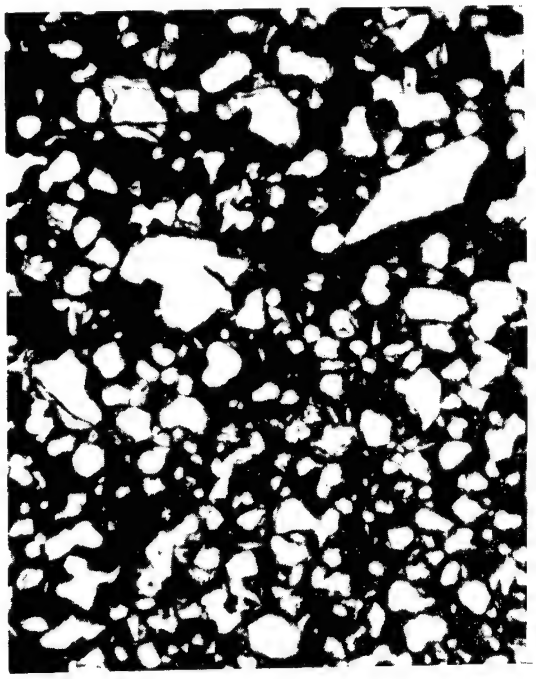

Figure 33 500X

Figure 34 250X

Figure 35 250X

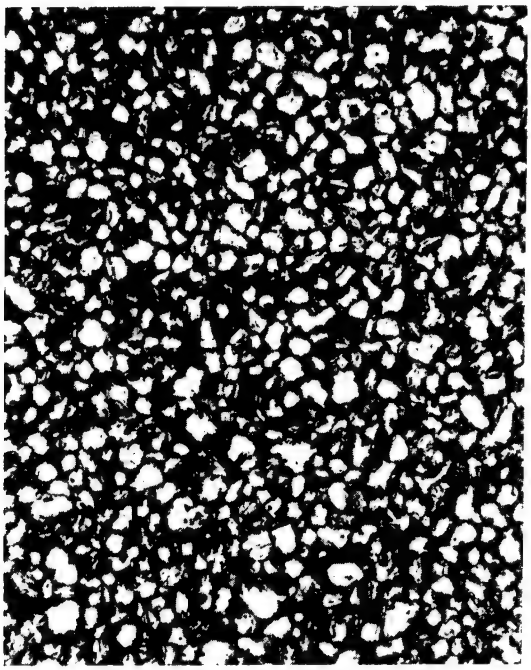

Figure 36 250X

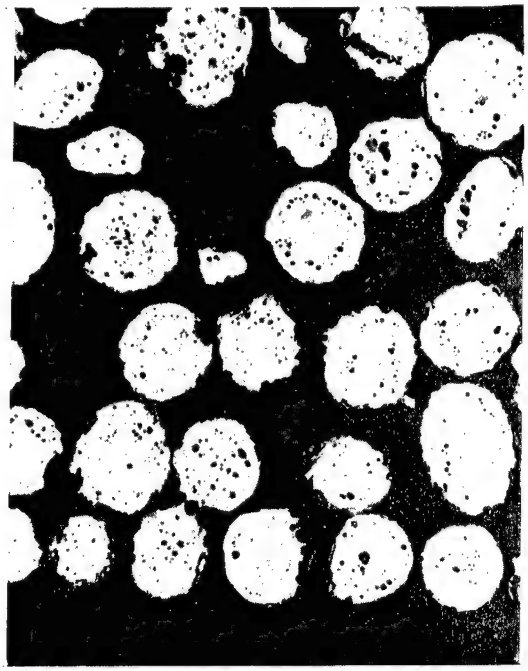

Figure 37 250X

Figure 38 250X

Figure 39 500X

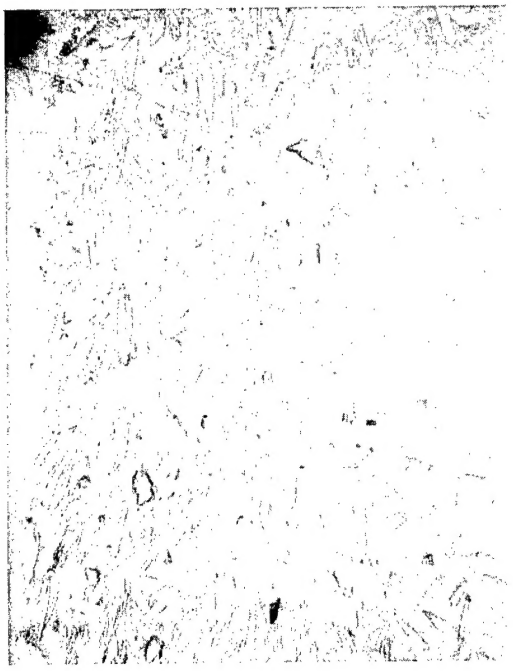

Figure 44 100x

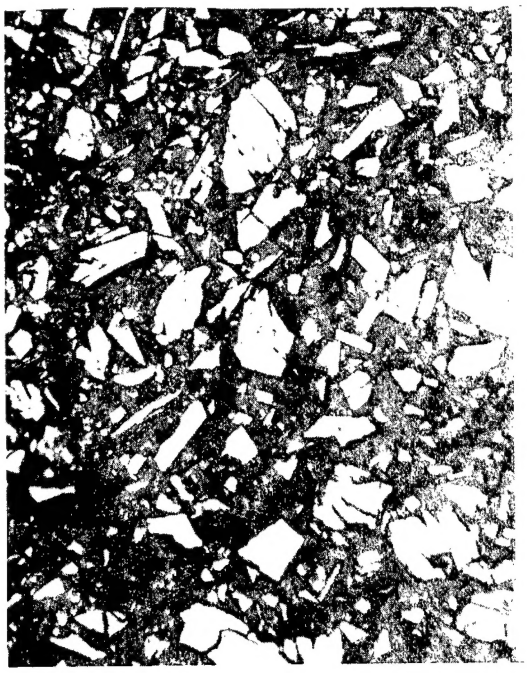

Figure 45 250x

Figure 46 250x

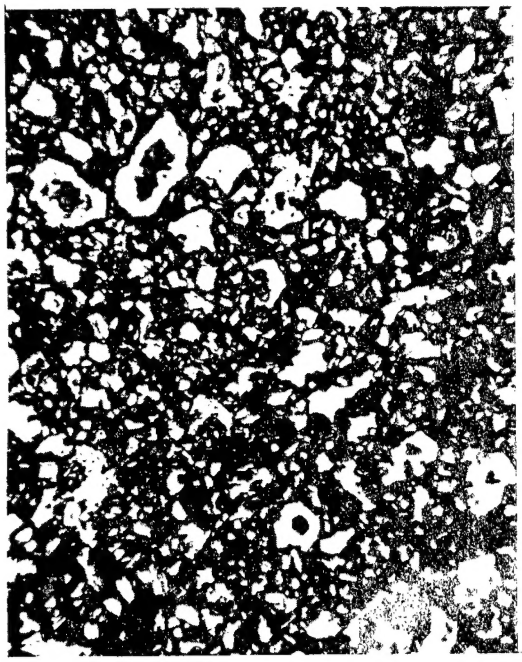

Figure 47 250x

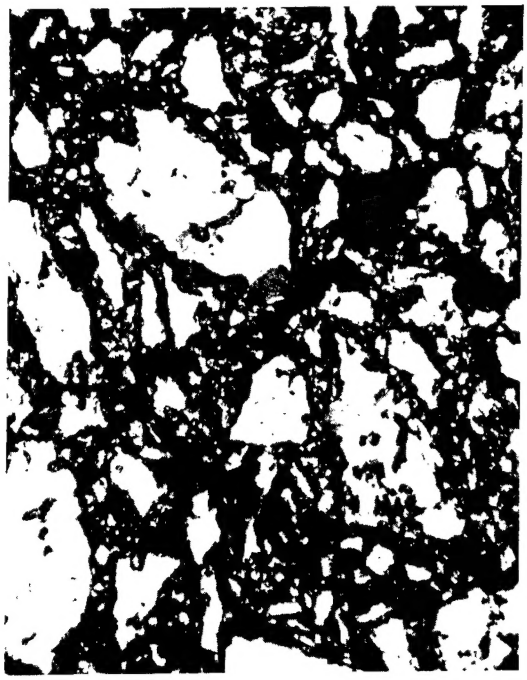

Figure 46 250×

Figure 46 500×

Figure 47 250×

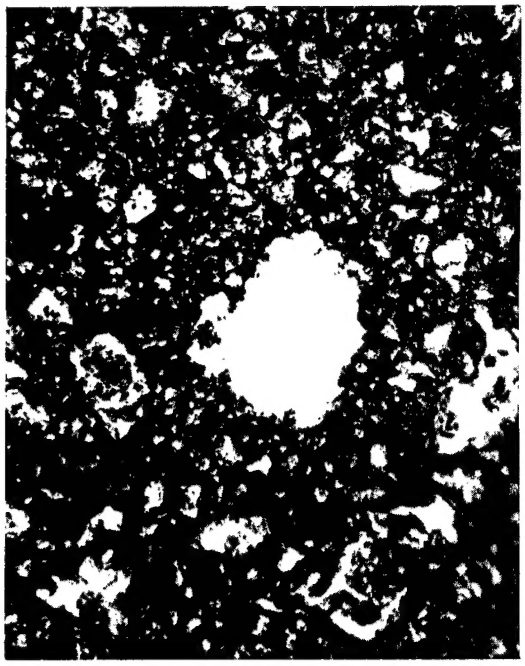

Figure 47 500×

Figure 48 250X

APPENDIX A

LIST OF ETCHANTS

The following list of etchants or procedures was submitted by the authors of some papers presented at the 17th A.E.C. Metallography Group Meeting.

Author	Etch
Crouse R.S.: (p. 60)	INOR-8 etchant. 2 parts 5% chromic acid 1 part HCl Immerse or swab.
Douglass, D.L.: (p. 85)	Etchant for thinning of uranium for transmission electron microscopy. 133 ml acetic acid 25 grams CrO_3 14 ml H_2O Cool below 15°C. Use constant magnetic stirring.
Gruber, W.J.: (p. 26)	Thorium etchant. After mechanical polishing, the thorium samples must be immediately placed in a vacuum. Surface oxidation, which can occur in a time period as short as 15 minutes, induces artifacts in the cathodically etched surface. The samples were vacuum cathodic etched for 30 minutes using argon gas. Etching was carried out with 2500 volts and about 25 milliamps while maintaining a 30 micron pressure. When etching, the voltage and pressure were kept constant while the amperage varied from sample to sample. Plutonium-aluminum etchant. Electrolyte: 49% methanol 49% distilled H_2O 2% HF Electropolish: Electropolish for 5 to 15 seconds using a current density of 0.3 amps/sq. in. to remove smeared metal. Care should be exercised to avoid overpolishing which can cause pitting and a relief effect. Electroetch: Electroetch for 25-45 seconds with a current density of 0.05 amps/sq. in. Best results are obtained if the electrolyte is thoroughly stirred prior to use.
Kegley, T.M.: (p. 111)	A thin pyroxylin film. 5% pyroxylin amyl acetate solution One drop is added to the specimen surface and spread evenly over the polished surface with a cotton swab.